Molecular phylogeny and frontal shield evolution of Cheilostome bryozoans

(Un)linking frontal shield evolution to phylogenetic relationships within Adeonidae

Marianne Nilsen Haugen

Master of Science
60 credits

Centre for Ecological and Evolutionary Synthesis
Department of Biosciences
Faculty of Mathematics and Natural Sciences

UNIVERSITY OF OSLO

September 2018

2018

Molecular phylogeny and frontal shield evolution of Cheilostome bryozoans: (Un)linking frontal shield evolution to phylogenetic relationships within Adeonidae.

Marianne Nilsen Haugen

http://www.duo.uio.no/

Trykk: Reprosentralen, Universitetet i Oslo

Acknowledgements

First and foremost, I will sincerely thank my wonderful supervisors, Lee Hsiang Liow, Kjetil Lysne Voie, Björn Berning and Russell Orr for giving me the opportunity to engage in a new and exciting research field. You have each and one of you safely guided me through an unknown, in the beginning quite scary, territory. I couldn't have asked for any better supervisors than you!

Lee Hsiang, your enthusiasm and passion for science, and bryozoans particularly, are something I truly admire. Thank you for the invaluable help and motivation, and for teaching me about being a critical and thorough scientist.

Kjetil, I thank you for all the wonderful help concerning the analyses and the manuscript.

Björn, I would like to thank you for sharing your bryozoan knowledge with me, skype-meetings and discussions, and for having patience with me, awaiting me to understand how frontal shield development works!

Russell, despite your terrible bad jokes, I have truly appreciated and enjoyed being your student for the last two years. You've thought me so much about lab-work, bioinformatics and phylogeny in a wonderful way. I'm really grateful for your patience, guidance and all your motivational talks.

Mali Hamre Ramsfjell, I thank you for providing me with wonderful SEM photos. I would also like to thank all the remaining members of BLEED. I will, believe it or not, miss endless rounds of bryozoan charades.

I also wish to thank Andrea Waeschenbach, Masato Hirose and Thomas Schwaha for providing me with sequences and samples, making this project possible. Additionally, I wish to thank Emanuela Di Martino for wonderful SEM photos and help with interpreting my results and answering questions regarding bryozoan systematics.

Lastly, I wish to thank my dearest friends, Lise and Nora, for being there for me during these two years. You've really meant a lot to me. And last but not least, thanks to my family for being supportive and enthusiastic all the way!

Marianne Nilsen Haugen

Abstract

The colonial marine invertebrate phylum Bryozoa, especially the order Cheilostomata, has a rich fossil record where their calcified skeleton reflects numerous key morphological traits. Some of these morphological traits are suggested to be taxonomically important and have thus contributed to the phylogenetic framework that bryozoologists use today. However, large parts of this phylogenetic framework, have not been fully subject to modern scrutiny. One such trait that has received overwhelming attention in the current phylogenetic framework is the frontal shield. Allowing for the physical protection of zooids, frontal budding and robust colonial growth, calcified frontal shields and skeletal reinforcements have undoubtedly been important for the success of ascophorine cheilostome bryozoans which are the most species-rich extant group of marine bryozoans. However, several current hypotheses suggest that neither of the two dominant shield types among ascophorine cheilostomes, umbonuloid and lepralioid, are monophyletic. For instance, the bryozoan families, Adeonidae and Smittinidae are found to exhibit both umbonuloid and lepralioid frontal shields, suggesting that it may not be exceedingly difficult to evolve between these apparently different frontal shield types. Recent molecular phylogenetic studies also suggest multiple independent origins of the umbonuloid and lepralioid frontal shields, albeit with limited statistical support.

In this study, I further investigate the hypothesis of the non-monophyly of umbonuloid and lepralioid frontal shields, through a robust multi-gene phylogeny consisting of 15 mitochondrial genes and two rRNA genes. To achieve this, I isolated DNA from 19 bryozoans, which I then genome-skimmed to acquire the mitochondrial genomes and rRNA operons. Combining my newly generated sequence data with previously published data, I inferred the phylogenetic relationships among 35 bryozoan species with both Maximum likelihood and Bayesian inference, and I also investigated their mitochondrial gene rearrangements. Specifically, my phylogeny focuses on resolving the phylogenetic relationships and gene rearrangements within the family Adeonidae. With highly resolved and well-supported nodes, my molecular phylogeny suggests independent origins of the two frontal shield types within the Adeonidae, and for bryozoans in general, further verified via an ancestral state reconstruction analysis. The result therefore validates previous hypotheses and casts doubt on the frontal shield as a good morphological trait for inferring evolutionary relationships among bryozoans.

Table of Contents

1 Introduction

Bryozoa is a phylum of aquatic, colonial invertebrates predominantly found in marine environments. The majority of bryozoan species have calcified skeletons, which are generally well-preserved, hence yielding a rich fossil record that dates back to the early Tremadocian (about 485–478 mya) (Ma, Taylor, Xia, & Zhan, 2015). Extant bryozoans are divided into three different classes: Phylactolaemata, Stenolaemata and Gymnolaemata, and about 6600 described species are found worldwide, with about 80 percent of all species found in the gymnolaemate order Cheilostomata (P. Bock, pers. comm., 2018). The phylogenetic relationships, both among bryozoan taxa and between other higher taxa, are subject to many questions and uncertainties, as the majority of phylogenetic and/or systematic studies are based largely or solely on morphological characters e.g. Dzik (1975); Cuffey and Blake (1991); Todd (2000); Ostrovsky, Gordon, and Lidgard (2009); Weaver, Cook, Bock, and Gordon (2018).

Other than being the most speciose and widespread order within Bryozoa, members of the Cheilostomata also have a wide range of morphological traits that are interesting evolutionarily, structurally and developmentally. Cheilostomes are a geologically young group with their first occurrence dating back about 160 mya to the Late Jurassic (Pohowsky, 1973). Cheilostomes remained low in taxonomic diversity (few species and genera) until a major radiation in the late Cretaceous (Taylor, 1988). Two major evolutionary innovations are hypothesized to be the drivers for this radiation: the development of non-planktotrophic larvae and the evolution of a hypostegal coelom and the associated calcified frontal shield (Taylor, 1988; Gordon & Voigt, 1996). Taylor (1988) hypothesized that brooded non-planktotrophic larvae restrict gene flow between populations which in turn promote allopatric speciation. A calcified frontal shield allows for physical protection of zooids, frontal budding and robust colonial growth, leading to significant adaptive evolution in colony form aiding competitive success and lower extinction rates (Lidgard, Carter, Dick, Gordon, & Ostrovsky, 2011). These innovations have very likely been important for the success of the most species-rich extant group of marine bryozoans, the ascophorans (McKinney & Jackson, 1989; Gordon & Voigt, 1996; Taylor, Casadío, & Gordon, 2008).

Members of Ascophora, now an informal higher taxon (Gordon, 2014), are cheilostomes that have calcified frontal shields above the ascus, a flexible-floored sac that lies beneath the frontal shield. Different frontal shield types have evolved, and their bearers thrived since the appearance of the first frontal shields in the late Cretaceous. Frontal shields are currently an

important trait for bryozoan systematics, where the current higher-level taxonomy of cheilostomes are based, for the most part, on the construction of the frontal wall, their associated tissues and skeletal elements which are related to the lophophore (feeding organ) eversion mechanism (Gordon, 2000). As such, four infraorders within Ascophora are recognized based on either of the four different frontal shield types: Acanthostegomorpha (spinocystal shield), Hippothoomorpha (gymnocystal shield), Umbonulomorpha (umbonuloid shield) and Lepraliomorpha (lepralioid shield).

Despite the purported evolutionary significance of frontal shields and additionally its importance for understanding bryozoan biology, the evolutionary history of this trait has been insufficiently investigated using independent molecular evidence. So far, only morphological models have been suggested for the development and evolution of the different kinds of frontal shields (Gordon, 2000). The best-supported hypotheses based on fossil evidence, argue that some members of Anasca (specifically calloporids), which are characterized by having zooids with membranous frontal wall without a calcified protective frontal shield, developed basally jointed spines around the frontal membrane to enhance protection of their soft parts (the polypide). Further, calcification or loss of cuticular spine joints created rigid spines (costae), and fusions among costae led to the rigid frontal costal shield (spinocyst) that defined a novel morphological grade, the cribrimorphs (Dick, Lidgard, Gordon, & Mawatari, 2009). From there on, two main pathways have been proposed: 1) progressive reduction in the area of the costal frontal shield and its eventual complete replacement by gymnocyst (exterior wall), giving a gymnocystal frontal shield, as found in the infraorder Hippothoomorpha or 2) overgrowth of the costal frontal shield by the surrounding kenozooids and subsequent reduction and loss of the costal field, giving an umbonuloid frontal shield with an underside roofing the ascus that has an outer cuticular layer, as in infraorder Umbonulomorpha. Thereafter, lepralioid frontal shield is believed to have derived from Umbonulomorpha by loss of the umbonuloid component of the frontal shield, leaving a cryptocystal frontal shield of interior wall which can be perforated by pseudopores (Gordon & Voigt, 1996; Gordon, 2000).

In chronological appearance in the fossil record since the Cenomanian (100.5–93.9 mya), spinocystal, umbonuloid, gymnocystal and lepralioid frontal shields have evolved possibly in the pathways stated above. However, hypotheses based on these fossil observations as well as recent morphological evidence, suggest that neither of the two dominant shield types, umbonuloid and lepralioid, are monophyletic (Gordon & Voigt, 1996). This is corroborated by

a recent molecular phylogenetic study by Knight, Gordon, and Lavery (2011) albeit with lacking statistical support. Additionally, accumulating evidence over the past few years also indicate that spinocystal and gymnocystal have a para- or even polyphyletic origin (Gordon, 2000), and the higher order taxa Acanthostegomorpha, Hippothoomorpha, Umbonulomorpha and Lepraliomorpha have for this reason already been discarded in the most recent classification of cheilostome Bryozoa (Gordon, 2014), although they are still being used on the Bryozoa Homepage (Bock, 2018), and the World Register of Marine Species for the sake of consistency (http://www.marinespecies.org/aphia.php?p=taxdetails&id=110722).

The phylogenetic positions of bryozoan taxa based solely on simple shared morphological characters are often incongruent with those based on independent molecular data (Waeschenbach, Taylor, & Littlewood, 2012; Taylor & Waeschenbach, 2015; Taylor, Waeschenbach, Smith, & Gordon, 2015). When using only morphological characters for systematic studies, interrelationships among taxa can be very hard to resolve, such as for the family Adeonidae, Busk, 1884, whose taxonomic status have been debated for decades. The family is divided in 10 extant genera with 106 described extant species which are found worldwide (Bock & Gordon, 2013), with the first observation of members of this family dating back to the Ypresian (56.0–47.8 mya) (Canu & Bassler, 1920). Genera in this family are found to possess either umbonuloid or lepralioid frontal shield and they also have extensive variation in their frontal pore complex. For this reason, Adeonidae was previously separated into two distinct families by Gregory (1893): Adeonidae and Adeonellidae, Gregory 1893. Despite their morphological differences, the two families are today merged, but the debate is ongoing since no molecular evidence has thus far been presented to investigate their relationship. In addition, the possession of two very different types of frontal shields by Adeonidae s.l. also implies that frontal shields may not be taxonomically relevant at family level, as suggested by Cook (1973) who conducted an extensive comparative morphological study of adeonid and adeonellid genera.

Therefore, the goals of my study are to disentangle and infer the phylogenetic relationships of cheilostome bryozoans, focusing on members of the family Adeonidae to reveal the nature of their frontal shield evolution, and consequently to increase the number of sequenced bryozoan taxa. I hypothesize that taxa within the family Adeonidae will form a monophyletic clade, but that the monophyly of the two types of frontal shields may not stand. In addition, I investigated mitochondrial gene rearrangements, as these has been suggested to encompass useful

phylogenetic information, and further explore if such rearrangements are congruent with species evolution (Boore, Collins, Stanton, Daehler, & Brown, 1995; Boore & Brown, 1998; Cameron, 2014).

For this reasoning, I conduct genome skimming on 19 bryozoan taxa that have never been subject to DNA sequencing, targeting the mitochondrial genome (15 genes) and the ribosomal operon (rRNA genes 18S and 28S). I also incorporate orthologous bryozoan sequence data provided by collaborators and those already present in Genbank to create a dataset, which I subject to phylogenetic inference with both Maximum likelihood (ML) and Bayesian analyses (BI). I present a well-supported phylogeny of 35 bryozoan taxa, and I present analyses of ancestral state reconstructions to aid my discussion of frontal shield evolution. I end by discussing the impact and implications of mitochondrial rearrangements on bryozoan evolution.

2 Methods

2.1 Taxon selection and sample preparation

19 bryozoan specimens sequenced for this study were collected globally by several bryozoologists (Table 1) and stored in 70–90% ethanol. Small fragments without visible contaminants (e.g. algae, other bryozoans or invertebrates) were isolated with a sterile scalpel for DNA isolation (~25 mg tissue per sample). Growing tips (distal ends in adeonids) or growing edges (in encrusting forms) were preferentially selected for isolation due to an increased chance of sampling live tissue. Morphological vouchers both retained in ethanol and dried were saved whenever possible, the latter was also used for Scanning Electron Microscopy (SEM). Additional sequences (17 taxa) were provided by collaborators or downloaded from Genbank (Table 1 and Appendix Table 1).

Table 1: Information of all unpublished taxa included in this study. Taxa downloaded from Genbank are not included here (Appendix Table 1). More precise location (if any) is found in the figure text with the voucher SEM's in the Appendix Figure 51-84. Sequencer: MNH = Marianne Nilsen Haugen (this study), EE = Emily Enevoldsen, AW = Andrea Waeschenbach and RJSO = Russell J. S. Orr

Species name	ID number	Collected by/Identified by	Date of collection	Location	Sequenced by
Adeona sp.	BLEED298	Phil Bock	03.12.2005	Australia	MNH
Adeonella calveti	BLEED38	Shipboard party/ Björn Berning	20.08.2006	Algeria	MNH
Adeonella pallasii	BLEED39	Katarina Achilleos	24.06.2016	Cyprus	MNH
Adeonellopsis japonica	BLEED49	Masato Hirose	11.10.2016	Japan	MNH
Adeonellopsis pentapora	BLEED50	Masato Hirose	27.06.2016	Japan	MNH
Adeonellopsis sp. 1	BLEED48	Abby Smith/ Thomas Schwaha	14.10.2016	New Zealand	MNH
Adeonellopsis sp. 2	BLEED301	Phil Bock	24.11.2005	Australia	MNH
Arachnopusia unicornis	BLEED221	Abby Smith	11.03.2011	New Zealand	MNH
Bitectipora retepora	BLEED180	Dennis Gordon	11.04.2015	New Zealand	MNH
Chiastosella sp.	AW459	-	-	-	AW
Chiastosella watersi	BLEED56	Dennis Gordon	20.05.2015	New Zealand	MNH

Cornuticella taurina	BLEED199	Dennis Gordon	20.05.2015	New Zealand	MNH
Costaticella bicuspis	BLEED103	Dennis Gordon	-	New Zealand	MNH
Cryptosula pallasiana	NZ011	-	-	-	AW
Escharoides angela	BLEED59	Dennis Gordon	28.03.2011	New Zealand	MNH
Euoplozoum sp.	BLEED322	NIWA	03.03.2011	New Zealand	RSJO
Eurystomella foraminigera	BLEED135	Dennis Gordon	02.2015	New Zealand	RJSO
Fenestrulina sp.	BLEED20	Kamil Zágoršek	-	South Korea	MNH
Laminopora contorta	BLEED373	Peter Wirtz/ Björn Berning	15.10.2015	Cape Verde	RJSO
Margaretta barbata	BLEED99	***Removed due to contamination.***			MNH
Micropora sp.	BLEED192	NIWA	11.04.2015	New Zealand	RJSO
Microporella ordo	BLEED64	NIWA	28.03.2011	New Zealand	MNH
Microporella sp.	BLEED387	Kamil Zágoršek	20.08.2015	China	EE
Orthoscuticella innominata	BLEED201	Dennis Gordon	20.05.2015	New Zealand	MNH
Oshurkovia littoralis (previously *Umbonula littoralis*)	-	-	-	-	AW
Pentapora foliacea	AW267	-	-	-	AW
Phidoloporidae indet.	AW006	-	-	-	AW
Reptadeonella violacea	BLEED41	Roland Melzer/ Björn Berning	15.03.2015	Croatia	MNH
Reteporella ligulata	AW286	-	-	-	AW
Steginoporella neozelanica	BLEED315	NIWA	05.07.2009	New Zealand	RJSO
Telopora watersi	BLEED139	Dennis Gordon	11.02.2015	New Zealand	MNH
Thalamoporella sp.	BLEED374	Judith Brown/ Björn Berning	06.09.2013	St. Helena	RJSO

2.2 DNA isolation and sequencing

Total genomic DNA (gDNA) was extracted using the DNeasy Blood & Tissue kit (QIAGEN), following the manufacturer's protocol, with the following modifications: Eluted once with 50 µl and then a second time with 100 µl AE (Elution buffer) to maximize DNA quantity, and these two were later pooled if needed (if DNA yield was low in 50 µl and additional yield was present in 100 µl). Colony fragments too small to remove from ethanol for drying were rinsed in PBS buffer prior to extraction. All samples were homogenized with the supplied lysis buffer (Qiagen) using a pestle. After isolation, a NanoDrop spectrometer (Thermofisher Scientific) was used for quantification and qualification of DNA yield.

Before further processing, purification of DNA was done, if needed, using Genomic DNA Clean & Concentrator™-10 (Zymo research). Quantification of DNA concentration was established using Qubit dsDNA BR Assay Kit. Verification of DNA concentration was checked using 1% agarose gel-electrophoresis with the nucleic acid dye GelRed. Lastly, DNA concentrations were normalized in order to gain an equal sequencing output: Two samples contained 0.1µg gDNA in 55 µl EB buffer (Qiagen), and the remaining samples contained 0.5µg in 55 µl EB buffer.

Nineteen samples (Table 1) were submitted to The Norwegian High-Throughput Sequencing Centre (NSC) at the University of Oslo in April 2017, where sample preparations and library prep were also carried out. Sequences were sequenced on an Illumina high-throughput sequencing platform (Hiseq 4000) with 150 bp paired-end reads and 350 bp insert size.

2.3 Sequence assembly

Quality of the raw sequence data retrieved from high-throughput sequencing was checked with FastQC (Andrews, 2010). Adaptors, low-quality bases and overrepresented sequences were removed using TrimGalore v.0.4.4 (Krueger, 2015). A thorough examination of which bioinformatic tool to use for assembly was conducted (see discussion) with SPAdes (Bankevich et al., 2012) found as the preferable choice. Reads were hence assembled using SPAdes 3.11.1 with k-mer length of 33, 55, 77, 99 and 121 (see Appendix Figure 1), using the Abel server at the University of Oslo. The assembly was polished and finished using Pilon, which attempts to correct single base differences and small indels, closing of gaps and identification of local misassemblies (Walker et al., 2014). The mitochondrial genome and ribosomal operon were

extracted from the assembly using CLC workbench 7 (Qiagen, Hilden, Germany) by creating a personal database of bryozoan sequences followed by BLAST (Basic Local Alignment Search Tool). Extracted sequences were then reconfirmed against the NCBInr database using MegaBLAST.

2.4 Gene annotation and alignments

The mitochondrial genomes were submitted to MITOS (Bernt et al., 2013) for annotation using the invertebrate mitochondrial genetic code, and ribosomal RNA was annotated using RNAmmer (Lagesen et al., 2007). MAFFT version 7 (Katoh & Standley, 2013) was used to align each of the separate 17 genes from all taxa (both those generated in this study and all orthologous sequences acquired from collaborators and Genbank). For protein-coding genes (*ATP6, ATP8, COX 1-3, CYTB, NADH 1-6* and *NADH4L)* model G-INS-i, which incorporates the possibility of global homology, was used to align amino acids. The Q-INS-i model, considering secondary RNA structure, was utilized for rRNA genes (18S, 28S, rrnL, rrnS). In both cases, default parameters were used. The single gene-alignments were improved manually using Mesquite Version 3.2 (Maddison & Maddison, 2001). Poorly aligned positions and divergent regions in each gene alignment were subsequently excluded using Gblocks (Castresana, 2000) with least stringent parameters. Gene-alignments were then concatenated using Catfasta2phyml.pl (https://github.com/nylander/catfasta2phyml). Three different datasets were created: 1) 18S + 28S, 2) mitochondrial genome and 3) 18S + 28S + mitochondrial genome. Datasets 1 and 2 were created to determine a congruent signal (topology) between the rRNA and mitochondrial genes (Appendix Figure 5 and 4).

2.5 Mitochondrial genomes

Mitochondrial genomes were manually closed with Mesquite after identifying sequence overlap at the 5' and 3' end using blast2 through NCBI. Seven mitochondrial genomes remained unclosed (no sequence overlap), and specific PCR primers were designed with the purpose of closing these (Appendix Table 3) (see also discussion). For primer design, Primer 3 Plus and NCBI primer blast were used (Untergasser et al., 2007; Ye et al., 2012), and OligoCalc (Kibbe, 2007) to check self-complementarity and to calculate primer annealing temperature (Tm). PCR was performed with DreamTaq DNA polymerase or Phusion high-fidelity DNA polymerase (Thermofisher Scientific) in the presence of 2.5% DMSO; and PCR was subsequently

conducted. The PCR conditions used are outlined in Table 2 in the Appendix. PCR products were examined using gel-electrophoresis (outlined previously) and cloned, using Zero Blunt® TOPO® PCR Cloning Kit. The PCR product was transformed into the chemically component *E. coli* cells, following the manufacturer's protocol. After 24 hours, 36 colonies were picked and subsequently amplified with PCR using the vector primers T3 and T7, quality checked with gel-electrophoresis, and sequenced with sanger sequencing at GATC Biotech (Germany). The cloned sequences were firstly extended with the raw Illumina reads using Tadpole (K-mer 33-121, part of the bbtools package: https://jgi.doe.gov/data-and-tools/bbtools/) before being used as "trusted contigs" with the unclosed mitochondrial genome in a new SPAdes assembly.

2.6 Phylogenetic analysis

ML were primarily run using Randomized Axelerated Maximum Likelihood (RAxML) v8.0.26 (Stamatakis, 2014) on all 17 single genes (four with nucleotides and 13 with amino acids) with 100 heuristic topology searches and up to 1000 bootstrap replicate searches. The RAxML "AUTO" parameter was used to establish the evolutionary model with the best fit. MtZoa and MtArt were the best evolutionary substitution models for protein coding genes. Ribosomal genes rrnL, rrnS, 18S and 28S were all best supported by the general time reversible (GTR) model. The final concatenated datasets were subsequently inferred with separate partitions for each of the 17 genes using the optimal evolutionary models for each as defined by RAxML, with 100 topology searches and 500 bootstrap searches under a gamma distribution model.

Taxa with unstable phylogenetic affinities were identified and removed using RogueNaRok based on evaluation of a 70% majority rule consensus tree (Aberer et al., 2013).

BI was performed using a modified version of MrBayes v3.2 (Huelsenbeck & Ronquist, 2001) incorporating the MtZoa evolutionary model (https://github.com/astanabe/mrbayes5d). The dataset was executed, as before, with 17 gene partitions under a separate gamma distribution. Two independent runs, each with three heated and one cold Markov Chain Monte Carlo (MCMC) chain, were started from a random starting tree. The MCMC chains were run for 40,000,000 generations with trees sampled every 1,000th generation. The posterior probabilities and mean marginal likelihood values of the trees were calculated after the burn-in phase, which was determined from the marginal likelihood scores of the initially sampled trees. The average split frequencies of the two runs were < 0.01, indicating the convergence of the MCMC chains.

2.7 Ancestral state reconstruction

An ML ancestral state reconstruction analysis was carried out in R (R Development Core Team, 2013) using the APE package, version 5.1 (Paradis, Schliep, & Schwartz, 2018) in order to investigate the probability of the path of frontal shield evolution, given my taxon sampling and phylogenic tree. Prior to the analysis, I pruned Cyclostomata and Ctenostomata from my tree, as they do not carry the trait of interest. Four character states: anascan, spinocystal, umbonuloid and lepralioid, were considered under two different transition models: An equal rates model, where all transitions between all character states are allowed and have the same rate, and a constrained model, where only the following transitions were allowed: anascan → spinocystal → umbonuloid → lepralioid (rate is equal for all permissible transitions). The constrained model was designed according to previous outlined hypotheses of the most probable way of frontal shield development, given observations from the fossil record and developmental models of zooid ontogeny. Note that the equal rates model and the constrained model each have only one parameter, the only difference being the number of permissible transitions between states in the two models. The relative fit of the two alternative models were assessed using the Akaike information criterion corrected for small samples (AICc) (Burnham & Anderson, 2003).

3 Results

3.1 Sequences and alignments

For this study, 18 new bryozoan taxa were successfully sequenced (one taxon was removed from the dataset due to contamination) (Table 1). Next-generation sequencing and a standard bioinformatic pipeline provided 11 closed mitochondrial genomes. Additional PCR, cloning and bioinformatic work gave two additional closed mitochondrial genomes, with five remaining unclosed. The targeted phylogenetic markers, namely, 15 mitochondrial genes and two rRNA genes, were annotated in the majority of taxa with the exceptions reported in Table 4 in the Appendix.

3.2 Phylogenetic relationships

BI and ML approaches yielded identical tree topologies and I present the inferred tree with ML bootstrap support values and BI posterior probability (Figure 1). I consider the following support values based on bootstrap percentage (BP) and posterior probability (PP): high support >90 BP/1.00PP, moderate support >80 BP/>0.97PP and low support >50 BP.

The individual ML and BI trees and all single gene trees (ML) are found in Figure 2–22 in the Appendix.

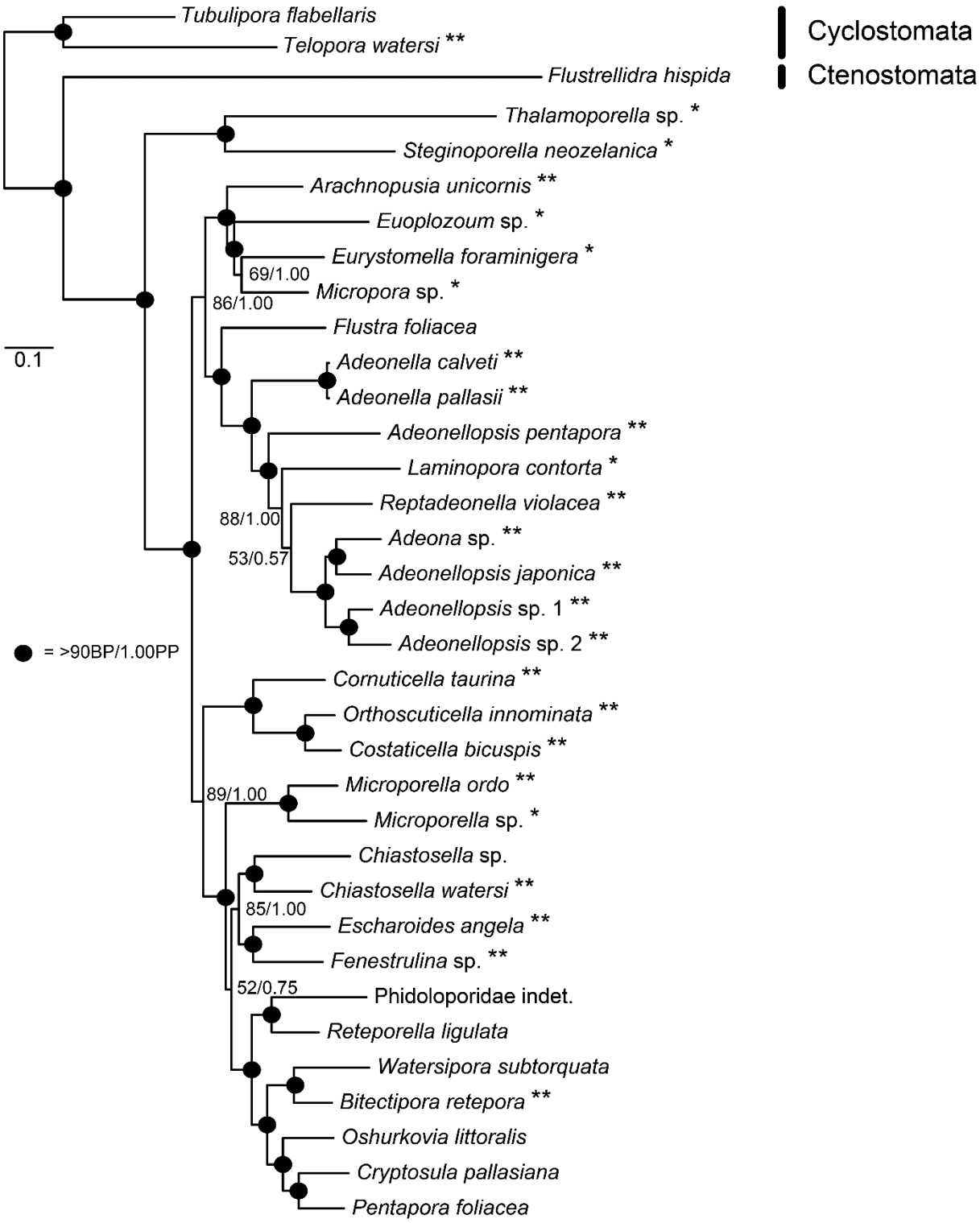

Figure 1. ML and BI tree topology of 35 bryozoan taxa. Numbers at the nodes refers to ML bootstrap support values (BP)/BI posterior probabilities (PP). Closed circles represent highly supported BP and PP values = >90BP/1.00PP. The branch length scale indicates number of substitutions per site as indicated from ML topology (note that branch lengths are highly similar for the BI analysis (Appendix Figure 3). Two asterisks indicate taxa that I handled and sent for sequencing, while a single asterisk indicates taxa that were sequenced by other members of BLEED.

The earliest diverging taxa are the fully supported cyclostome outgroup taxa *Telopora watersi* and *Tubulipora flabellaris,* which form a sister relationship with the ctenostome *Flustrellidra hispida*. Subsequent is the highly supported (98BP/1.00PP) monophyletic cheilostome ingroup.

The most basal cheilostome lineage is formed by two anascan taxa (see Figure 2 for color codes) with full support: *Thalamaporella* sp. and *Steginoporella neozelanica,* which are sister to, and excluded from the highly supported (99BP/1.00PP) main cheilostome assemblage.

The main cheilostome assemblage is divided into two major clades which both are moderately supported. The first clade (86BP/1.00PP) encompasses both anascans and ascophorans, leading to polyphyly of the two informal suborders, Anasca and Ascophora. This clade is further divided in to clades: one that incorporates two anascan taxa, *Euoplozoum* sp. and *Micropora* sp. accompanied by two ascophoran taxa, *Arachnopusia unicornis* and *Eurystomella foraminigera,* and the second clade with the anascan *Flustra foliacea* placing basal to Adeonidae with high support (96BP/1.00PP). The adeonids, represented by the genera *Adeona, Adeonellopsis, Reptadeonella, Laminopora* and *Adeonella,* form a fully supported monophyletic clade. On the other hand, the now discarded family Adeonellidae, with the genera *Laminopora* and *Adeonella,* is found to be paraphyletic.

The other large, moderately supported, cheilostome clade is comprised solely of ascophoran taxa, in which the fully supported clade of *Orthoscuticella innominata, Costaticella biscuspis, Cornuticella taurina,* all members of the family Catenicellidae, is sister to the remaining large clade of ascophorans with moderate support (89BP/1.00PP). Catenicellidae belongs to the superfamily Catenicelloidea, to which the family Eurystomellidae, with *E. foraminigera* (in a more basal position) also belongs, leading to polyphyly of this superfamily.

Next, two species of the genus *Microporella* are excluded, with full support, from the inclusion of the remaining clade of ascophorans. In the next large clade to diverge, albeit with low support (52BP/0.75PP), *Chiastosella watersi, Chiastosella* sp., *Escharoides angela* and *Fenestrulina* sp., are found to be sister to the fully supported clade of Phidoloporidae indet., *Reteporella ligulata, Watersipora subtorquata, Bitectipora retepora, Oshurkovia littoralis, Cryptosula pallasiana* and *Pentapora foliacea*.

Watersipora and *Bitectipora*, both within the same superfamily Smittinoidea, form the sister clade to *O. littoralis*, *C. pallaisana* and *P. foliacea* with full support. *Pentapora foliacea* is also currently assigned to the superfamily Smittinoidea making this superfamily paraphyletic.

3.3 Frontal shields distribution

Spinocystal, umbonuloid and lepralioid frontal shields are all found to be polyphyletic (Figure 2). Note that gymnocystal frontal shields are not represented in the phylogeny, and are hence not considered further. Based on this topology and the taxa present in the phylogeny, both the spinocystal and the lepralioid shields have evolved independently at least twice and the umbonuloid shield has evolved independently at least four times. This consequently implies that the informal Ascophoran infraorders Acanthostegomorpha, Lepraliomorpha and Umbonulomorpha are all polyphyletic.

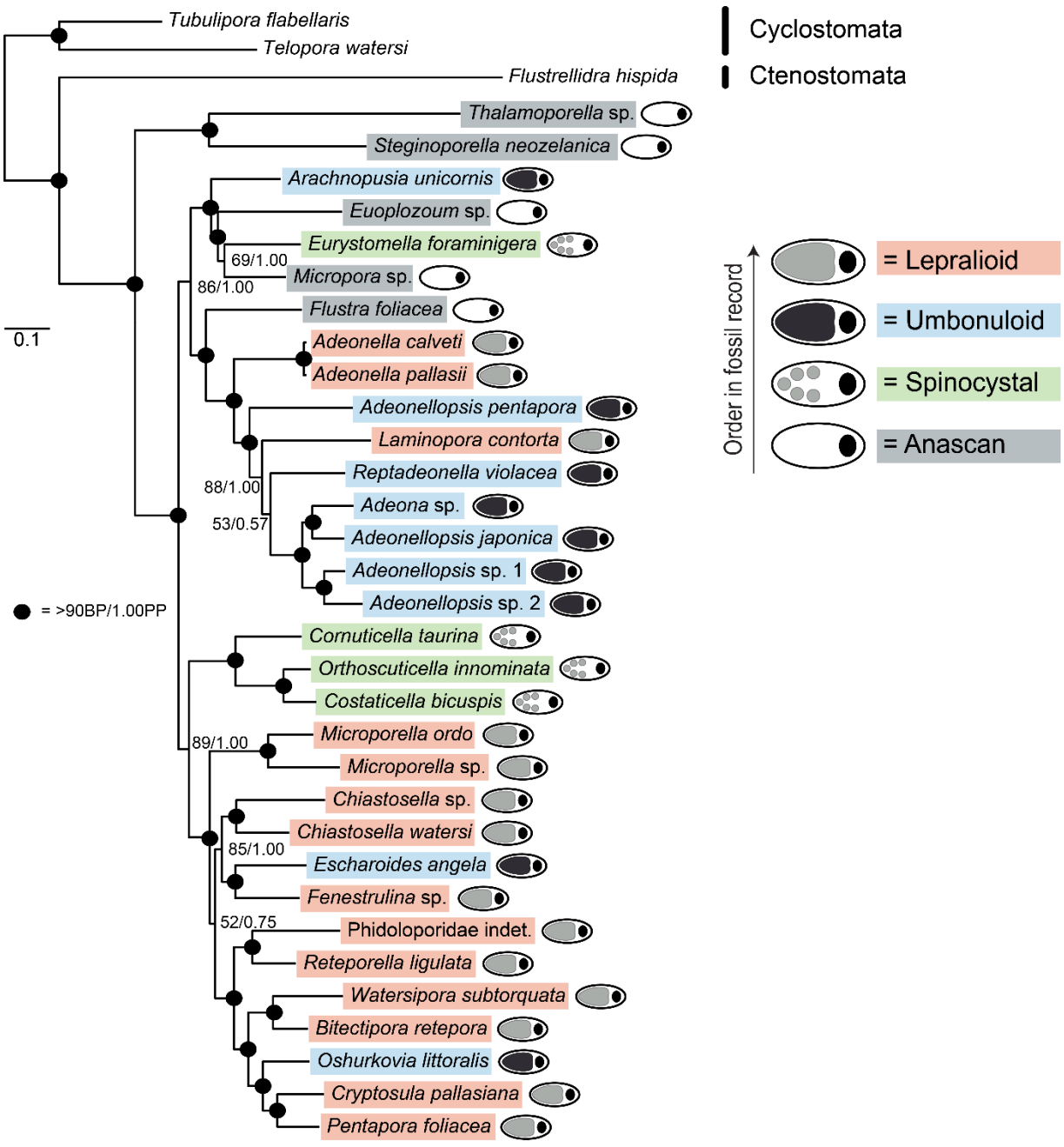

Figure 2. The phylogenetic distribution of frontal shield types integrated in the same tree topology as found in Figure 1. Taxa with lepralioid shields are highlighted in red, umbonuloid shields in blue, spinocystal shields in green and anascan-grade taxa are highlighted in grey.

3.4 Ancestral state reconstruction

Table 2. Parameters, Log Likelihood, AICc and AICc weight for the two considered models for the ancestral state reconstruction analysis. The constrained model was the preferred model as indicated by AICc and AICc weight.

Model	Parameters (K)	Log Likelihood	AICc	AICc weight
Equal rates	1	-31.4677	-60.8022	0.0007
Constrained	1	-38.7416	-75.3499	0.9993

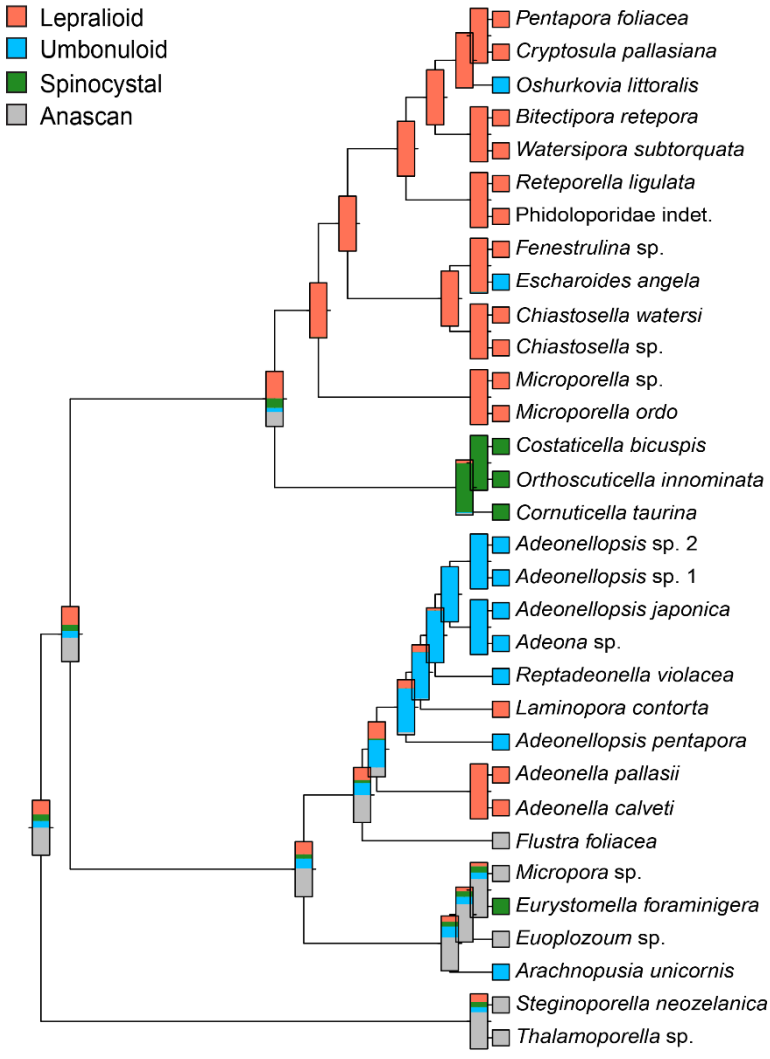

Figure 3. Ancestral state reconstruction of frontal shield types with four different states: Anascan-grade in grey, spinocystal in green, umbonuloid in blue and lepralioid in red. The ancestral states given at each internal node is given as a likelihood ratio that adds to 1, and the different colors indicate the four different states' likelihood values, respectively. This tree is based on the ML tree topology and the constrained model of ancestral state reconstruction.

The constrained model was the preferred model, as this model was 14.6 AICc units better than the equal rates model, and hence chosen for this analysis. Given the topology and frontal shield states found at the terminal nodes, this analysis provides the likelihood of the character states at the internal nodes. For the basal lineages, the most likely ancestral state is anascan, but also lepralioid has non-negligible support, while the spinocystal and umbonuloid states are less supported. For the clade with *Flustra foliacea* and the adeonids, the most likely ancestral state is anascan, but some support is also present for all the other three states. Umbonuloid is the most likely ancestral state for adeonids. For the second large ascophoran clade, the most likely ancestral state is found to be lepralioid.

3.5 Mitochondrial size and rearrangements

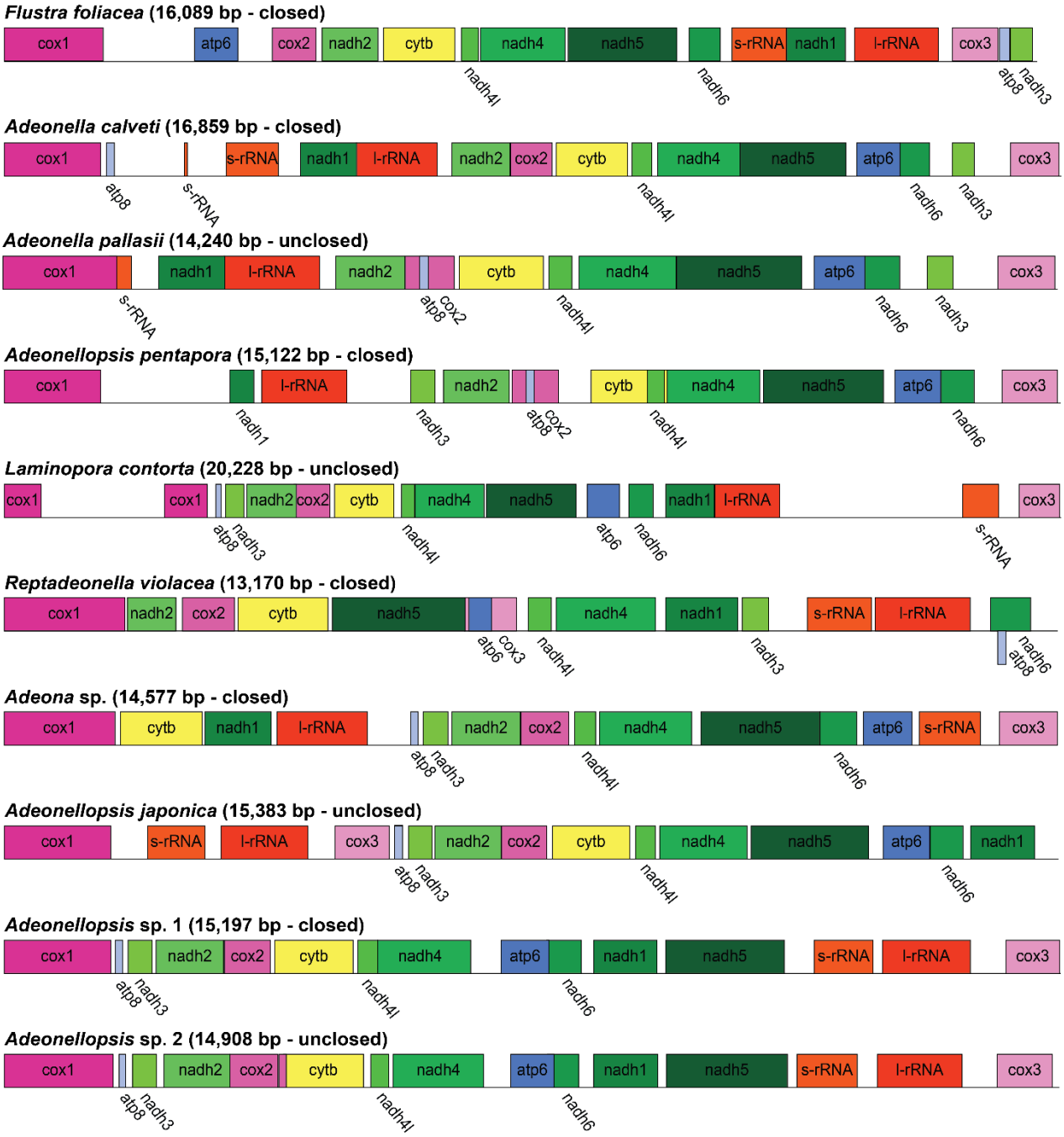

Figure 4. Mitochondrial gene order in *Flustra foliacea* and the adeonids. All mitochondrial genomes are arranged to start with *COX 1*. tRNAs and introns are removed for better visualization. Box size and placement represent gene length and position respectively, and the order of taxa follows that of the tree topology in Figures 1 and 2. The only missing gene among these taxa is s-rRNA (rrnS) from *Adeonellopsis pentapora*.

A few mitochondrial gene blocks are retained among the adeonids and its sister taxon in the current phylogeny, *Flustra foliacea* (Figure 4). For instance, *NADH4L* followed by *NADH4* and *NADH5* are found in adeonids and *F. foliacea*, with the exception of *Reptadeonella violacea*. Note that this gene block is also found in 15 of the remaining 25 taxa (see Figure 51–84 in the Appendix for all 35 mitochondrial genomes). *ATP6* and *NADH6* are also found clustered in eight of the ten selected taxa (Figure 4), where *R. violacea* and *F. foliacea* are the exceptions. *COX1* and *COX3* are found together in all except *R. violacea* and *A. japonica* (Figure 4), whereas in the remaining 25 taxa this order is only present in three taxa: *Chiastosella watersi, Arachnopusia unicornis* and *Euoplozoum* sp. (Appendix Figure 57, 78 and 79).

Despite the above-mentioned resemblances, the majority of gene arrangements in both the selected taxa (Figure 4) and the remaining taxa (Appendix Figure 51–84), are seemingly random and without any clear congruence to species evolution.

Considering the 25 closed mitochondrial genomes used in this study (13 from this study and 12 from collaborators and Genbank), mitochondrial genome length varies considerably. The shortest bryozoan mitochondrial genome currently known is the genome of the ctenostome *Flustrellidra hispida* which is 13026 bp (Genbank accession: NC_008192). Of the newly sequenced taxa in my study, the shortest mitochondrial genome found is *Reptadeonella violacea* with 13170 bp. The largest bryozoan mitochondrial genome reported to date is from *Celleporella hyalina* (Genbank accession: NC_018344, not included in this study) with 17265 bp, and the largest found in this study is *Adeonella calveti* with 16859 bp. Genomes of the newly sequenced taxa are found within the range of other reported bryozoan genomes where the variation is likely due to non-coding intergenic regions. Note that both the shortest and longest genomes in my study are found within family Adeonidae.

4 Discussion

4.1 Phylogenetic relationships

The available sequence data for Cheilostomata has been substantially increased with my study, both in terms of the number of newly sequenced taxa as well as in the number of genes analyzed. This gives us an opportunity to investigate the phylogenetic relationships among cheilostome bryozoans where the inferred topology is largely fully or highly resolved. Occasional lower support for some taxon relationships, as well as differences in support between both methods (ML and BI), was only found where taxon sampling might be low and where taxa were found to have unstable phylogenetic affinity.

The most comprehensive cheilostome bryozoan molecular phylogenies to date are found in Waeschenbach et al. (2012) and Orr et al. (2018), using seven and six genes and 32 and 33 cheilostome taxa, respectively. Of the 32 taxa used in Waeschenbach et al. (2012), seven taxa are represented in both phylogenies (including the ctenostome *Flustrellidra hispida*) in addition to five genera represented by different species. Orr et al. (2018) and this study accommodate 13 of the same taxa (including *F. hispida*), seven of which were sequenced for this study and the remaining six were provided by collaborators or downloaded from Genbank. The phylogenetic topology presented here is congruent with those in Waeschenbach et al. (2012) and Orr et al. (2018) in a broad sense. However, statistical support for relationships is substantially improved here compared to the above-mentioned studies, and increased taxon sampling within the adeonids allows us to study the evolution of the frontal shield and mitochondria within this bryozoan family for the first time.

Among the earliest divergent clades, a comparable topology is found in all three phylogenies. While anascans are the earliest diverging cheilostomes, neither Anasca nor Ascophora, are monophyletic, corroborating earlier results (Dick et al., 2009; Fuchs, Obst, & Sundberg, 2009; Knight et al., 2011; Waeschenbach et al., 2012).

The earliest-known strictly umbonuloid-shielded genus is the Santonian (86.3–83.6 mya) *Staurosteginopora* (Voigt, 1991; Gordon, 2000), which belongs to the family Arachnopusiidae, here represented by the extant taxon *Arachnopusia unicornis*. *Arachnopusia unicornis* is here found to be sister to the anascan *Euoplozoum* sp., the spinocyctal *Eurystomella foraminigera* and the anascan *Micropora* sp. As Uttley and Bullivant (1971) remarked, the species *A.*

unicornis is subject to "bewildering variation" particularly with regard to the appearance of the frontal shield (Gordon, 1989). In addition, this species has even been attributed to *Cribilina* (Hincks, 1881) and to the family Cribrilinidae (Levinsen, 1909). According to Levinsen (1909), the frontal shield in *Arachnopusia* "is formed by the coalescence of a number of branched, originally hollow, and later partially solid spines which springs from the lateral wall". This cribrimorph (spinocystal) frontal shield development is the reason why Levinsen included the genus among the Cribilinidae. However, Gordon (2000) found the distinct ring scar typical for umbonuloid shields on the underside of the frontal shield of *A. unicornis*, and hence placed the genus with the umbonuloids. The turbulent taxonomic history of this genus reflects the considerable morphological variation evident in the oldest family of Umbonulomorpha (Gordon, 1993) and hence may explain the basal position of this umbonuloid taxa. However, Knight et al. (2011) also found *A. unicornis* to have a basal position in a clade otherwise containing species from the suborder Flustrina. This said, a thorough examination of the development of the frontal shield accompanied by DNA sequencing is needed to validate the true nature of *Arachnopusia's* frontal shield and phylogenetic positioning, respectively.

The phylogenetic positioning of family Adeonidae has never been examined with molecular data, and my results suggest that the adeonids are sister to *Flustra foliacea* which is a less calcareous, erect, bilaminar anascan. However, previous molecular studies have already implied numerous other taxa in close approximation to *F. foliacea* (Knight et al., 2011; Waeschenbach et al., 2012; Orr et al., 2018), indicating that taxon sampling basal to the adeonids must be substantially improved in future studies to shed light on the family's phylogenetic positioning.

The second large cheilostome clade, which solely comprises of ascophoran taxa, (Figure 1), has a topology which is similar to that of Waeschenbach et al. (2012) and Orr et al. (2018). One of the two lineages to diverge first, are three members of the monophyletic family Catenicellidae, which are typified by erect jointed colonies and spinocystal frontal shields with (*Costaticella*) or without (*Orthoscuticella*, *Cornuticella*) costae and having large pseudopores. Note, however, that *E. foraminigera* currently belongs to the same superfamily (Catenicelloidea) but it has a rather basal position in my tree, indicating that Catenicelloidea is not a monophyletic taxon.

As found by Orr et al. (2018), the genera *Fenestrulina* and *Microporella*, which previously have been placed in the same family (Taylor & Mawatari, 2005), are not monophyletic suggesting the separation of the family Microporellidae. My result is congruent with this, although taxon

sampling for these genera is low. Low taxon sampling is also reflected in the difference in topology between this study and Orr et al. (2018). Here, *Microporella* is excluded from and sister to the remaining ascophoran clade, whereas in Orr et al. (2018), *Fenestrulina* is excluded from the remaining ascophoran clade.

Given the topology here, we find that superfamily Smittinoidea (genera *Pentapora*, *Watersipora* and *Bitectipora*) is paraphyletic. Additionally, *Watersipora*, *Pentapora* and *Bitectipora* have a smittinoid ovicell type (or lepralielliform *sensu* Ostrovsky (2013)), which in this tree topology therefore is found to have evolved independently twice.

Additional to the above mentioned molecular phylogenetic studies, a handful of others have been conducted, although with only one to three genes and few taxa (Dick, Freeland, Williams, & Coggeshall-Burr, 2000; Hao, Li, Sun, & Yang, 2005; Fuchs et al., 2009; Jiao, Yang, Zhao, Shi, & Hao, 2009; Tsyganov-Bodounov, Hayward, Porter, & Skibinski, 2009). A degree of consensus has emerged from these studies: Ctenostomata are paraphyletic to the inclusion of the Cheilostomata, Ascophora are polyphyletic with Flustrina being closely associated with Hippothoomorpha, and Umbonulomorpha form a clade with the Lepraliomorpha. However, conflicting results are evident due to a lack of phylogenetic signal or contaminant sequences as found by Waeschenbach et al. (2012). This study is in accordance with the consensus of Ascophora being polyphyletic. Additionally, here I find Flustrina, Umbonulomorpha, Acanthostegamorpha and Lepraliomorpha to all be polyphyletic, indicating that higher order systematics should not be based on a single morphological trait, like the frontal wall/shield type.

4.2 Adeonids

A main goal of my study was to resolve the questions regarding the controversial interrelationships of the members of the family Adeonidae, which has been discussed for many decades by e.g. Busk (1884); Hincks (1887); Gregory (1893); Levinsen (1909); Waters (1912); Bassler (1953); Harmer (1957); Cook (1973); Hayward (1983); Lidgard (1996).

The family name Adeonidae was formally introduced by Busk (1884) while Gregory (1893) established the family Adeonellidae by arguing that the genus *Adeonella* did not belong in Adeonidae because of the structure of the median pore and primary orifice, which differs significantly from other members of Adeonidae. Harmer (1957), who made a subsequent major contribution towards an understanding of the morphology of *Adeonella*, and of the superficially

similar *Adeona*, combined them within the single family Adeonidae. Later, Cook (1973) conducted a comparative morphological study of both adeonid and adeonellid genera, and established conclusively that this large grouping is at least diphyletic, and that the Adeonellidae (genera *Adeonella* and *Laminopora*) differs radically from the Adeonidae (*Adeona*, *Adeonellopsis*, *Reptadeonella* and *Bracebridgia*) in the mode of development of the calcified frontal wall of the autozooid, and in the homology of the frontal pore complex. However, Cook (1973) also anticipated that, with further studies on adeonids and other cheilostome taxa, the ontogeny of the frontal shield and protrusion apparatus may prove to be phylogenetically insignificant.

The earliest adeonid species found, belong to the genera *Adeonellopsis*, *Bracebridgia*, *Meniscopora*, *Poristoma* and *Schizostomella*, and are reported from the early Eocene (Ypresian), dating back between 56 and 47.8 million years. However, if it can be verified that the genus *Anarthropora*, which is currently placed in the Exechonellidae, also belongs to the Adeonidae, the fossil record of the family extends back to the Late Cretaceous (Danian 66–61.6 mya). The species in these genera are all likely to have an umbonuloid frontal shield (B. Berning, pers. comm., 2018). The majority of modern adeonids are found in the tropical to subtropical Indo-Pacific and South Atlantic, and the family has in recent years also gained attention, as a number of new species have been erected, and several known species revised (Grischenko & Mawatari, 2002; Amui, 2005; Rosso & Novosel, 2010; Almeida, Souza, Sanner, & Vieira, 2015; Hirose, 2016). Despite this attention, the molecular phylogenetic positioning of adeonids have never been examined before. The sequence data contributed by this study can confirm the monophyly of the family and its sister relationship to the anascan *F. foliacea.* However, I anticipate that this sister relationship will become more distant when more cheilostomes from this basal region are sequenced. Additionally, in my topology (Figure 1), the four sequenced *Adeonellopsis* taxa do not group together, suggesting that the genus *Adeonellopsis* is polyphyletic. The topology I inferred therefore suggests that *Reptadeonella*, *Laminopora* and *Adeona* are descendants of an *Adeonellopsis*-like ancestor. The first occurrence of genus *Adeonellopsis* dates back to at least the Ypresian (56–47.8 mya), and *Reptadeonella* to at least the Burdigalian (20.43–15.97 mya), *Laminopora* to the Miocene (23–5.3 mya) and *Adeona* to the Oligocene (33.9–23 mya), according to the Paleobiology Database (data accessed 01/08/18). Note that the inferred topology does not conflict with the available chronological fossil observations of these genera.

The assumptions drawn by Cook (1973) are consistent with my inference based on molecular sequence data. My study unequivocally rejects the monophyly of the two families (Adeonidae and Adeonellidae) and thus, the two types of frontal shield, umbonuloid and lepralioid do not form monophyletic clades within the family Adeonidae. However, *Laminopora contorta* dissected the two families, Adeonidae and Adeonellidae resulting in the paraphyly of both. This enforces the importance of taxon sampling and future studies should hence ideally include a larger number of taxa, especially other representatives of *Laminopora* and other unsampled adeonid genera like *Triporula, Bracebridgia, Kubaninella, Anarthropora* or *Dimorphocella* to verify the conclusions drawn here. Nonetheless, this study shows the frontal shield to be a poor morphological character for inferring family level taxonomy of the adeonids. However, frontal shield types currently remain consistent within genera.

4.3 Models for frontal shield evolution

The evolution of a calcified frontal shield is thought to be one of the main drivers leading to the great flourishing of cheilostome diversity in the Late Cretaceous (Gordon & Voigt, 1996). Multiple morphological models for evolution and development have been proposed (Gordon & Voigt, 1996; Gordon, 2000), and our current understanding of frontal shield evolution are mostly based on these models, supplemented by molecular studies such as that of Dick et al. (2009); Knight et al. (2011).

As mentioned in the introduction, lepralioid frontal shields are inferred to have derived from Umbonulomorpha by loss of the umbonuloid component of the frontal shield, leaving a cryptocystal frontal shield of interior wall. Both these shield types, umbonuloid and lepralioid, provide similar calcified ‘roofs’ over the body cavity, but differ in the pattern and sequence of skeletal morphogenesis, and in geometric relationships to epithelia and coelomic chambers (Lidgard et al., 2011). Sandberg (1977) pointed out that the only way to discriminate between these two major shield morphologies is to examine the calcareous microstructure of the inner face of the calcareous shield. However, not only are umbonuloid and lepralioid shields problematic to disentangle from each other. Some taxa, like superfamily Catenicelloidea as found in this study, have structures that are characteristic of both spinocystal- and gymnocystal shield type, evidencing the evolutionary transition from the former to the latter by the reduction of the spinocystal component of the frontal shield in favor of the gymnocystal part. Hence, although mostly composed of a gymnocystal part, the frontal shields in *Eurystomella*

foraminigera and in the catenicellids (*C. taurina*, *O. innominata* and *C. bicuspis*) still contain a vestigial spinocystal component and are here as such considered as having a spinocystal frontal shield (Figure 2). For these reasons, a morphological examination of the interior of the skeleton and the frontal shield structures should be conducted for all included taxa in order to verify the nature of the trait and associated structures. However, due to time constraints, this was deemed to be outside the scope of this study.

Fossil evidence also suggests that umbonuloid shields arose in the Cretaceous prior to the appearance of lepralioid shields in the Paleogene (Gordon & Voigt, 1996). Thereafter, lepralioid frontal shields are believed to have evolved repeatedly from umbonuloid precursors. This hypothesis was explicitly tested by Knight et al. (2011) using five genes and 56 taxa, but their most robust dataset only consisted of three genes. Albeit with low support values and incongruent topologies between different datasets, the work by Knight et al. (2011) represents a big leap in our understanding of the molecular interrelationships of the different types of frontal shields. Knight et al. (2011) rejected the monophyly of three of the four types of frontal shield, the umbonuloid, gymnocystal and the lepralioid, confirmed with multiple independent origins of these, and they also confirmed the hypothesis of multiple origins of the lepralioid shield. I further examine the hypothesis of multiple independent origins of the represented different shield types, with an improved phylogeny inferred using a much greater number of genes. My results, validated by a topology with high statistical support, are congruent with the results from Knight et al. (2011), and I find all three represented shield types, umbonuloid, spinocystal and lepralioid polyphyletic.

A formal ancestral state reconstruction analysis was conducted in order to better understand the evolution of the different frontal shields represented in my study (Figure 3). The results indicate which of the four states, anascan, spinocystal, umbonuloid or lepralioid, are most likely at each of the internal nodes. Two models were tested: an equal rates model, where all transitions between the four states are permissible and have the same rate, and a constrained model, in which only the following transitions between frontal shields were allowed: anascan → spinocystal → umbonuloid → lepralioid. It was the constrained model that had the best relative fit according to the model's AICc scores, therefore, only the results from this model are discussed. I would like to stress, however, that the results from the models performing ancestral reconstructions are conditioned on the given phylogeny and the data on frontal shields at the branch tips. Taxon sampling may accordingly affect the estimated ancestral states on internal

nodes. Furthermore, these models do not consider other available evidence from the fossil record, information that may also have affected the estimated ancestral states.

At the root of the tree, all four states are present, but the state with the highest likelihood is anascan, as anticipated, as the first cheilostomes appearing in the fossil record were of anascan-grade. Further among the basal taxa, the dominant state is anascan, but the relative likelihood of being both spinocystal and umbonuloid is not negliable, but most likely have the states in *A. unicornis* and *E. foraminigera* evolved from an anascan somewhere along the branch from their most recent common ancestor.

Having an anascan state is most likely at the internal node for the clade of *F. foliacea* and the adeonids. This anascan have subsequently evolved an umbonuloid shield, giving rise to the adeonids. The lepralioid *Adeonella* and *Laminopora* have thereafter developed a lepralioid shield from an umbonuloid ancestor in accordance with the previous outlined hypotheses. As mentioned previously, the genus *Adeonellopsis* is in this topology polyphyletic, and presumably have the genera *Laminopora, Reptadeonella* and *Adeona* developed from an *Adeonellopsis*-like ancestor. Whether or not *Adeonella* are also descended from *Adeonellopsis*, which appears early in the fossil record, remains to be tested, but the results from this analysis indicate an umbonuloid ancestral state, which might suggest this scenario to be true, with the possibility that it could also be a different umbonuloid adeonid genus.

For the second large ascophoran clade, the internal node has a higher probability of being lepralioid. However, there is also a non-negligible probability for this ancestor to be anascan, which is more in accordance with the anticipated development of the spinocystal shield found in the catenicellid clade. From the next branching point, the ancestral states are solely lepralioid. Despite the presence of the two umbonuloid taxa, there is no support of having an umbonuloid ancestral state. This is contradictory to previous outlined hypotheses that lepralioid shields have developed from umbonuloid precursors. In this analysis, it seems as the umbonuloid shield found in *O. littoralis* and *E. angela* have originated independently from a lepralioid ancestor. However, the fossil record provides evidence for a much earlier occurrence of umbonuloid shields than of lepralioid shields (Gordon & Voigt, 1996), while also the ontogeny of zooids (sequence of formation of the skeleton, orifice and polypide) shows that taxa with a lepralioid frontal shield are derived (e.g. Cook, 1973).

Considering the given frontal shield distribution in this study, all three shield types have evolved independently at least twice, and the constrained model in the ancestral state

reconstruction analysis is favored, indicating that the hypothesized pathway of evolution is supported in this tree, with the present taxon sampling. However, with the appearance of the two umbonuloid taxa clustered within the large lepralioid clade, I open up for the possibility that other pathways of development are possible, despite the above-mentioned evidence. This, however, needs a deeper sampling and an increased investigation of both extant and fossil taxa to conclude further.

Bryozoans in general have a complex morphology with multiple morphological characters that are subject to a high degree of variation. We know for instance that variation in zooidal morphology is even observed in single colonies as a result of different environmental conditions or predation pressure (Jackson & Cheetham, 1990; Schwaninger, 1999; Yagunova & Ostrovsky, 2008; Lombardi, Cocito, Gambi, & Taylor, 2015). But, in bryozoology, we have little knowledge of the genetic basis of phenotypic expression, which adds to the difficulties of explaining the evolution and development of selected traits. Some things we do know: The development of a calcified frontal shield and the ascus are regarded as key innovations, presumably as a result of high predation pressure. Dick et al. (2009) investigated if the origin of these structures is historically contingent or not. Mirroring a common evolutionary scenario in Late Cretaceous taxa, leading from an anascan state zooid to one with a spinocystal shield and on to one with a largely gymnocystal shield and a well-developed ascus, they presented the case of such an evolutionary sequence in the extant bryozoan genus *Cauloramphus*, which may have taken less than 12 million years. They argue that the origin of these structures are highly likely with sufficient possibilities afforded by time. Parallel and convergent evolution of the frontal shield trait is also hypothesized by e.g. Cook (1973). This bulk of evidence, including results from Knight et al. (2011), indicate that frontal shields can, and already have, originated independently at multiple occasions, and hence may be relatively easily derivable.

To firmly establish whether or not frontal shields are a good taxonomical trait requires a deeper taxon sampling. Here I show that the three represented shield types are polyphyletic, and especially for the adeonids, I will argue that frontal shields are not a good taxonomical trait at family level. With a general high variation in bryozoan morphological characters, there are difficulties in determining which characteristics are important taxonomically. Calcified structures, like frontal shields, are easily preserved in fossils and have gained extensive attention as taxonomically important traits, but further questions are raised if these really are suitable for taxonomical inference. Soft parts like degenerated polypides (brown bodies),

parietal muscles and anus location, may also be morphological synapomorphies for Stenolaemata and Gymnolaemata and hence be important taxonomically (Waeschenbach et al., 2012). However, to investigate this, either living or histologically prepared specimens are necessary, and many bryozoans have proven to be difficult to cultivate under laboratory conditions making this approach tedious.

4.4 Mitochondrial gene order

An additional goal of this study was to examine the mitochondrial gene order, as the sequencing method used provide the mitochondrial genome of all sequenced taxa. However, some mitochondrial genomes remained unclosed, however with all genes present. An attempt was made to close these. First, I conducted a thorough examination of which bioinformatic tool to use for assembling the reads. With the advent of numerous different sequencing techniques, choosing the appropriate mitochondrial assembly method has proven to be important, as different methods may produce dissimilar results as found in a study by Velozo Timbó, Coiti Togawa, M. C. Costa, A. Andow, and Paula (2017). There are multiple assemblers available, and among these I tested SPAdes (Bankevich et al., 2012), Novoplasty (Dierckxsens, Mardulyn, & Smits, 2017), MitoBIM (https://github.com/chrishah/MITObim), Stampy (Lunter & Goodson, 2011) and Norgal (Al-Nakeeb, Petersen, & Sicheritz-Pontén, 2017). However, some of these programs require both high sequence coverage or the use of a reference genome to guide assemblies. With few bryozoan mitochondrial genomes sequenced, prior to this study, and with those available being taxonomically diverse, an optimal reference was unavailable. Also, use of a reference genomes can bias assemblies and even propagate errors (Velozo Timbó et al., 2017). SPAdes, a *de novo* assembler, proved to be the most successful, despite not being able to close all the mitochondrial genomes (11 of 18 became closed). *De novo* assembly may however be challenged by short read length, missing data, repetitive regions, polymorphisms and sequencing errors (Lischer & Shimizu, 2017). Repetitive regions were observed in the unclosed mitochondrial genomes, upon visualization of read mapping files, which could not be resolved with the 150PE Illumina reads. To close the remaining mitochondrial genomes, primer design and PCR was attempted with subsequent cloning due to unspecific annealing and multiple PCR products. The additional sequences allowed for two additional mitochondrial genomes to be annotated and closed. Nonetheless, genome skimming combined with an adequate bioinformatic pipeline has proven successful for phylogenetic purposes, increasing both taxa and resolution to the bryozoan tree. 13 closed mitochondrial genomes are a major

contribution for bryozoan sequence data which increases the number of sequenced mitochondria's of bryozoan species from eight (published) to 21 (22.08.2018). In addition, I add five partial mitochondrial genomes.

With a total of 35 mitochondrial genomes in this study, both complete and partial (18 provided by me and additional 17 from collaborators or Genbank), a goal of this study was, as mentioned, to investigate mitochondrial gene rearrangements. Gene order data has been suggested to contain useful phylogenetic information, since mitochondrial gene arrangements commonly remains unchanged over long periods of evolutionary time and may therefore retain the signal of ancient common ancestry (Boore et al., 1995; Boore & Brown, 1998). Boore (1999) stated that gene arrangements are relatively stable within major groups, but variable between them and hence have great potential for resolving phylogenetic relationships. However, in a later study by the same author (Mueller & Boore, 2005) they stated that previous conclusions were "early and with limited sampling" and hence concluded that "animal mitochondrial genomes possess unexpected diversity both in gene order and in the presence, extent, and distribution of noncoding sequence". Considerable variation in mitochondrial gene order has been documented in several different organismal groups including fungi (Aguileta et al., 2014), birds (Mindell, Sorenson, & Dimcheff, 1998), gastropods (Rawlings, Collins, & Bieler, 2001) and flatworms (Le et al., 2000), making it possible to question the utility of gene order as a phylogenetic character. Tandem duplication via slipped-strand mispairing, followed by a random deletion of genes are anticipated as mechanisms causing the rearrangements (Boore & Brown, 1998; Brugler & France, 2008).

Due to the lack of sequenced bryozoan mitochondrial genomes, evolution of mitochondrial gene order has not been much investigated in bryozoology. However, the number of sequenced mitochondrial genomes is now increasing, and studies are becoming possible. But, a broader taxonomic sampling is necessary for using mitochondrial gene order for phylogenetic analyses (Mindell et al., 1998), and for this reason only a comparison of *F. foliacea* and the adeonids are conducted in this study as seen in Figure 4. Yet, a presentation of the mitochondrial genome of all 35 taxa are found in the Appendix (Appendix Figure 51–84).

Without prior knowledge, one could anticipate that bryozoans would resemble patterns found in other invertebrates like corals (Lin et al., 2014) or annelids (Weigert et al., 2016), where gene order is highly conserved among closely related taxa and even among more distant related taxa. However, this seems not to be the case for bryozoans. Generally, bryozoans possess a high level

of mitochondrial gene rearrangements, especially between distant related taxa, but also among closely related taxa (R. Orr, pers. comm., 2018). But, as seen in Figure 4, some gene blocks are retained in the majority of the selected taxa. The retained block of *NADH4L + NADH4 + NADH5,* which is found in 24 of the 35 taxa in this study, is according to Weigert et al. (2016) found in the putative ground pattern of the entire grouping of Lophotrochozoa. This block is, however, the only block that is conserved to a certain degree within the total 35 bryozoan taxa included in this study.

If the phylogenetic relationship is close, one would expect certain gene blocks or positions to be retained. Here we find the block *COX1 + COX3* to be conserved for the phylogenetic grouping of *F. foliacea* and the adeonids. Additionally, there are large similarities in the two species of *Adeonella* and between *A.* sp. 1, *A.* sp. 2 and *A. japonica*. However, *A. pentapora* differ significantly from the other members of the genus *Adeonellopsis*. Four genes, *NADH1,* l-rRNA (rrnL), *ATP8,* and *COX2* have moved, and the amount of difference may reflect the polyphyletic relationship of this genus found in my topology. Being so different from the other members of the same genus, one would question if this specimen truly is an *Adeonellopsis.* Through SEM verification (Appendix Figure 28), this is however verified to be the case (B. Berning, pers. comm., 2018).

Despite the difference between *A. pentapora* and the other members of *Adeonellopsis,* it might seem like a certain conservation of gene order is evident at genus level. Species from different genera have a higher degree of variation, like *Adeona* sp. and *A. japonica*, which are fully resolved sister taxa, but where five genes have changed positions in a seemingly random fashion. In a similar fashion, gene order identity is found in the two species of *Microporella* (Appendix Figure 39 and 51). However, some similarities are also found at family level: In the family Catenicellidae, the only gene order difference detected is in *Cornuticella taurina* where the block of *ATP8* and *NADH3* have moved to the other side of *COX1*.

Conserved gene regions between closely related species may reflect the relatedness and common ancestral states, hence the close relationships I found in my inferred topology. For this reason, I anticipate that the large amount of rearrangements found, also reflects low taxon sampling, suggesting a huge unsampled or unknown bryozoan diversity. With a denser taxon sampling, we might expect to see, more systematic patterns, as seen for corals and annelids (Lin et al., 2014; Weigert et al., 2016). But, these results also indicate the importance of considering taxonomical level when comparing and studying rearrangements. With a longer evolutionary

timespan from the last common ancestor, there is a higher possibility for both mutations, rearrangements and selection to occur as I demonstrate here: Taxa from different families and genera are more different than within a family or genus.

Lastly, the gene alignments used for this phylogenetic analysis, do not consider gene order when estimating phylogenetic relationships: Only the sequence of amino acids or nucleotides within the genes are considered. For this reason, a statistical approach (e.g. Aguileta et al. 2014) is necessary to verify and establish the utility of gene order as a phylogenetic character. This was beyond the scope of this study, but should be considered in future studies with a broader taxon sample.

5 Conclusion

With a robust dataset and by far the highest number of genes used in a bryozoan phylogeny to date, I have inferred the phylogenetic positioning of 35 bryozoan taxa in a topology with high statistical support. The family Adeonidae, which has never before been placed in a molecular phylogenetic context, is here shown to be a monophyletic clade, which supports the merging of the two previously separated families Adeonidae and Adeonellidae. I argue that frontal shields are not a good family level taxonomical trait for the adeonids. Accordingly, all three represented frontal shield types (spinocystal, umbonuloid and lepralioid) and therefore the infraorders Acanthostegamorpha, Umbonulomorpha and Lepraliomorpha, are in this study found to be polyphyletic, indicating that this trait might not even be a good taxonomical trait for the entire order Cheilostomata, especially not for higher order systematics. The convergent evolution of this trait also highlights the importance of incorporating molecular markers when inferring bryozoan relationships.

6 Future perspectives and final remarks

Despite the ongoing effort to sequence bryozoan taxa, more work is needed, and a deeper taxon sampling is in great need to verify and resolve remaining parts of the bryozoan tree. Furthermore, mitochondrial genes within the sampled bryozoans, shows a high degree of rearrangements which are in contrast to other invertebrates. A dense taxon sampling combined with a statistical approach should be carried out to further explore which, if any, phylogenetic congruence is evident between mitochondrial gene evolution and species evolution.

One taxon in my dataset was removed due to contamination. Whether this is due to colony overgrowth or due to a sequencing error, is yet to be determined. Contamination due to overgrowth of either neighboring colonies or other organisms is a commonly known problem since bryozoans live in close proximity with other biota. For this reason, some sequences deposited in Genbank have been shown to be contaminated as found by Waeschenbach et al. (2012) (see supplementary material) and thereby removed accordingly in this study (Appendix Table 4). Additionally, I encountered some issues regarding the closing of the mitochondrial genome. Repetitive regions over 150 bp are the primary issue, and in future studies, longer reads from either Nanopore or PacBio will be needed to close these genomes. Alternatively, long range PCR, all though a non PCR based method is preferred.

References

Aberer, A. J., Krompass, D., & Stamatakis, A. (2013). Pruning Rogue Taxa Improves Phylogenetic Accuracy: An Efficient Algorithm and Webservice. *Systematic Biology, 62*, 162-166.

Aguileta, G., de Vienne, D. M., Ross, O. N., Hood, M. E., Giraud, T., Petit, E., & Gabaldón, T. (2014). High Variability of Mitochondrial Gene Order among Fungi. *Genome Biology and Evolution, 6*, 451-465.

Al-Nakeeb, K., Petersen, T. N., & Sicheritz-Pontén, T. (2017). Norgal: extraction and de novo assembly of mitochondrial DNA from whole-genome sequencing data. *BMC Bioinformatics, 18*, 510.

Almeida, A. C. S., Souza, F. B. C., Sanner, J., & Vieira, L. M. (2015). Taxonomy of recent Adeonidae (Bryozoa, Cheilostomata) from Brazil, with the description of four new species. *Zootaxa, 4013*, 348-368.

Amui, A.-M. (2005). Adeonellas from the Gulf of Aden including one new species. *Zootaxa, 1012*, 45-52.

Andrews, S. (2010). FastQC: a quality control tool for high throughput sequence data.

Bankevich, A., Nurk, S., Antipov, D., Gurevich, A. A., Dvorkin, M., Kulikov, A. S., Lesin, V. M., Nikolenko, S. I., Pham, S., Prjibelski, A. D., Pyshkin, A. V., Sirotkin, A. V., Vyahhi, N., Tesler, G., Alekseyev, M. A., & Pevzner, P. A. (2012). SPAdes: A New Genome Assembly Algorithm and Its Applications to Single-Cell Sequencing. *Journal of Computational Biology, 19*, 455-477.

Bassler, R. S. (Ed.) (1953). *Part G. Bryozoa*. Lawrence: Geological Society of America and University of Kansas Press.

Bernt, M., Donath, A., Jühling, F., Externbrink, F., Florentz, C., Fritzsch, G., Pütz, J., Middendorf, M., & Stadler, P. F. (2013). MITOS: improved de novo metazoan mitochondrial genome annotation. *Molecular Phylogenetics and Evolution, 69*, 313-319.

Bock, P. E. (2018). Bryozoa Homepage. Retrieved from http://bryozoa.net/famsys.html, 18.08.2018

Bock, P. E., & Gordon, D. P. (2013). Phylum Bryozoa Ehrenberg, 1831. *Zootaxa, 3703*, 67-74.

Boore, J. L. (1999). Animal mitochondrial genomes. *Nucleic Acids Research, 27*, 1767-1780.

Boore, J. L., & Brown, W. M. (1998). Big trees from little genomes: mitochondrial gene order as a phylogenetic tool. *Current Opinion in Genetics & Development, 8*, 668-674.

Boore, J. L., Collins, T. M., Stanton, D., Daehler, L. L., & Brown, W. M. (1995). Deducing the pattern of arthropod phytogeny from mitochondrial DNA rearrangements. *Nature, 376*, 163-165.

Brugler, M. R., & France, S. C. (2008). The Mitochondrial Genome of a Deep-Sea Bamboo Coral (Cnidaria, Anthozoa, Octocorallia, Isididae): Genome Structure and Putative

Origins of Replication Are Not Conserved Among Octocorals. *Journal of Molecular Evolution, 67*, 125.

Burnham, K. P., & Anderson, D. R. (2003). *Model selection and multimodel inference: a practical information-theoretic approach*: Springer Science & Business Media.

Busk, G. (1884). Report on the Polyzoa. Part I. The Cheilostomata. *Report of the Scientific Results of the Voyage of H.M.S. Challenger during the years 1873-76, 10*, 1-216.

Cameron, S. L. (2014). Insect Mitochondrial Genomics: Implications for Evolution and Phylogeny. *Annual Review of Entomology, 59*, 95-117.

Canu, F., & Bassler, R. S. (1920). North American early Tertiary Bryozoa. *Bulletin of the United States National Museum, 106*, 1-879.

Castresana, J. (2000). Selection of conserved blocks from multiple alignments for their use in phylogenetic analysis. *Molecular Biology and Evolution, 17*, 540-552.

Cook, P. L. (1973). Preliminary notes on the ontogeny of the frontal body wall in the Adeonidae and Adeonellidae (Bryozoa, Cheilostomata). *Bulletin of the British Museum (Natural History), Zoology, 25*, 243-263.

Cuffey, R. J., & Blake, D. B. (1991). Caldistic analysis of the phylum Bryozoa. In F. P. Bigey (Ed.), *Bryozoaires Actuels et Fossiles: Bryozoa Living and Fossil* (Vol. 1, pp. 97-108).

Dick, M. H., Freeland, J. R., Williams, L. P., & Coggeshall-Burr, M. (2000). Use of 16S mitochondrial ribosomal DNA sequences to investigate sister-group relationships among gymnolaemate bryozoans. In A. Herrera Cubilla & J. B. C. Jackson (Eds.), *Proceedings of the 11th International Bryozoology Association Conference* (pp. 197-210). Panama City: Smithsonian Tropical Research Institute, Balboa, Republic of Panama.

Dick, M. H., Lidgard, S., Gordon, D. P., & Mawatari, S. F. (2009). The origin of ascophoran bryozoans was historically contingent but likely. *Proceedings of the Royal Society of London, B, 276*, 3141-3148.

Dierckxsens, N., Mardulyn, P., & Smits, G. (2017). NOVOPlasty: de novo assembly of organelle genomes from whole genome data. *Nucleic Acids Research, 45*.

Dzik, J. (1975). The origin and early phylogeny of the cheilostomatous Bryozoa. *Acta Palaeontologica Polonica, 20*, 395-423.

Fuchs, J., Obst, M., & Sundberg, P. (2009). The first comprehensive molecular phylogeny of Bryozoa (Ectoprocta) based on combined analyses of nuclear and mitochondrial genes. *Molecular Phylogenetics and Evolution, 52*, 225-233.

Gordon, D. P. (1989). The marine fauna of New Zealand: Bryozoa: Gymnolaemata (Cheilostomatida Ascophorina) from the western South Island continental shelf and slope. *New Zealand Oceanographic Institute Memoir, 97*, 1-158.

Gordon, D. P. (1993). Bryozoan frontal shields: studies on umbonulomorphs and impacts on classification. *Zoologica Scripta, 22*, 203-221.

Gordon, D. P. (2000). *Towards a phylogeny of cheilostomes - morphological models of frontal wall/shield evolution.* Paper presented at the Proceedings of the 11th International Bryozoology Association Conference, 1998, Panama City.

Gordon, D. P. (2014). Bryozoa: Cheilostomata. Interim Classification for Treatise. *NIWA, Wellington*.

Gordon, D. P., & Voigt, E. (1996). The kenozooidal origin of the ascophorine hypostegal coelom and associated frontal shield. In D. P. Gordon, A. M. Smith, & J. A. Grant-Mackie (Eds.), *Bryozoans in Space and Time* (pp. 89-107). Wellington: NIWA.

Gregory, J. W. (1893). On the British Palaeogene Bryozoa. *Transactions of the Zoological Society of London, 13*, 219-279.

Grischenko, A. V., & Mawatari, S. F. (2002). *Kubaninella*: a new genus of Adeonidae (Bryozoa: Cheilostomata) from the Western Kamchatka shelf of the Sea of Okhotsk. In P. N. Wyse Jackson, C. J. Buttler, & M. E. Spencer Jones (Eds.), *Bryozoan Studies 2001* (pp. 125-130). Lisse: Balkema.

Hao, J., Li, C., Sun, X., & Yang, Q. (2005). Phylogeny and divergence time estimation of cheilostome bryozoans based on mitochodrial 16S rRNA sequences. *Chinese Science Bulletin, 50*, 1205-1211.

Harmer, S. F. (1957). The Polyzoa of the Siboga Expedition, Part IV. Cheilostomata, Ascophora. II. In *Siboga Expeditie* (Vol. 28d, pp. 641-1147). Leiden: Brill.

Hayward, P. J. (1983). Biogeography of *Adeonella* (Bryozoa, Cheilostomata): a preliminary account. *Bulletin of Marine Science, 33*, 582-596.

Hincks, T. (1881). Contributions towards a general history of the marine Polyzoa. Part VI. Polyzoa from Bass's Straits. *Annals and Magazine of Natural History, ser. 5, 8*, 1-14.

Hincks, T. (1887). Critical notes on the Polyzoa. *Annals and Magazine of Natural History, ser. 5, 19*, 150-164.

Hirose, M. (2016). Diversity and distribution of adeonid bryozoans (Cheilostomata: Adeonidae) in Japanese waters. *European Journal of Taxonomy, 203*, 1-41.

Huelsenbeck, J., & Ronquist, F. (2001). MrBayes: Bayesian inference of phylogenetic trees. *Bioinformatics, 17*, 754-755.

Jackson, J. B. C., & Cheetham, A. H. (1990). Evolutionary significance of morphospecies: a test with cheilostome Bryozoa. *Science, 248*, 579-583.

Jiao, X. X., Yang, Q., Zhao, H. B., Shi, Q. H., & Hao, J. S. (2009). Molecular phylogenetic relationships of the cheilostomatous bryozoans based on 18S rRNA gene sequences. *Acta Zootaxonomica Sinica, 34*, 513-521.

Jullien, J., & Calvet, L. (1903). Bryozoaires provenant des campagnes de l'*Hirondelle* (1886-1888). *Résultats des Campagnes Scientifiques du Prince de Monaco, 23*, 1-188.

Katoh, K., & Standley, D. M. (2013). MAFFT Multiple Sequence Alignment Software Version 7: Improvements in Performance and Usability. *Molecular Biology and Evolution, 30*, 772-780.

Kibbe, W. A. (2007). OligoCalc: an online oligonucleotide properties calculator. *Nucleic Acids Research, 35*, W43-W46.

Knight, S., Gordon, D. P., & Lavery, S. D. (2011). A multi-locus analysis of phylogenetic relationships within cheilostome bryozoans supports multiple origins of ascophoran frontal shields. *Molecular Phylogenetics and Evolution, 61*, 351-362.

Krueger, F. (2015). Trim Galore. *A wrapper tool around Cutadapt and FastQC to consistently apply quality and adapter trimming to FastQ files*.

Lagesen, K., Hallin, P., Rødland, E. A., Stærfeldt, H.-H., Rognes, T., & Ussery, D. W. (2007). RNAmmer: consistent and rapid annotation of ribosomal RNA genes. *Nucleic Acids Research, 35*, 3100-3108.

Le, T. H., Blair, D., Agatsuma, T., Humair, P.-F., Campbell, N. J. H., Iwagami, M., Littlewood, D. T. J., Peacock, B., Johnston, D. A., Bartley, J., Rollinson, D., Herniou, E. A., Zarlenga, D. S., & McManus, D. P. (2000). Phylogenies Inferred from Mitochondrial Gene Orders—A Cautionary Tale from the Parasitic Flatworms. *Molecular Biology and Evolution, 17*, 1123-1125.

Levinsen, G. M. R. (1909). *Morphological and Systematic Studies on the Cheilostomatous Bryozoa*. Copenhagen: Nationale Forfatteres Forlag.

Lidgard, S. (1996). Zooid skeletal morphogenesis of some Australian and New Zealand *Adeonellopsis* (Cheilostomatida). In D. P. Gordon, A. M. Smith, & J. A. Grant-Mackie (Eds.), *Bryozoans in Space and Time* (pp. 167-177). Wellington: NIWA.

Lidgard, S., Carter, M. C., Dick, M. H., Gordon, D. P., & Ostrovsky, A. N. (2011). Division of labor and recurrent evolution of polymorphisms in a group of colonial animals. *Evolutionary Ecology, 26*, 233-257.

Lin, M.-F., Kitahara, M. V., Luo, H., Tracey, D., Geller, J., Fukami, H., Miller, D. J., & Chen, C. A. (2014). Mitochondrial Genome Rearrangements in the Scleractinia/Corallimorpharia Complex: Implications for Coral Phylogeny. *Genome Biology and Evolution, 6*, 1086-1095.

Lischer, H. E. L., & Shimizu, K. K. (2017). Reference-guided de novo assembly approach improves genome reconstruction for related species. *BMC Bioinformatics, 18*, 474.

Lombardi, C., Cocito, S., Gambi, M. C., & Taylor, P. D. (2015). Morphological plasticity in a calcifying modular organism: evidence from an in situ transplant experiment in a natural CO_2 vent system. *Royal Society open science, 2*, 140413.

Lunter, G., & Goodson, M. (2011). Stampy: A statistical algorithm for sensitive and fast mapping of Illumina sequence reads. *Genome Research, 21*, 936-939.

Ma, J., Taylor, P. D., Xia, F.-S., & Zhan, R. (2015). The oldest known bryozoan: *Prophyllodictya* (Cryptostomata) from the lower Tremadocian (Lower Ordovician) of Liujiachang, south-western Hubei, central China. *Palaeontology, 58*, 925-934.

Maddison, W. P., & Maddison, D. R. (2001). Mesquite: a modular system for evolutionary analysis. Version 3.2 http://www.mesquiteproject.org.

McKinney, F. K., & Jackson, J. B. C. (1989). *Bryozoan Evolution*. Boston: Unwin Hyman.

Mindell, D. P., Sorenson, M. D., & Dimcheff, D. E. (1998). Multiple independent origins of mitochondrial gene order in birds. *Proceedings of the National Academy of Sciences, 95*, 10693-10697.

Mueller, R. L., & Boore, J. L. (2005). Molecular Mechanisms of Extensive Mitochondrial Gene Rearrangement in Plethodontid Salamanders. *Molecular Biology and Evolution, 22*, 2104-2112.

Orr, R. J. S., Waeschenbach, A., Enevoldsen, E. L. G., Boeve, J. P., Haugen, M. N., Voje, K. L., Zágoršek, K., Smith, A. M., Gordon, D. P., & Liow, L. H. (2018). Bryozoan genera *Fenestrulina* and *Microporella* no longer confamilial; multi-gene phylogeny supports separation *Zoological Journal of the Linnean Society 2018, In Press*.

Ostrovsky, A. N. (2013). *Evolution of Sexual Reproduction in Marine Invertebrates. Example of Gymnolaemate Bryozoans*. Dordrecht: Springer.

Ostrovsky, A. N., Gordon, D. P., & Lidgard, S. (2009). Independent evolution of matrotrophy in the major classes of Bryozoa: transitions among reproductive patterns and their ecological background. *Marine Ecology Progress Series, 378*, 113-124.

Paradis, E., Schliep, K., & Schwartz, R. (2018). ape 5.0: an environment for modern phylogenetics and evolutionary analyses in R. *Bioinformatics, 1*.

Pohowsky, R. A. (1973). A Jurassic cheilostome from England. In G. P. Larwood (Ed.), *Living and Fossil Bryozoa* (pp. 447-461). London: Academic Press.

R Development Core Team. (2013). R: A language and environment for statistical computing. R Foundation for Statistical Computing, Vienna.

Rawlings, T. A., Collins, T. M., & Bieler, R. (2001). A major mitochondrial gene rearrangement among closely related species. *Molecular Biology and Evolution, 18*, 1604-1609.

Rosso, A., & Novosel, M. (2010). The genus *Adeonella* (Bryozoa, Ascophora) in the Mediterranean, with description of two new living species and rediscovery of a fossil one. *Journal of Natural History, 44*, 1697-1727.

Sandberg, P. A. (1977). Ultrastructure, mineralogy, and development of bryozoan skeletons. In R. M. Woollacott & R. L. Zimmer (Eds.), *Biology of Bryozoans* (pp. 143-181). New York: Academic Press.

Schwaninger, H. R. (1999). Population structure of the widely dispersing marine bryozoan *Membranipora membranacea* (Cheilostomata): implications for population history, biogeography, and taxonomy. *Marine Biology, 135*, 411-423.

Stamatakis, A. (2014). RAxML version 8: a tool for phylogenetic analysis and post-analysis of large phylogenies. *Bioinformatics, 30*, 1312-1313.

Taylor, P. D. (1988). Major radiation of cheilostome bryozoans: triggered by the evolution of a new larval type? *Historical Biology, 1*, 45-64.

Taylor, P. D., Casadío, S., & Gordon, D. P. (2008). A rare form of frontal shield development in the new cheilostome bryozoan genus *Uharella* from the Eocene of Antarctica. *Paläontologische Zeitschrift, 82*, 262-268.

Taylor, P. D., & Mawatari, S. F. (2005). Preliminary overview of the cheilostome bryozoan *Microporella*. In H. I. Moyano, J. M. Cancino, & P. N. Wyse Jackson (Eds.), *Bryozoan Studies 2004* (pp. 329-339). Leiden: Balkema.

Taylor, P. D., & Waeschenbach, A. (2015). Phylogeny and diversification of bryozoans. *Palaeontology, 58*, 585-599.

Taylor, P. D., Waeschenbach, A., Smith, A. B., & Gordon, D. P. (2015). In search of phylogenetic congruence between molecular and morphological data in bryozoans with extreme adult skeletal heteromorphy. *Systematics and Biodiversity, 13*, 525-544.

Todd, J. A. (2000). The central role of ctenostomes in bryozoan phylogeny. In A. Herrera Cubilla & J. B. C. Jackson (Eds.), *Proceedings of the 11th International Bryozoology Association Conference* (pp. 104-135). Balboa, R.P.: Smithsonian Tropical Research Institute.

Tsyganov-Bodounov, A., Hayward, P. J., Porter, J. S., & Skibinski, D. O. F. (2009). Bayesian phylogenetics of Bryozoa. *Molecular Phylogenetics and Evolution, 52*, 904-910.

Untergasser, A., Nijveen, H., Rao, X., Bisseling, T., Geurts, R., & Leunissen, J. A. M. (2007). Primer3Plus, an enhanced web interface to Primer3. *Nucleic Acids Research, 35*, W71-W74.

Uttley, G. H., & Bullivant, J. S. (1971). Biological results of the Chatham Islands 1954 Expedition, Part 7, Bryozoa Cheilostomata. *New Zealand Oceanographic Institute Memoir, 57*, 1-61.

Velozo Timbó, R., Coiti Togawa, R., M. C. Costa, M., A. Andow, D., & Paula, D. (2017). Mitogenome sequence accuracy using different elucidation methods. *PloS one, 12*, e0179971.

Voigt, E. (1991). Mono- or polyphyletic evolution of cheilostomatous bryozoan divisions? In F. P. Bigey (Ed.), *Bryozoaires Actuels et Fossiles: Bryozoa Living and Fossil* (pp. 505-522). Nantes: Bulletin de la Société Sciences Naturelles de l'Ouest de la France, Mémoire HS 1.

Waeschenbach, A., Taylor, P. D., & Littlewood, D. T. J. (2012). A molecular phylogeny of bryozoans. *Molecular Phylogenetics and Evolution, 62*, 718-735.

Walker, B. J., Abeel, T., Shea, T., Priest, M., Abouelliel, A., Sakthikumar, S., Cuomo, C. A., Zeng, Q., Wortman, J., Young, S. K., & Earl, A. M. (2014). Pilon: An Integrated Tool for Comprehensive Microbial Variant Detection and Genome Assembly Improvement. *PloS one, 9*.

Waters, A. W. (1912). A structure in *Adeonella* (*Laminopora*) *contorta* (Michelin), and some other Bryozoa, together with remarks on the Adeonidae. *Annals and Magazine of Natural History, ser. 8, 9*, 489-500.

Weaver, H., Cook, P., Bock, P., & Gordon, D. P. (2018). *Australian Bryozoa Volume 2: Taxonomy of Australian Families*: CSIRO Publishing.

Weigert, A., Golombek, A., Gerth, M., Schwarz, F., Struck, T. H., & Bleidorn, C. (2016). Evolution of mitochondrial gene order in Annelida. *Molecular Phylogenetics and Evolution, 94*, 196-206.

Yagunova, E. B., & Ostrovsky, A. N. (2008). Encrusting bryozoan colonies on stones and algae: variability of zooidal size and its posssible causes. *Journal of the Marine Biological Association of the United Kingdom, 88*, 901-908.

Ye, J., Coulouris, G., Zaretskaya, I., Cutcutache, I., Rozen, S., & Madden, T. L. (2012). Primer-BLAST: a tool to design target-specific primers for polymerase chain reaction. *BMC Bioinformatics, 13*, 134.

Appendix

Appendix Table 1. Accession number of sequences retrieved from Genbank. Where accession number is not listed, the sequence has not been submitted to Genbank or no sequence are available. Three of the available sequences was removed due to contamination (Appendix Table 4 for more information).

ID number	Species name	Accession number mt genome	Accession number 18S	Accession number 28S
NZ011	*Cryptosula pallasiana*		JN680940	JN681038
	Flustra foliacea	JQ061319	FJ196110	FJ196139 (Removed)
	Flustrellidra hispida	NC_008192	FJ409601	FJ409577
	Oshurkovia littoralis (previously *Umbonula*)		JN680953	JN681046
AW267	*Pentapora foliacea*		JN680941	
AW006	Phidoloporidae indet.			JN681049
	Tubulipora flabellaris	NC_015646	EU650325 (Removed)	DQ333340 (Removed)
	Watersipora subtorquata	NC_011820	JN680947	DQ33334

Appendix Table 2. PCR cycling profile for Phusion high-fidelity polymerase. A temperature gradient was used to see which temperature was the preferred one for the different primers.

	Temperature	Time	Cycles
Initial denaturation	98 °C	30 sec	1
Denaturation	98 °C	10 sec	35
Annealing	41 – 59 °C	30 sec	35
Extension	72 °C	1.5 min	35
Final extension	72 °C	10 min	1

Appendix Table 3. Successful primers used for Phusion high-fidelity PCR. These PCR products were further used for cloning. *Adeonella calveti* and *Adeonellopsis* sp. 1 became closed and *Arachnopusia unicornis* was reduced from two fragments to one.

Species	**Reverse primer**	**Sequence**	**Forward primer**	
Adeonella calveti	601 R	GTTGTATAACCGCGGATGCT	15173 F	TGAAGGGACTTTTTGCCATT
Adeonella calveti	101 R	GGATACAATCCTCCCCTTCC	15527 F	TGTTCGAAAGGCCAAATAGG
Adeonellopsis sp. 1	266 R	ATCAAGACATCGACCGGCTT	13832 F	GCTTTATCGGTTTTATTGCACTCT
Adeonellopsis sp. 1	305 R	ATAACCGCGGGTGCTGGCAC	14775 F	GGTGTACGGAGCTGGCTTAA
Arachnopusia unicornis	345 R	TGAAGGTGTACCTAGTTGGA	748 R (RC)	AGTGGTGGTTAGGTTGATTA

Appendix Table 4. Missing or excluded genes from the concatenated dataset.

Species	**Missing genes**	**Reason**
Telopora watersi	ATP 8	Not annotated
Tubulipora flabellaris	ATP 8	Not annotated
Thalamoporella sp.	ATP 8	Not annotated
Steginoporella neozelanica	ATP 8	Not annotated
Microporella sp.	28S	Not yet sequenced
Pentapora foliacea	28S	Not yet sequenced
Chiastosella sp.	18S & 28S	Not yet sequenced
Reteporella ligulata	18S & 28S	Not yet sequenced
Phidoloporidae indet.	18S	Not yet sequenced
Cornuticella taurina	18S & 28S	Not yet sequenced
Tubulipora flabellaris	18S (EU650325)	Contaminated. See Waeschenbach et al. (2012)
Tubulipora flabellaris	28S (DQ333340)	Contaminated. See Waeschenbach et al. (2012)
Flustra foliacea	28S (FJ196139)	Contaminated. A. Waeschenbach, pers. comm, 2018

FastQC: FastQC provides a set of analyses with quality information and you can see if your data has any problems which you should be aware of before doing any further analysis (Andrews, 2010)
TrimGalore: Quality and adapter trimming of FastQ files (Krueger, 2015).
SPAdes. *De novo* genome assembler (Bankevich et al., 2012).
Pilon: Improves draft genome assemblies by correcting bases, fixing mis-assemblies and filling gaps (Walker et al., 2014).
CLC workbench 7 (Qiagen bioinformatics): Software which allows for DNA, RNA, and protein sequence data analysis.
BLAST: Basic Local Alignment Search Tool. BLAST finds regions of similarity between biological sequences. The program compares nucleotide or protein sequences to sequence databases and calculates the statistical significance (https://blast.ncbi.nlm.nih.gov/Blast.cgi).
Mitos: MITOS is a free web server for the annotation of metazoan mitochondrial genomes (Bernt et al., 2013).
RNAmmer: A free web server for annotation of ribosomal RNA (Lagesen et al., 2007).
MAFFT: A multiple alignment program for amino acid or nucleotide sequences. This is an iterative refinement method using Needleman-Wunsch algorithm, with two major gap penalties: gap open penalty and gap extension penalty (Katoh & Standley, 2013).
Gblocks: Eliminates poorly aligned positions and divergent regions of a DNA or protein alignment so that it becomes more suitable for phylogenetic analysis (Castresana, 2000).
Mesquite: Software used to visualize sequence data and alignments (Maddison & Maddison, 2001).
RAxML: Randomized Axelerated Maximum Likelihood. A popular program for phylogenetic analyses of large datasets under maximum likelihood (Stamatakis, 2014).
MrBayes5d: A modified version of MrBayes v3.2 (Huelsenbeck & Ronquist, 2001) which incorporates the MtZoa evolutionary model (https://github.com/astanabe/mrbayes5d).
Catfasta2phyml.pl: Software used to concatenate all gene-alignments into one final dataset (https://github.com/nylander/catfasta2phyml).
RougeNaRok: A tool for identifying rouge taxa; a class of taxa with uncertain position in a phylogenetic tree (Aberer, Krompass, & Stamatakis, 2013).
Tadpole: Tadpole is a kmer-based assembler, with additional capabilities of error-correcting and extending reads. https://jgi.doe.gov/data-and-tools/bbtools/bb-tools-user-guide/tadpole-guide/
K-mer: Substrings of length k that are contained in a string. Illumina reads are 150bp, but this breaks down the sequence into smaller k-mers to better find overlaps between the reads which ideally creates longer contigs. SPAdes use a range of k-mers when creating the assembly. Small k-mers result in shorter contigs with lots of connections, while large k-mers can result in longer contigs with fewer connections. The ideal k-mer size depends on the read length and the read depth and sequence complexity. If you have longer reads and/or higher read depth, you can use larger k-mers which are useful in resolving complex areas of the graph.

Appendix Figure 1. Bioinformatic tools and abbreviations.

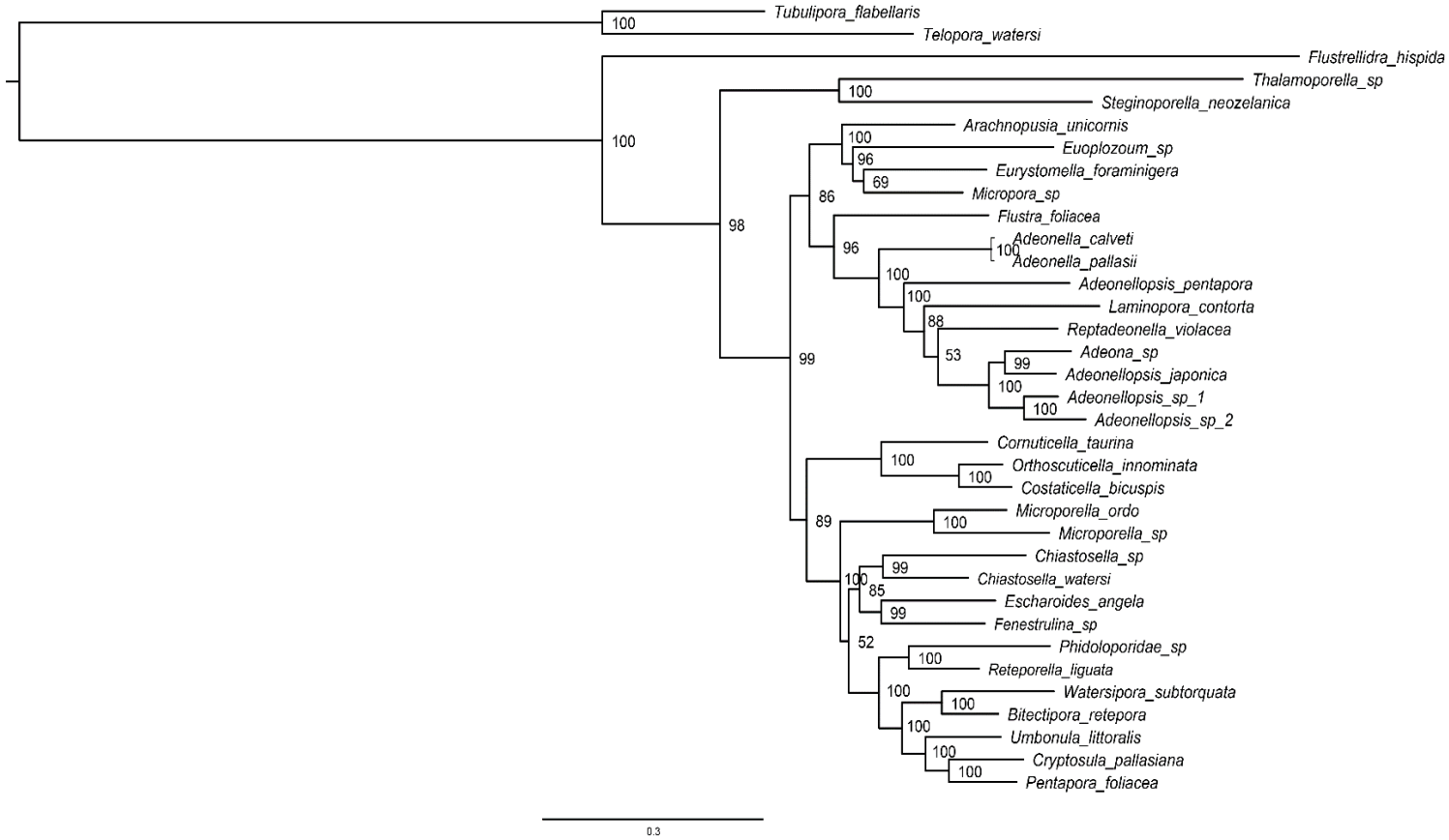

Appendix Figure 2. Maximum likelihood (ML) tree of all 35 taxa and 17 genes with bootstrap support values. ML analysis conducted with RAxML with preferred evolutionary model for each gene. Scale bar indicate number of substitutions per site.

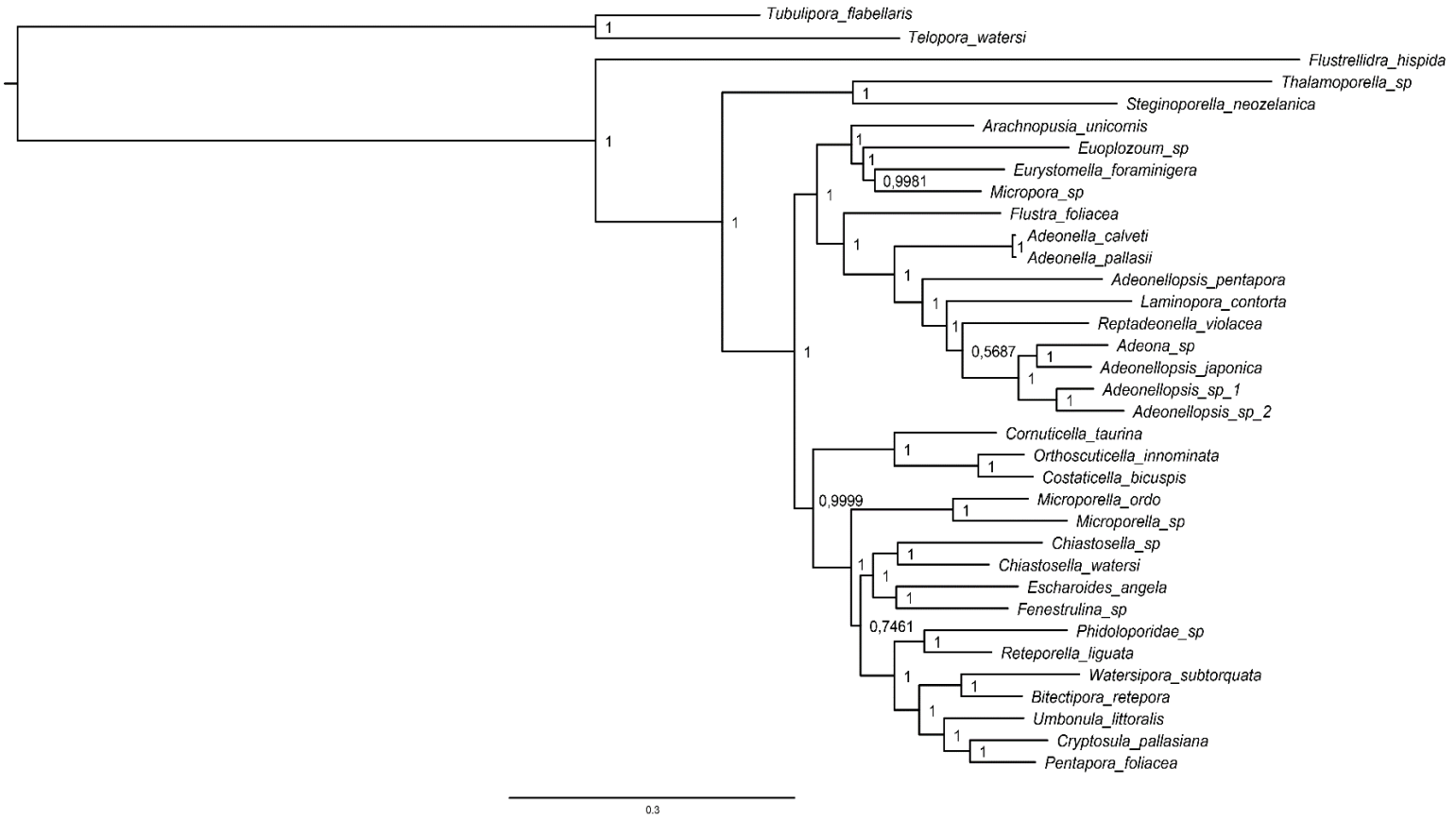

Appendix Figure 3. Bayesian inference tree (BI) of 35 taxa and 17 genes with posterior probability values. BI analyis conducted with MRBayes5d and with preferred evolutionary models for each gene. Scale bar indicate number of substitutions per site.

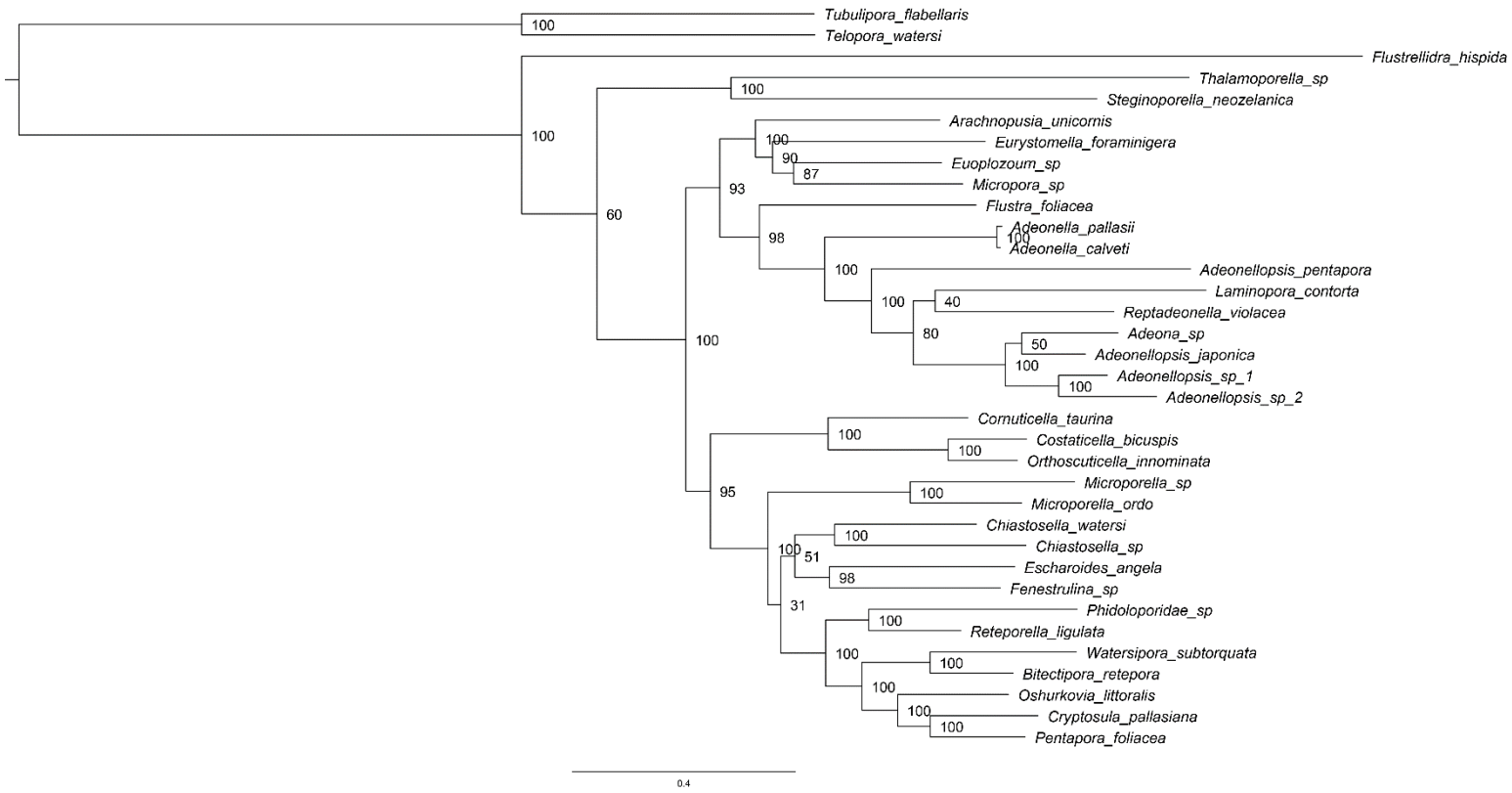

Appendix Figure 4. ML tree of 15 mitochondrial genes and all 35 taxa, with bootstrap support values. ML analysis conducted with RAxML with preferred evolutionary model for each gene. Scale bar indicate number of substitutions per site.

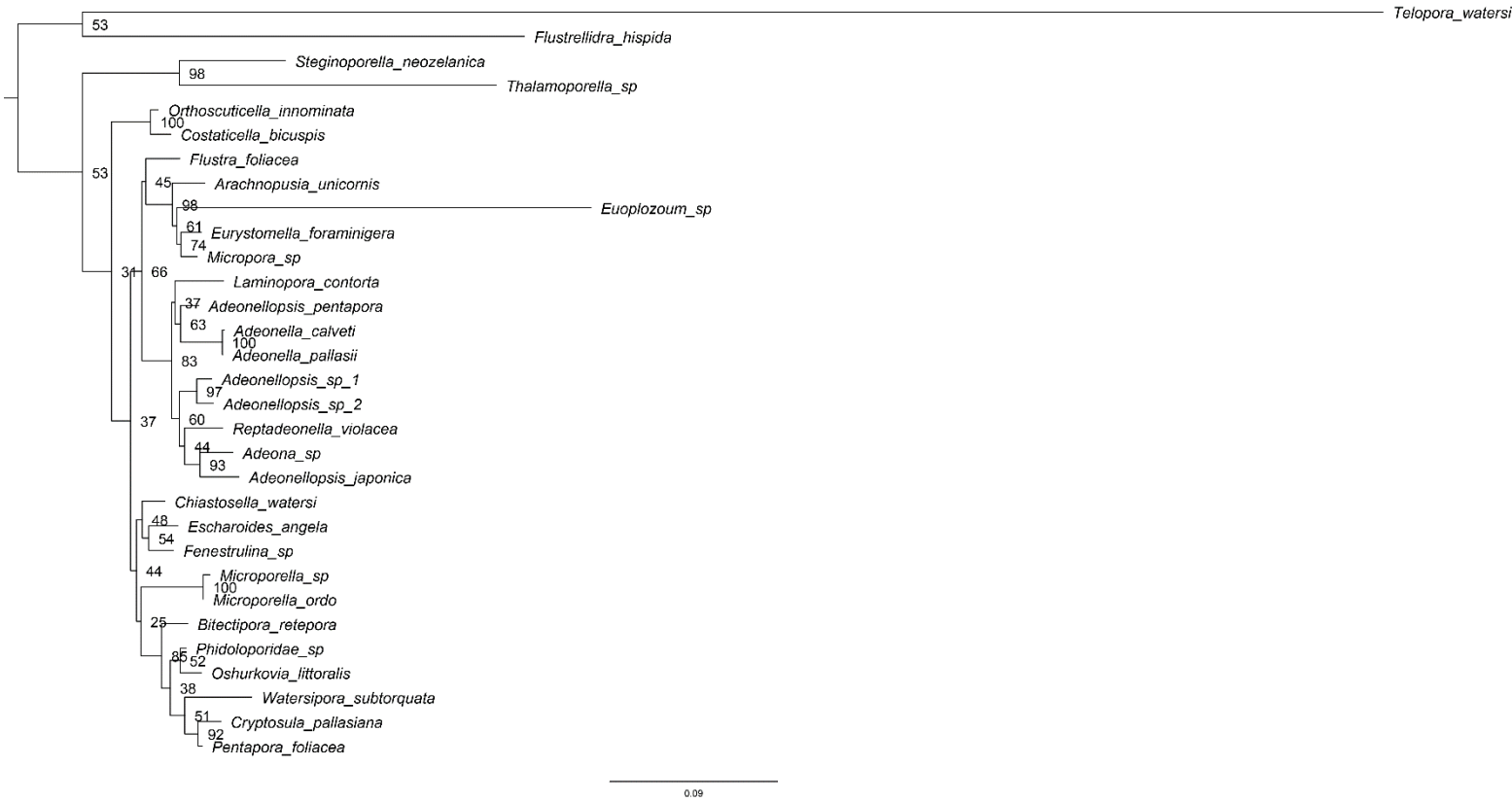

Appendix Figure 5. Ribosomal 18S and 28S. ML conducted in RAxML with evolutionary model GTR and gamma distribution.

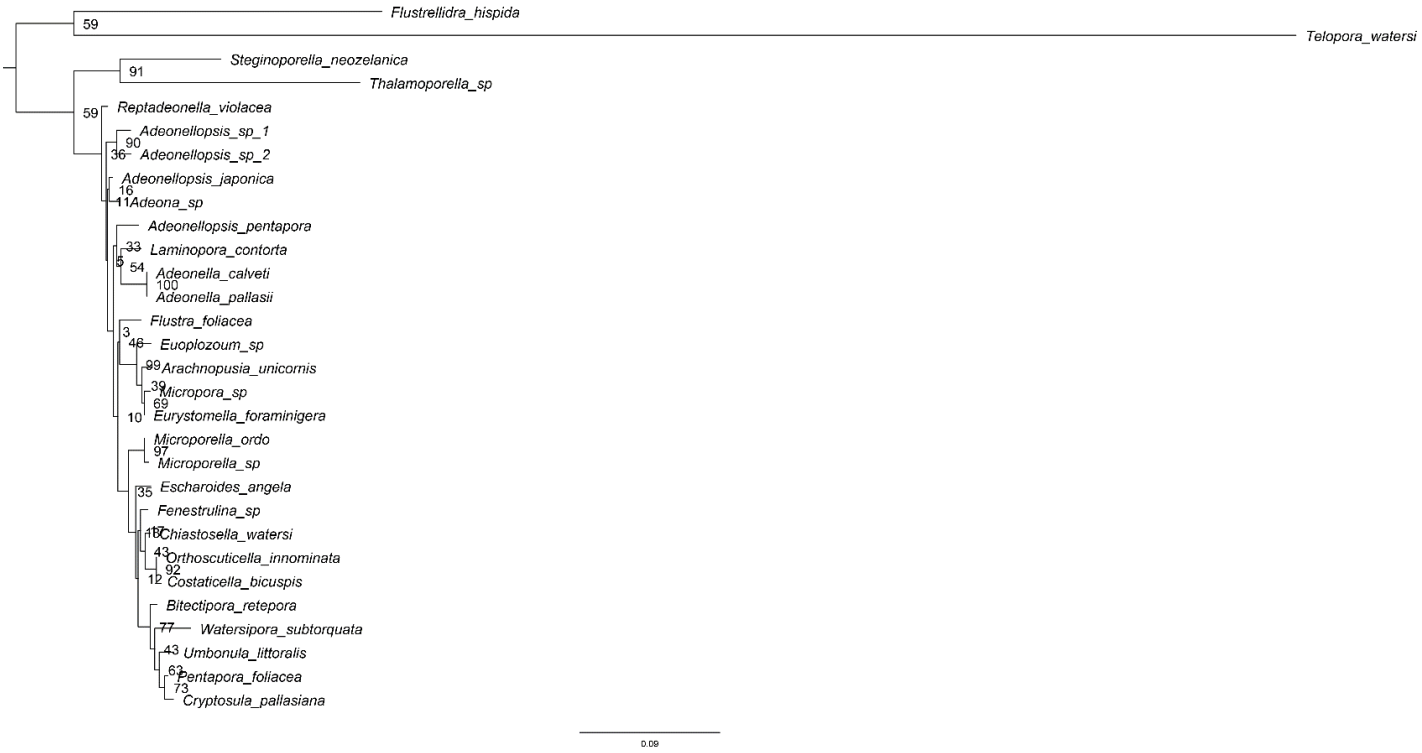

Appendix Figure 6. Ribosomal 18S. ML conducted in RAxML with evolutionary model GTR and gamma distribution. Contains 1828 nucleotides. Please note: *Umbonula littoralis* has a new formal name: *Oshurkovia littoralis* as seen in the main text.

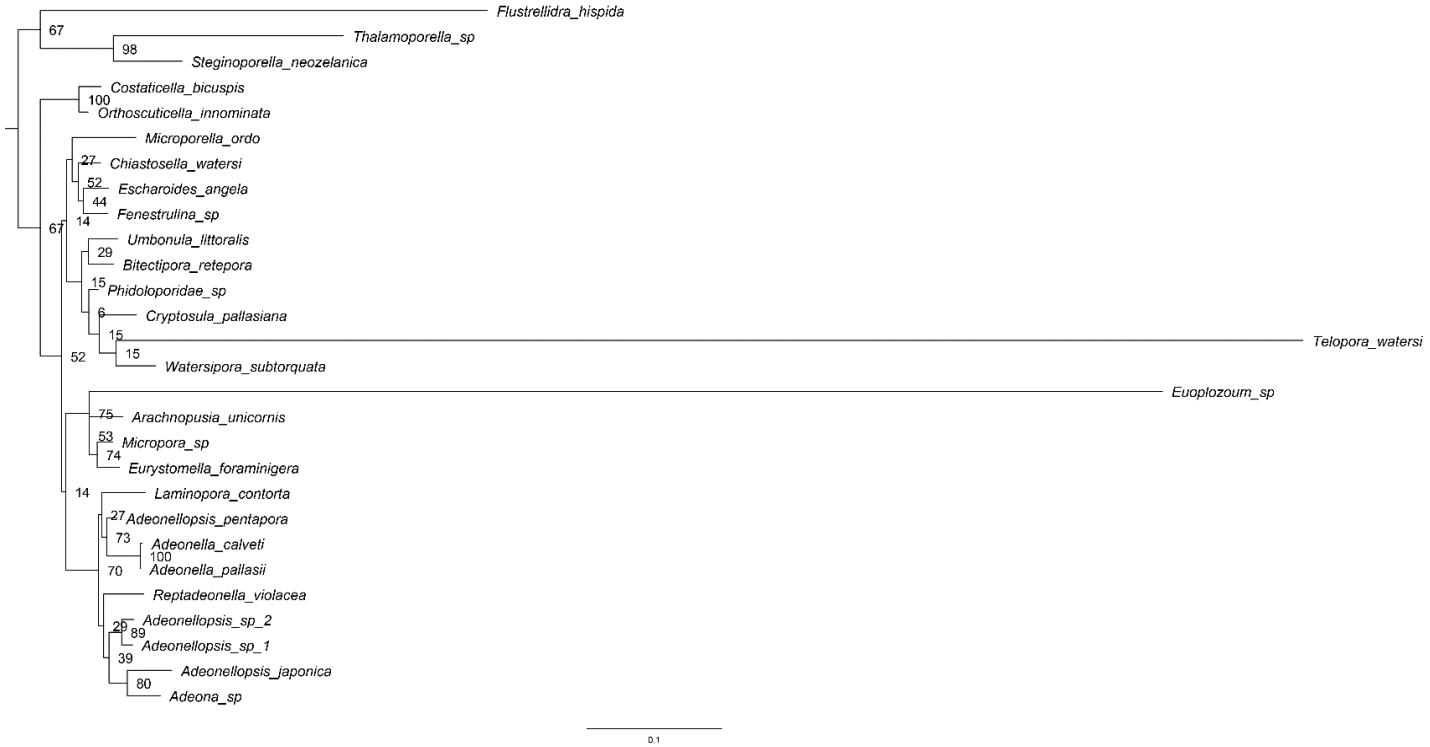

Appendix Figure 7. Ribosomal 28S. ML conducted in RAxML with evolutionary model GTR and gamma distribution. Contains 3614 nucleotides. Please note: *Umbonula littoralis* has a new formal name: *Oshurkovia littoralis* as seen in the main text.

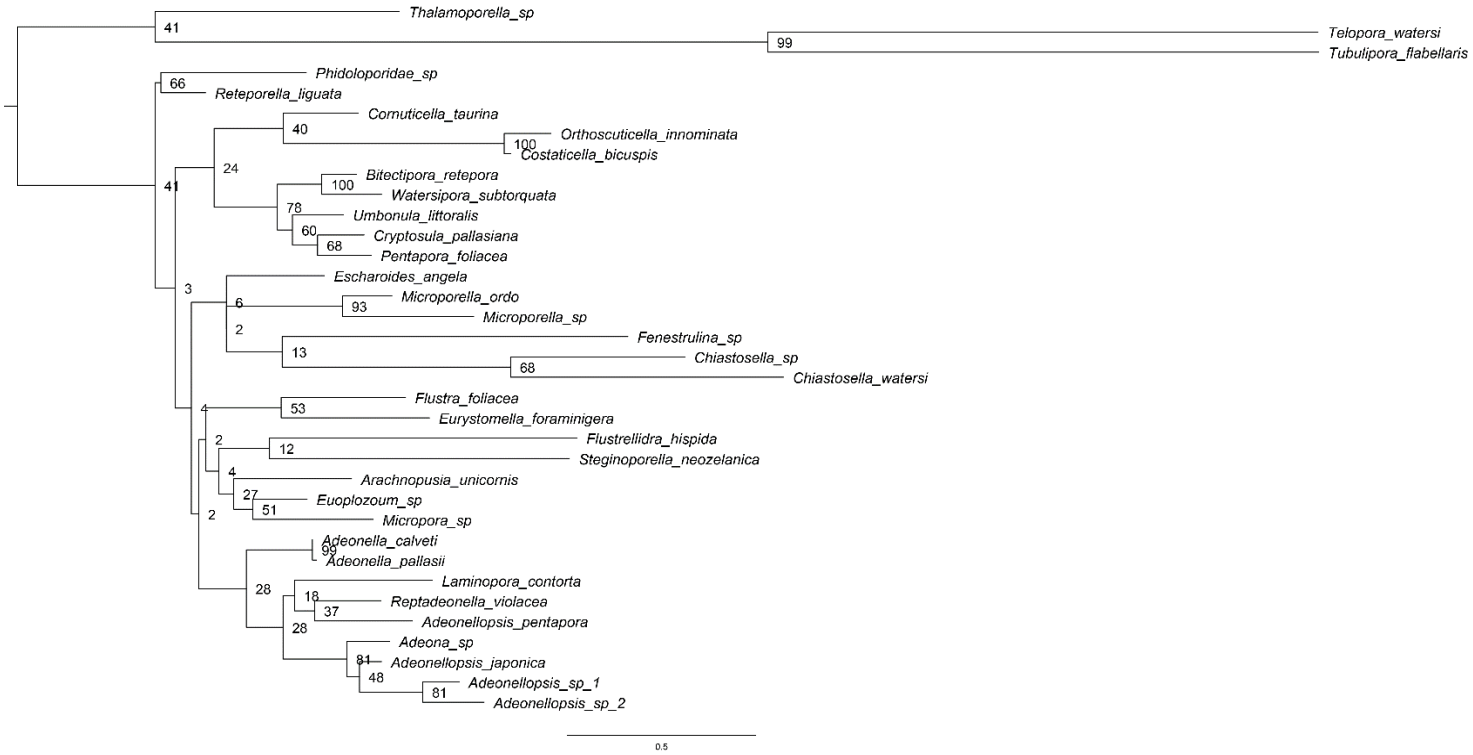

Appendix Figure 8. Mitochondrial ATP6. ML conducted in RAxML with evolutionary model MtZoa and gamma distribution. Contains 157 amino acids. Please note: *Umbonula littoralis* has a new formal name: *Oshurkovia littoralis* as seen in the main text.

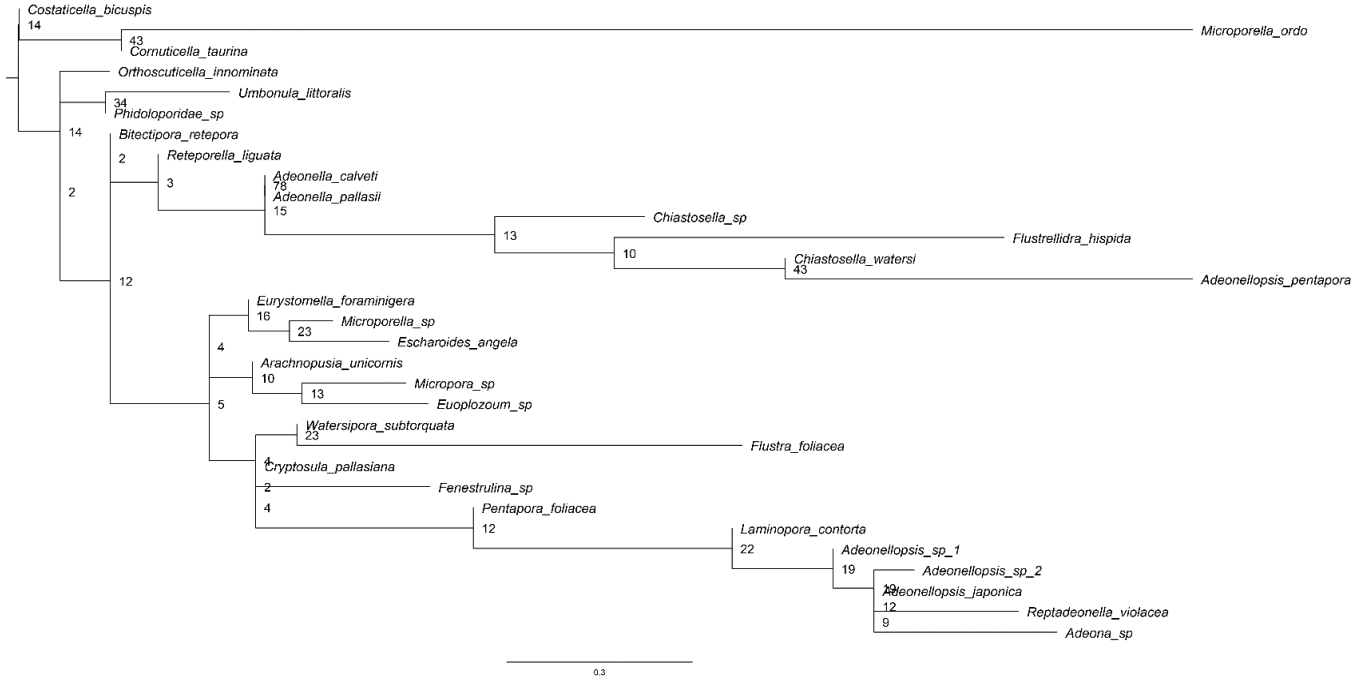

Appendix Figure 9. Mitochondrial *ATP8*. ML conducted in RAxML with evolutionary model MtArt and gamma distribution. Contains 13 amino acids. Please note: *Umbonula littoralis* has a new formal name: *Oshurkovia littoralis* as seen in the main text.

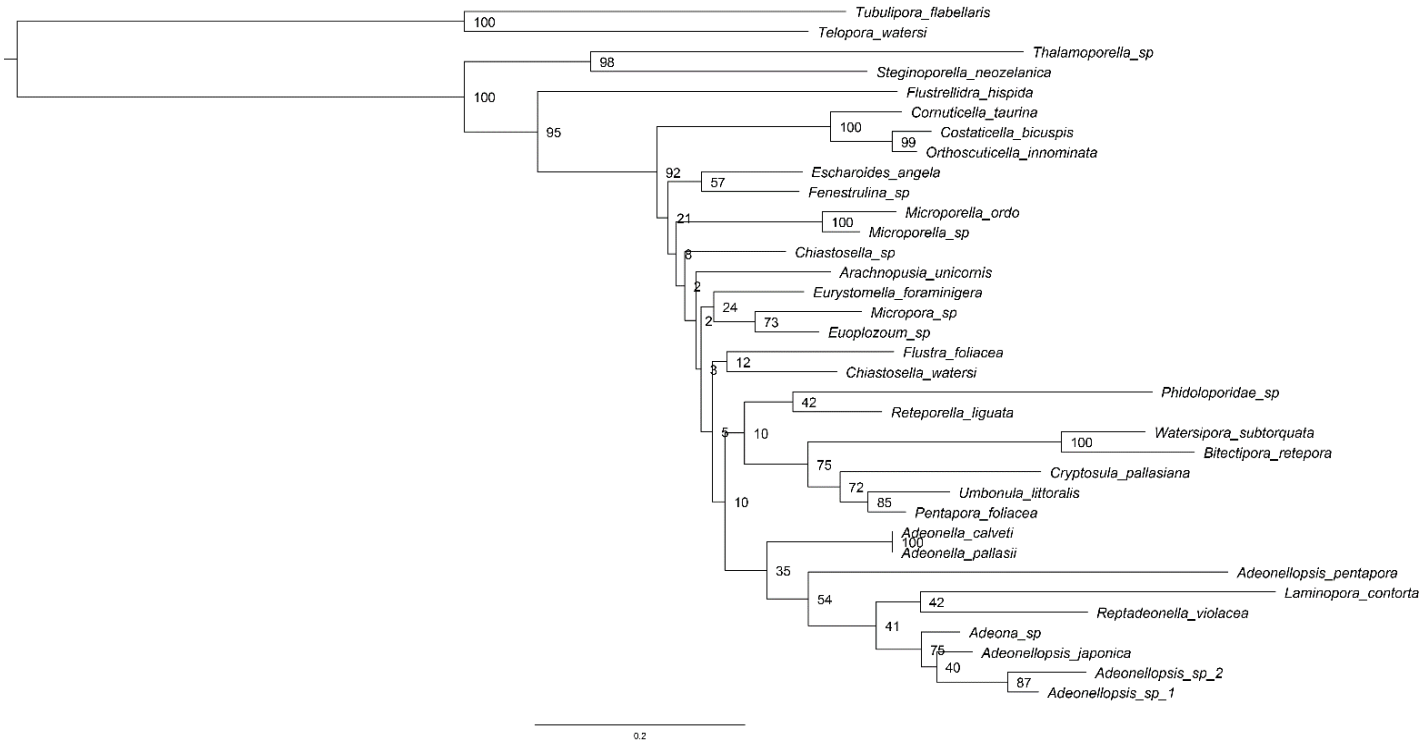

Appendix Figure 10. Mitochondrial *COX1*. ML conducted in RAxML with evolutionary model MtZoa and gamma distribution. Contains 501 amino acids. Please note: *Umbonula littoralis* has a new formal name: *Oshurkovia littoralis* as seen in the main text.

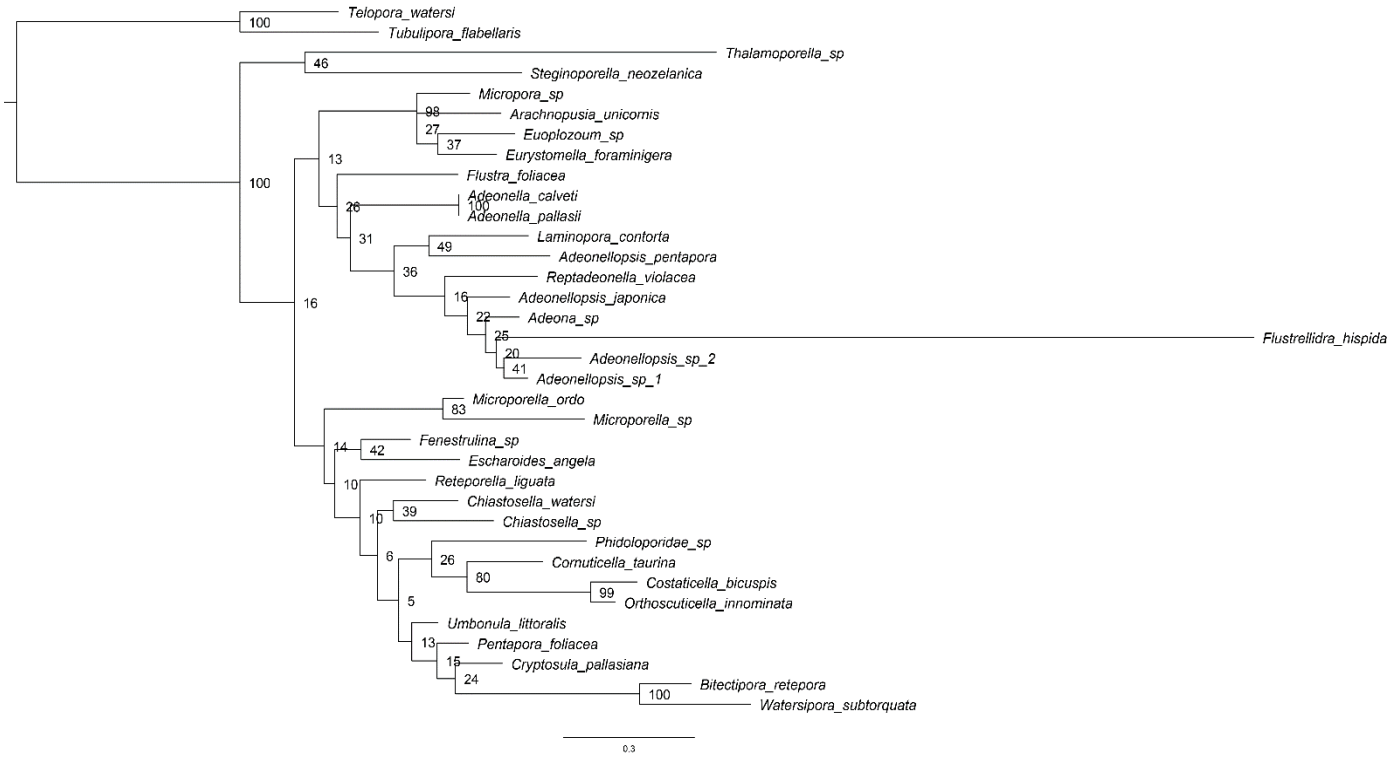

Appendix Figure 11. Mitochondrial *COX2*. ML conducted in RAxML with evolutionary model MtZoa and gamma distribution. Contains 199 amino acids. Please note: *Umbonula littoralis* has a new formal name: *Oshurkovia littoralis* as seen in the main text.

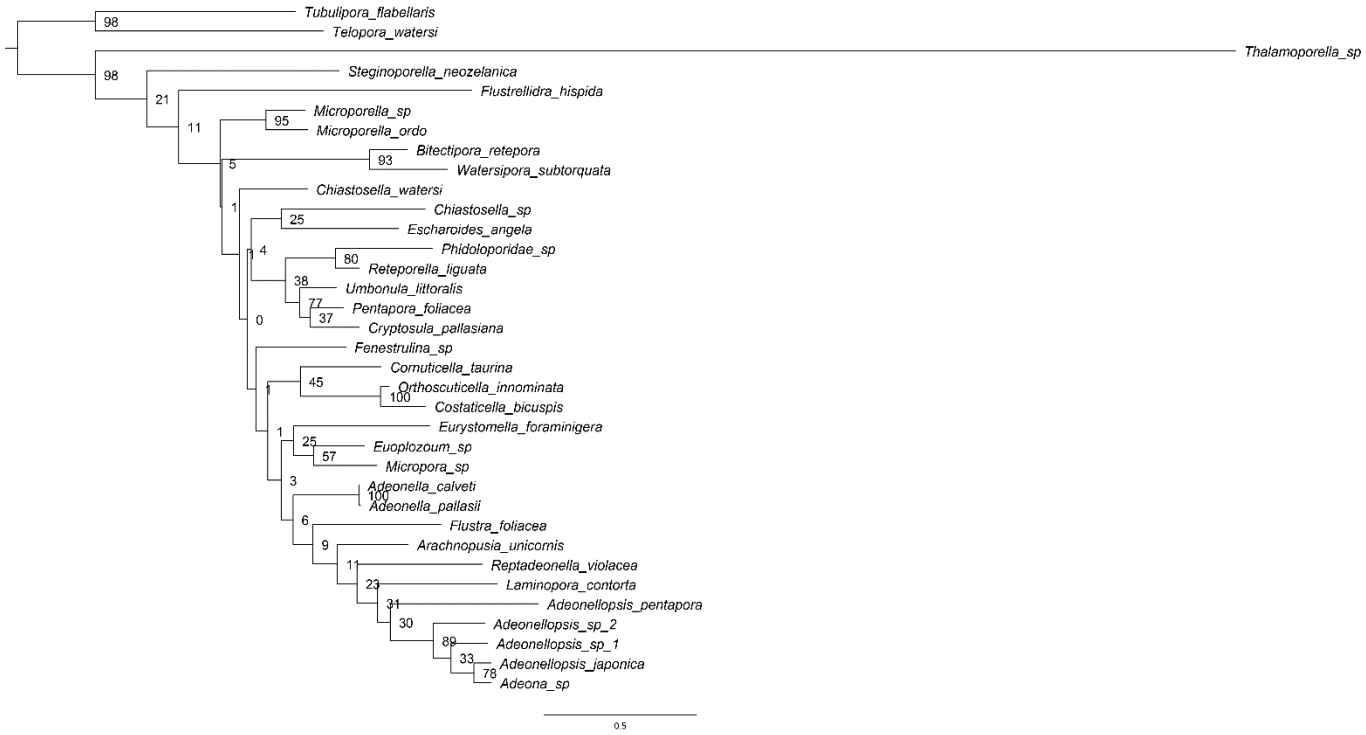

Appendix Figure 12. Mitochondrial *COX3*. ML conducted in RAxML with evolutionary model MtZoa and gamma distribution. Contains 253 amino acids. Please note: *Umbonula littoralis* has a new formal name: *Oshurkovia littoralis* as seen in the main text.

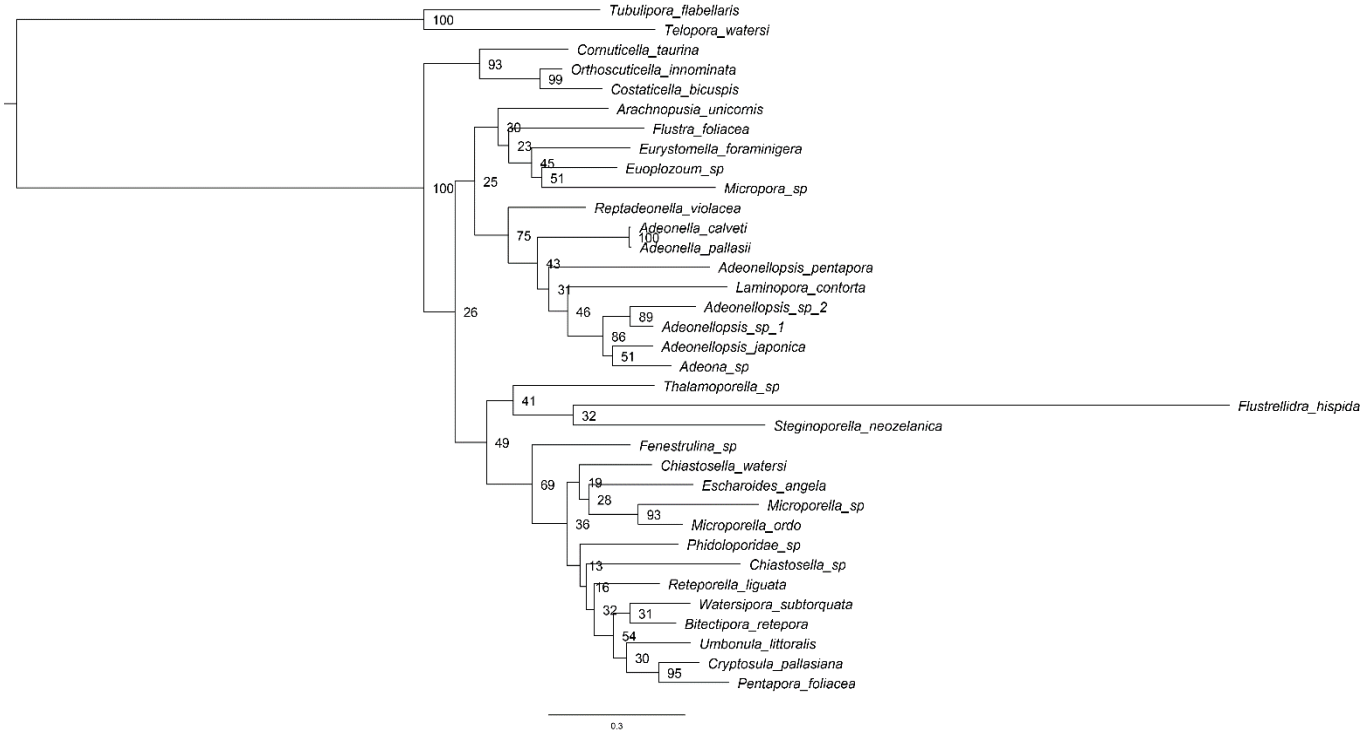

Appendix Figure 13. Mitochondrial *CYTB*. ML conducted in RAxML with evolutionary model MtZoa and gamma distribution. Contains 340 amino acids. Please note: *Umbonula littoralis* has a new formal name: *Oshurkovia littoralis* as seen in the main text.

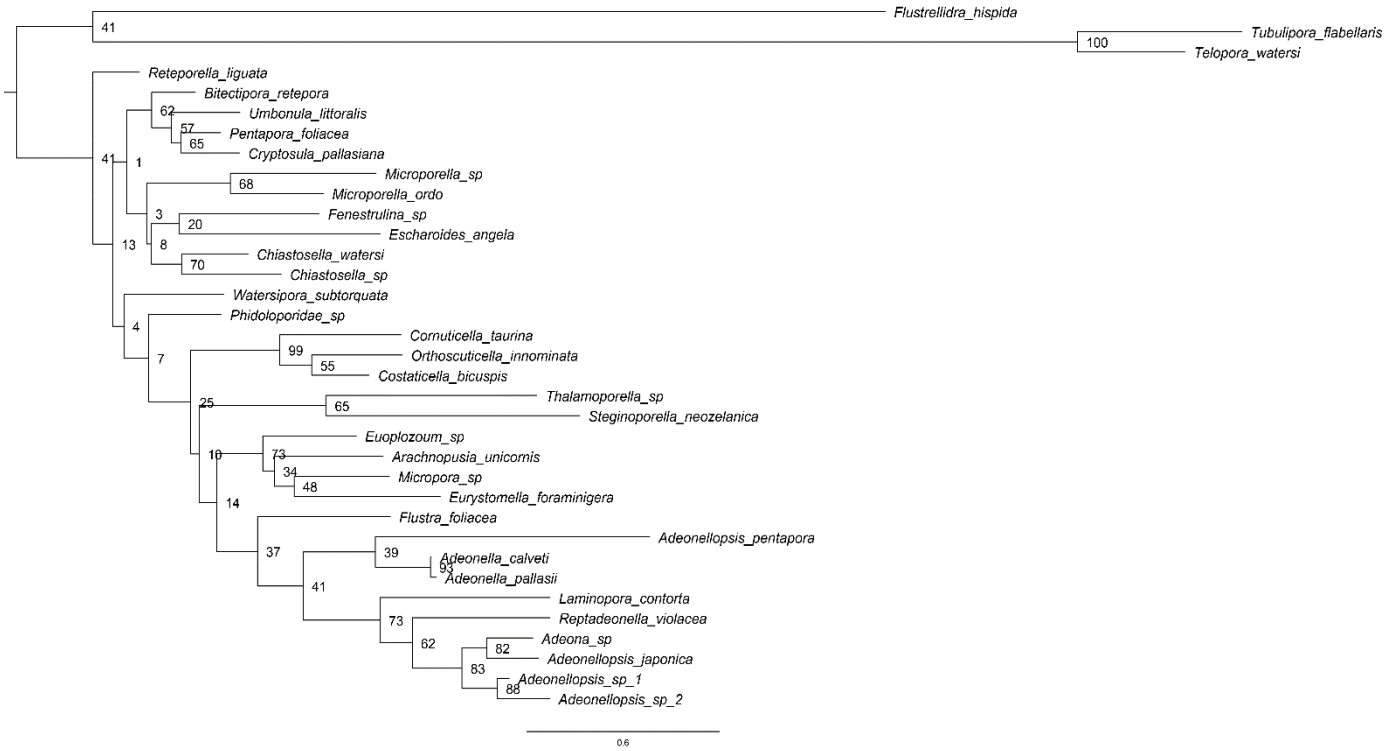

Appendix Figure 14. Mitochondrial *NADH1*. ML conducted in RAxML with evolutionary model MtArt and gamma distribution. Contains 266 amino acids. Please note: *Umbonula littoralis* has a new formal name: *Oshurkovia littoralis* as seen in the main text.

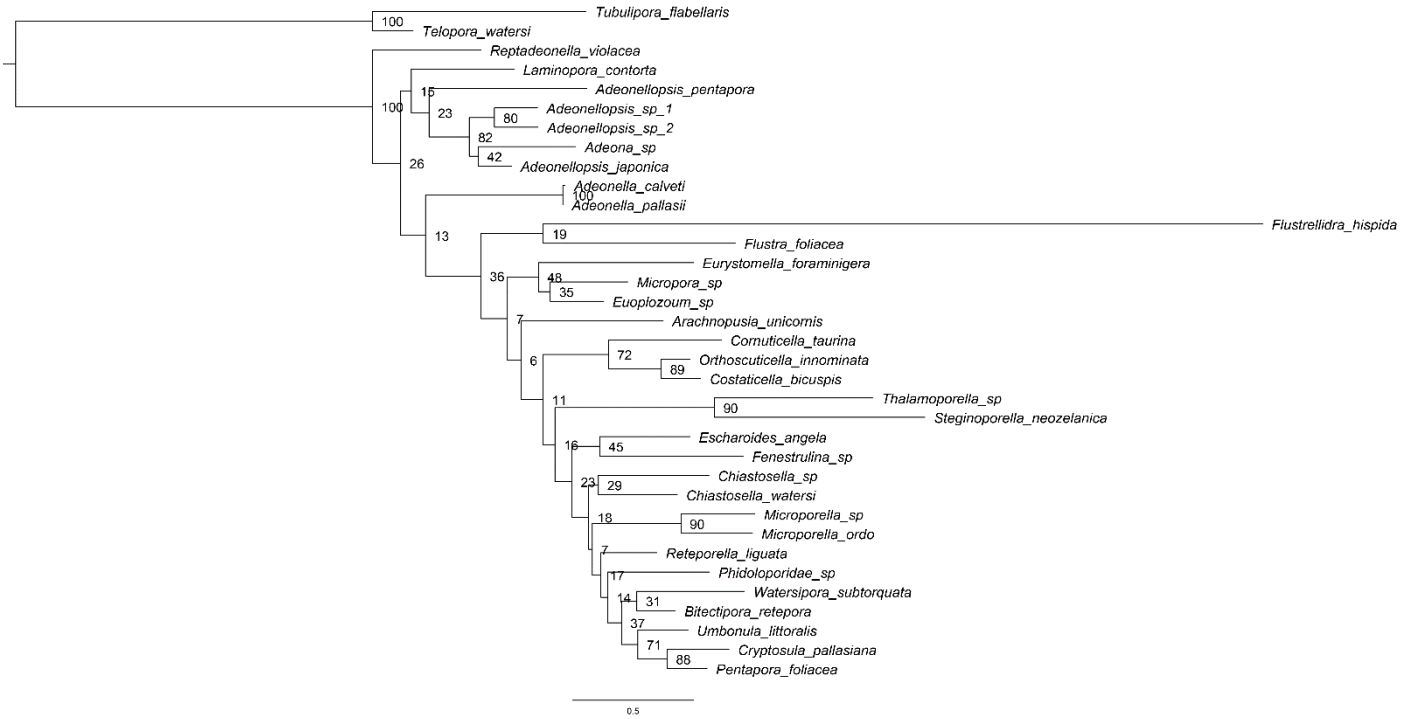

Appendix Figure 15. Mitochondrial *NADH2*. ML conducted in RAxML with evolutionary model MtArt and gamma distribution. Contains 197 amino acids. Please note: *Umbonula littoralis* has a new formal name: *Oshurkovia littoralis* as seen in the main text.

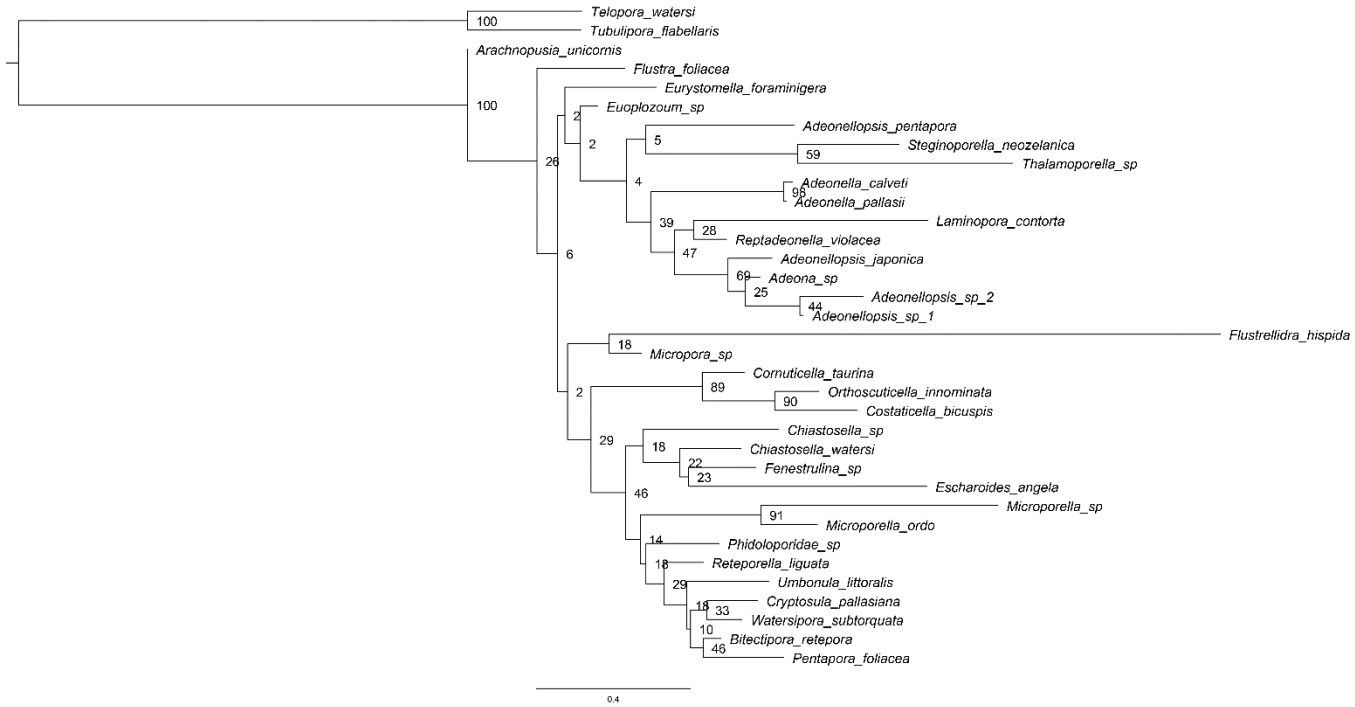

Appendix Figure 16. Mitochondrial *NADH3*. ML conducted in RAxML with evolutionary model MtZoa and gamma distribution. Contains 96 amino acids. Please note: *Umbonula littoralis* has a new formal name: *Oshurkovia littoralis* as seen in the main text.

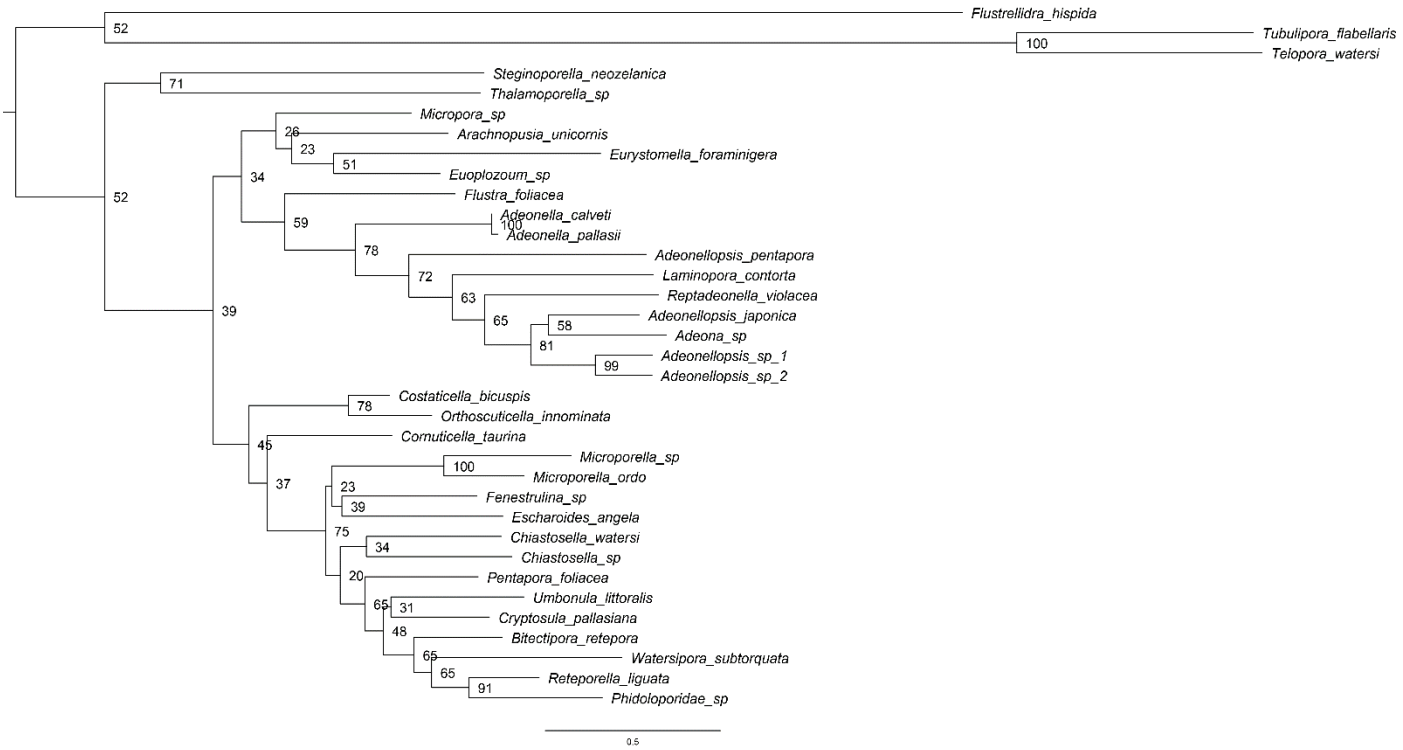

Appendix Figure 17. Mitochondrial *NADH4*. ML conducted in RAxML with evolutionary model MtArt and gamma distribution. Contains 337 amino acids. Please note: *Umbonula littoralis* has a new formal name: *Oshurkovia littoralis* as seen in the main text.

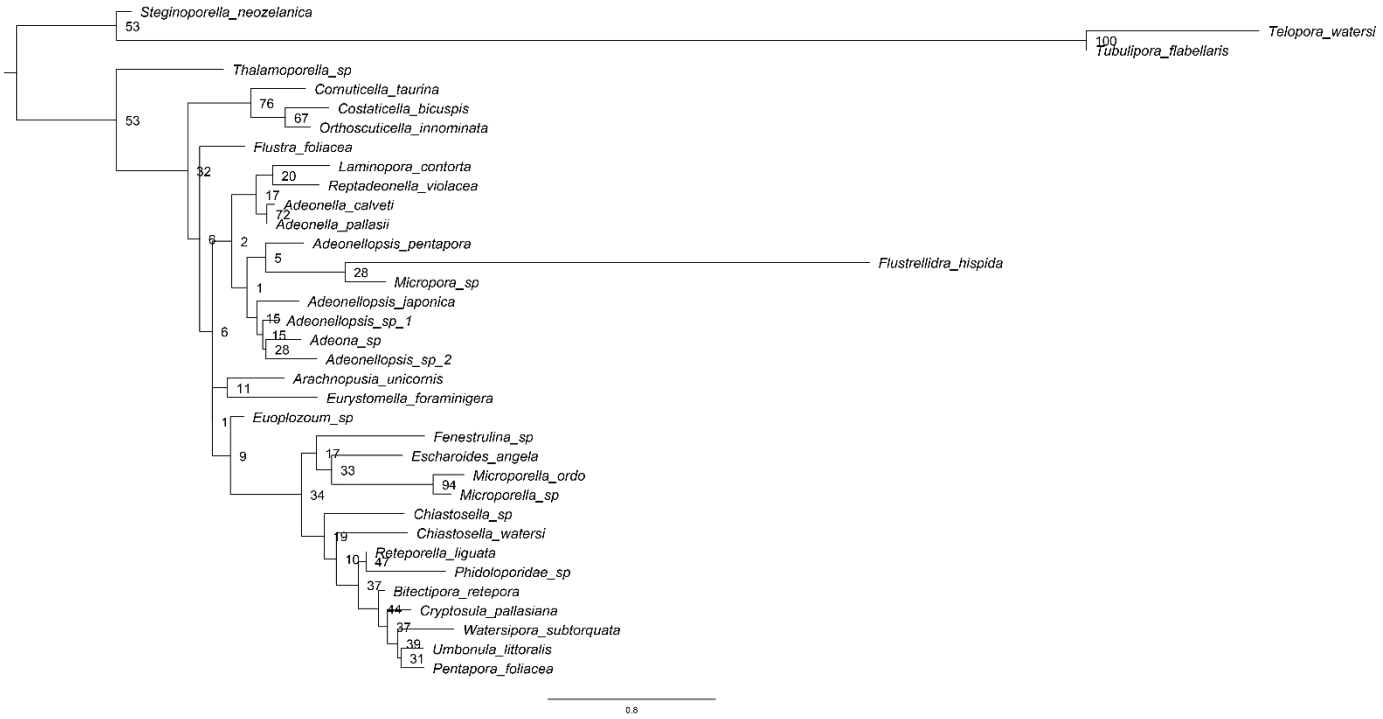

Appendix Figure 18. Mitochondrial *NADH4L*. ML conducted in RAxML with evolutionary model MtArt and gamma distribution. Contains 63 amino acids. Please note: *Umbonula littoralis* has a new formal name: *Oshurkovia littoralis* as seen in the main text.

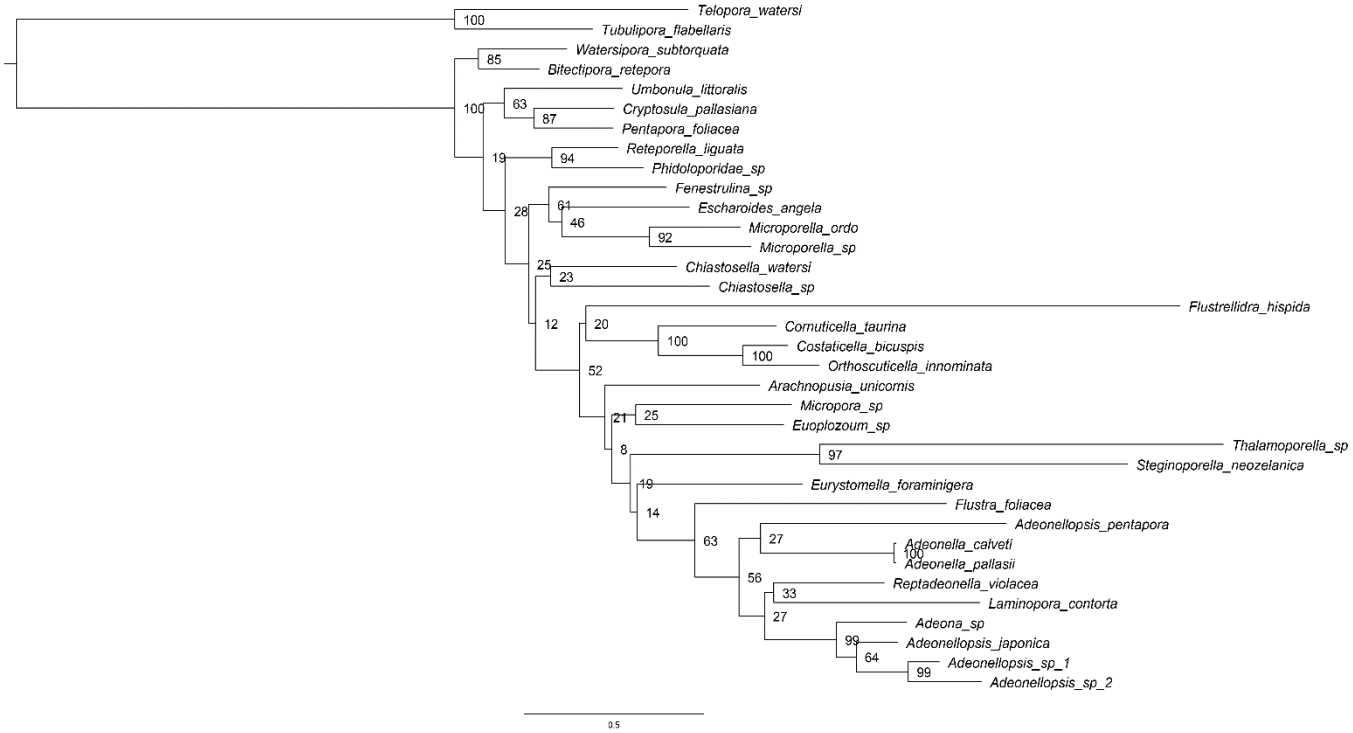

Appendix Figure 19. Mitochondrial *NADH5*. ML conducted in RAxML with evolutionary model MtArt and gamma distribution. Contains 457 amino acids. Please note: *Umbonula littoralis* has a new formal name: *Oshurkovia littoralis* as seen in the main text.

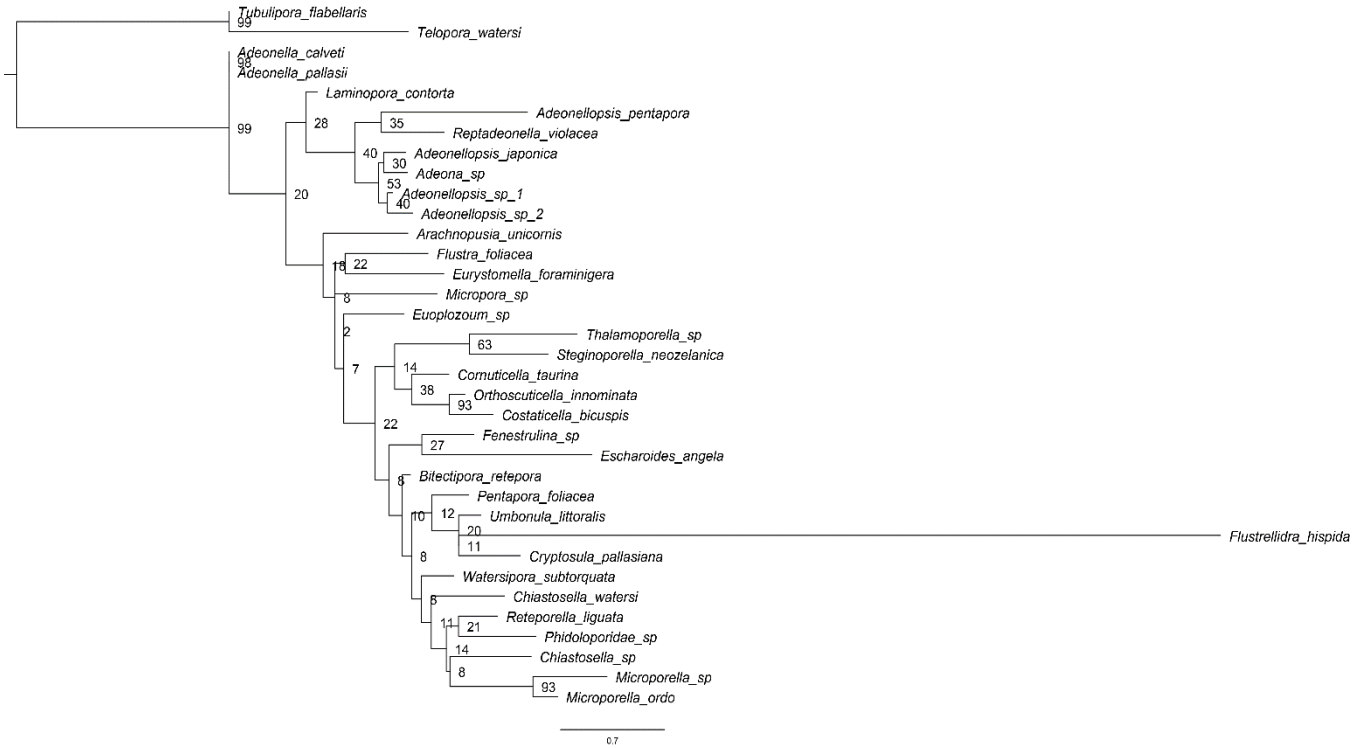

Appendix Figure 20. Mitochondrial *NADH6*. ML conducted in RAxML with evolutionary model MtArt and gamma distribution. Contains 91 amino acids. Please note: *Umbonula littoralis* has a new formal name: *Oshurkovia littoralis* as seen in the main text.

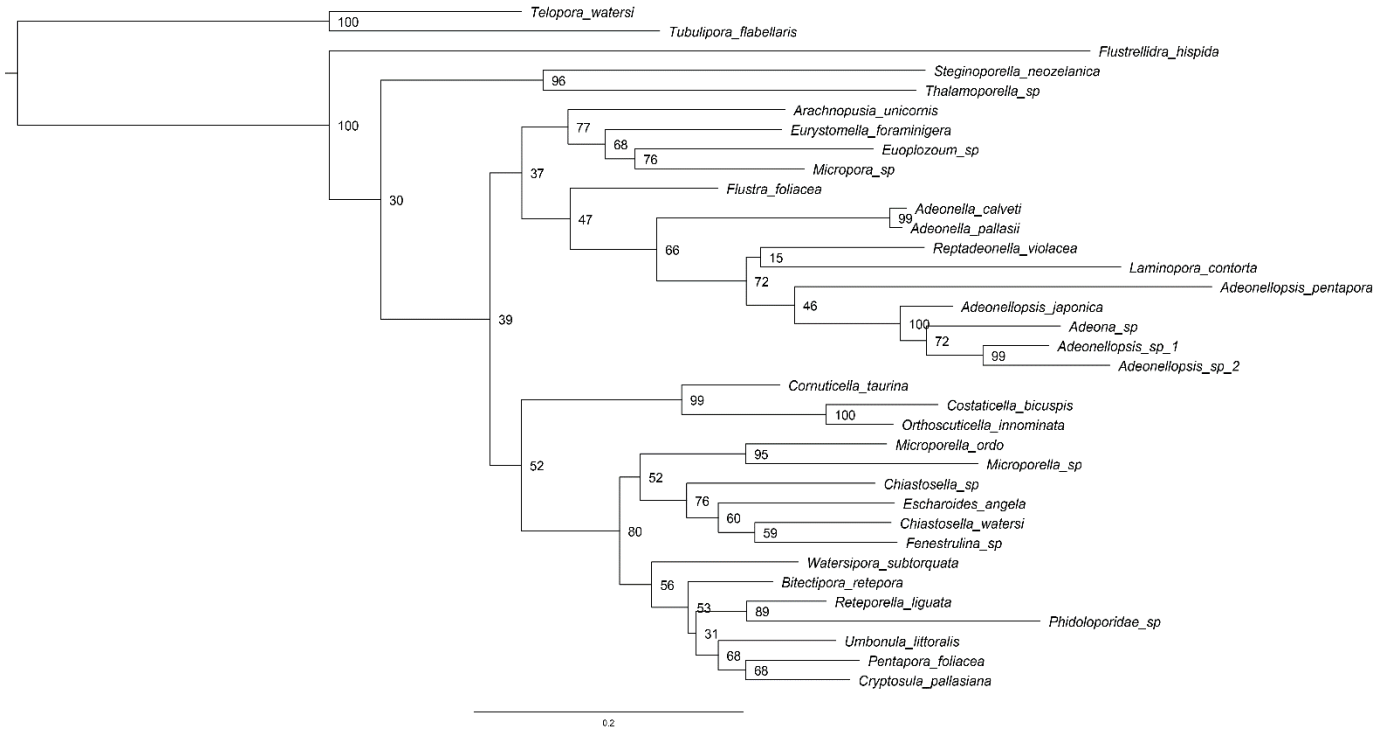

Appendix Figure 21. Mitochondrial rrnL. ML conducted in RAxML with evolutionary model GTR and gamma distribution. Contains 866 nucleotides. Please note: *Umbonula littoralis* has a new formal name: *Oshurkovia littoralis* as seen in the main text.

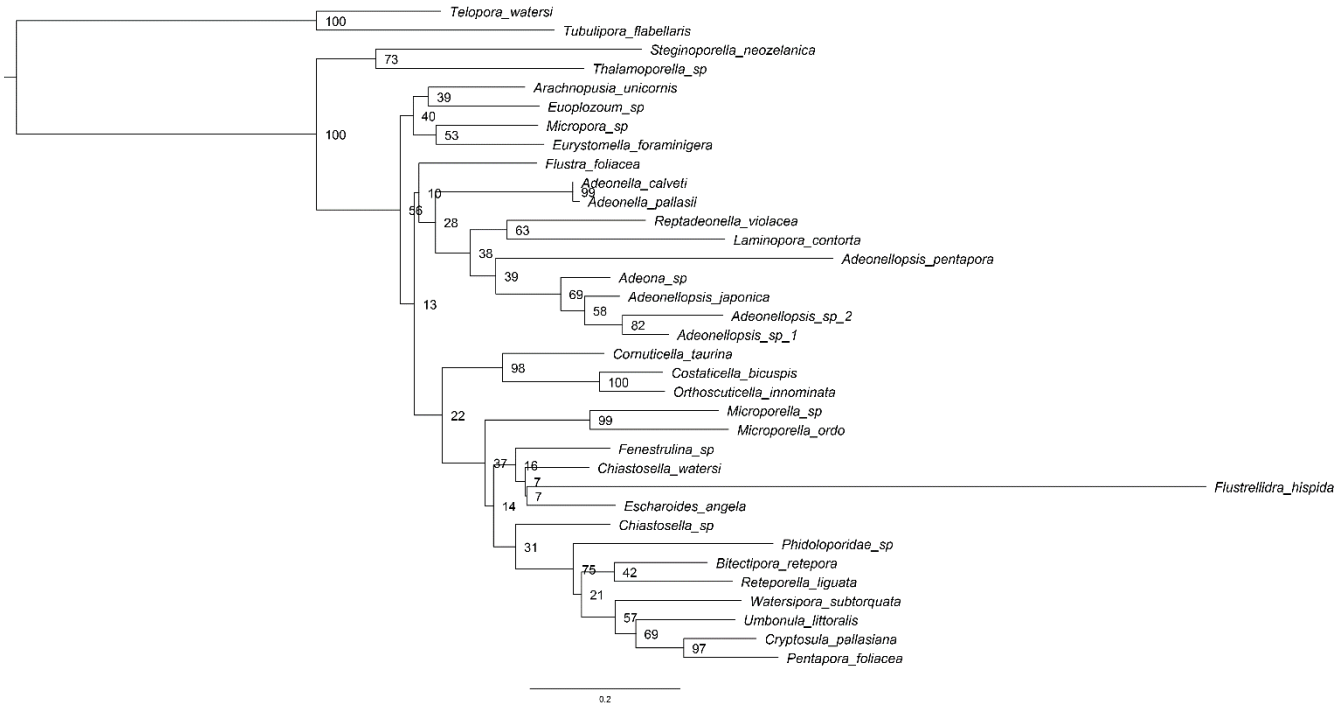

Appendix Figure 22. Mitochondrial rrnS. ML conducted in RAxML with evolutionary model GTR and gamma distribution. Contains 670 nucleotides. Please note: *Umbonula littoralis* has a new formal name: *Oshurkovia littoralis* as seen in the main text.

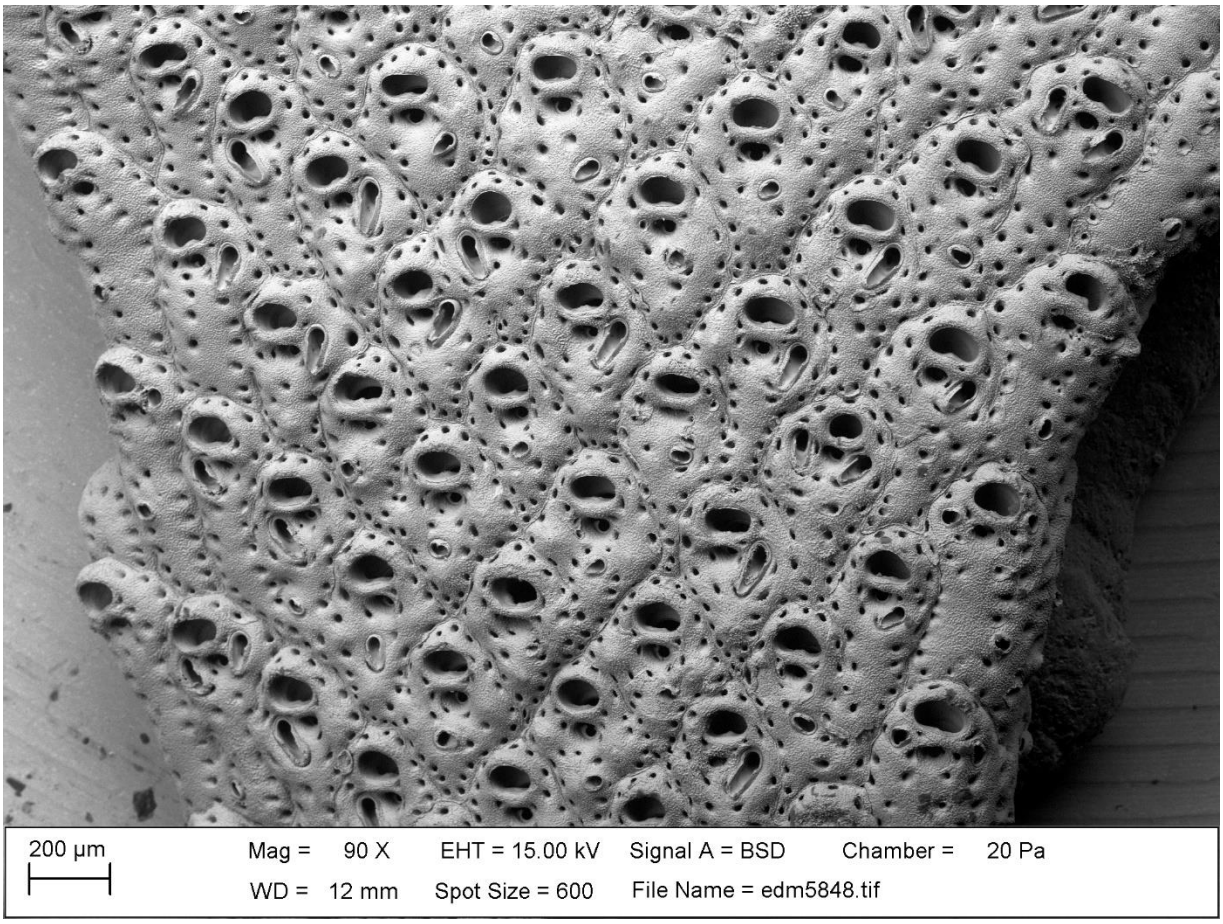

Appendix Figure 23. SEM, ***Adeonella calveti*** Canu & Bassler, 1930
Specimen ID: BLEED 38, Locality: Off Oran, Algeria, Photo credits: Emanuela Di Martino

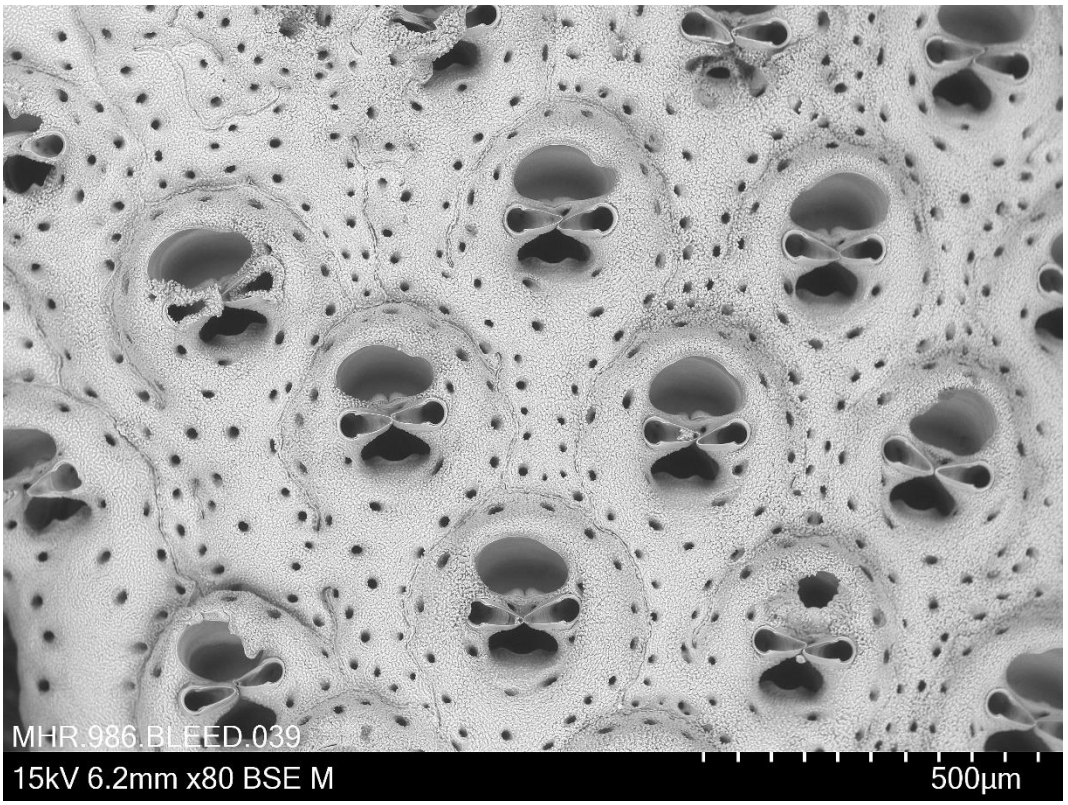

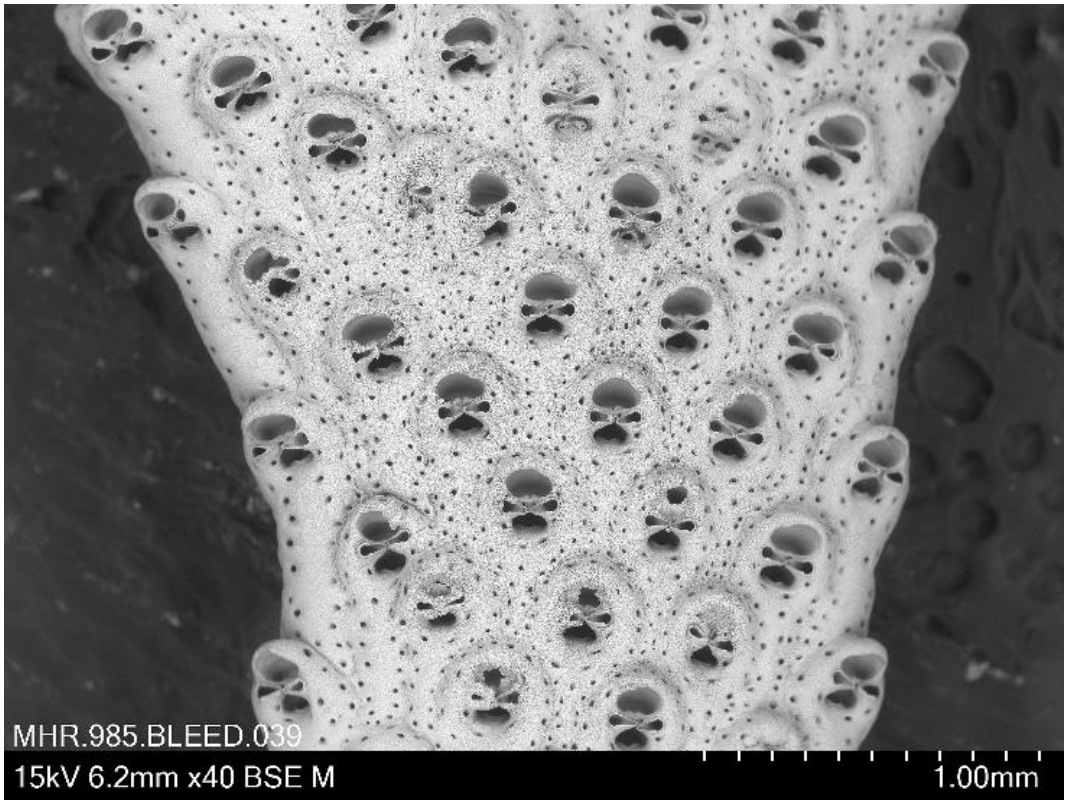

Appendix Figure 24. SEM, ***Adeonella pallasii*** Heller, 1867
Specimen ID: BLEED 39, Locality: Cyprus, Photo credits: Mali Hamre Ramsfjell

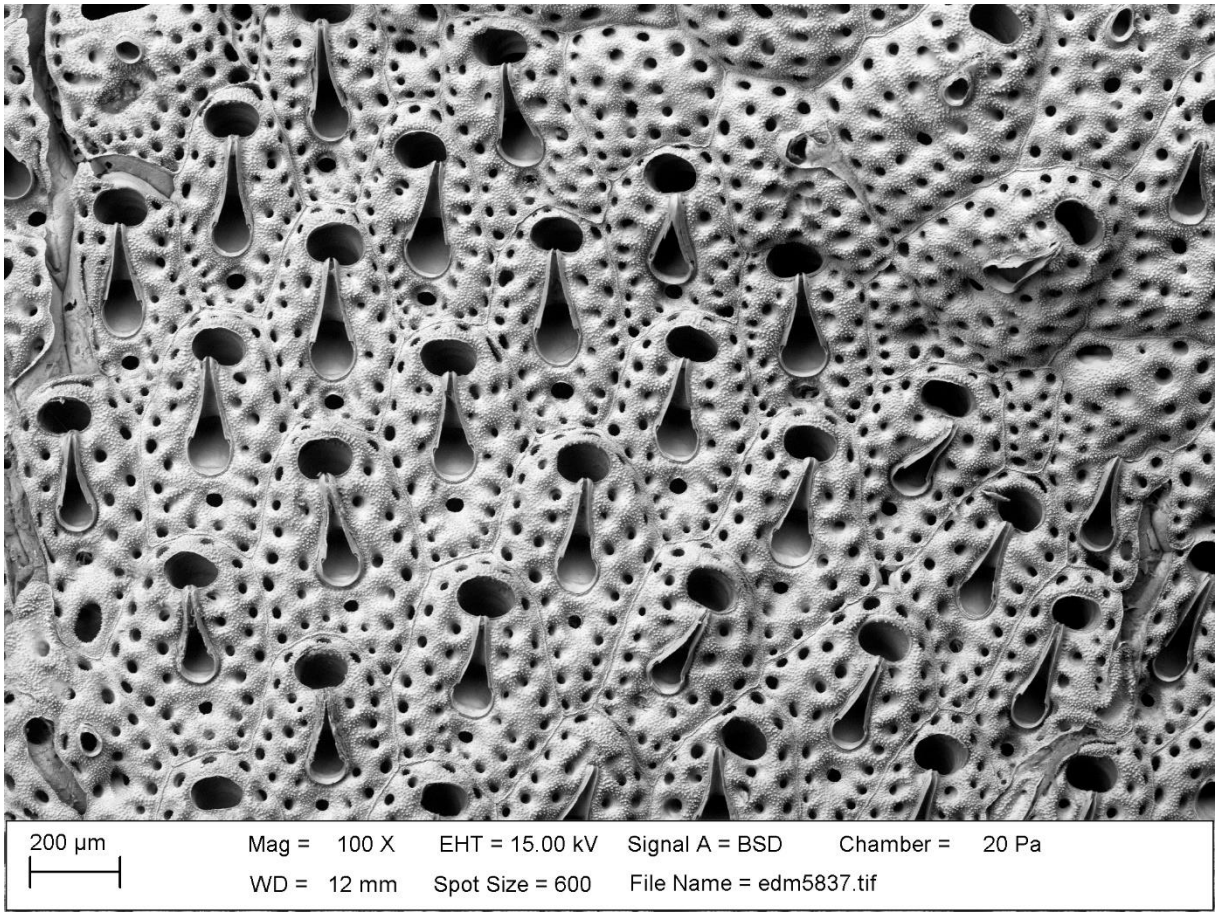

Appendix Figure 25. SEM, ***Reptadeonella violacea*** Johnston, 1847
Specimen ID: BLEED 41, Locality: off Rovinj, Croatia, Photo credits: Emanuela Di Martino

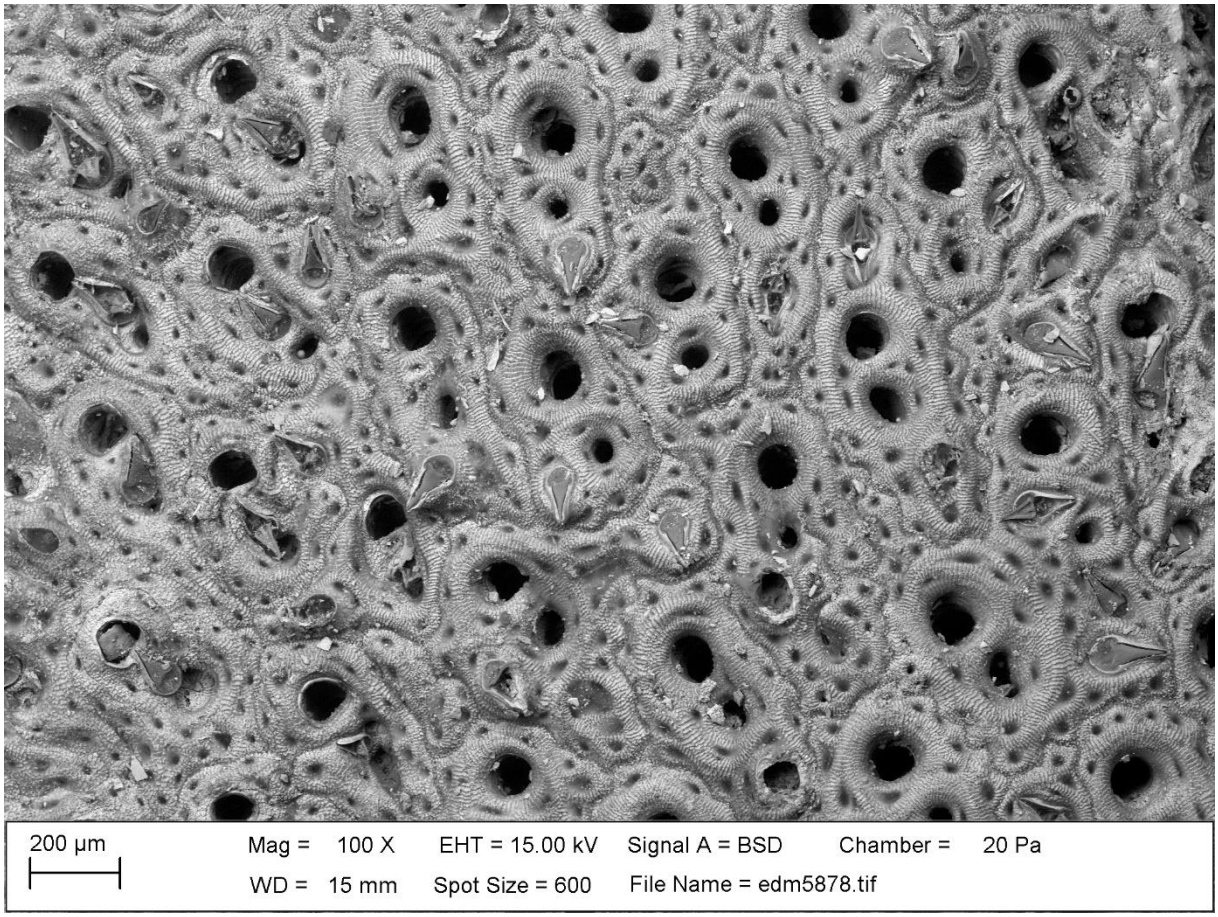

Appendix Figure 26. SEM, ***Adeonellopsis* sp. 1**
Specimen ID: BLEED 48, Locality: S New Zealand, Photo credits: Emanuela Di Martino

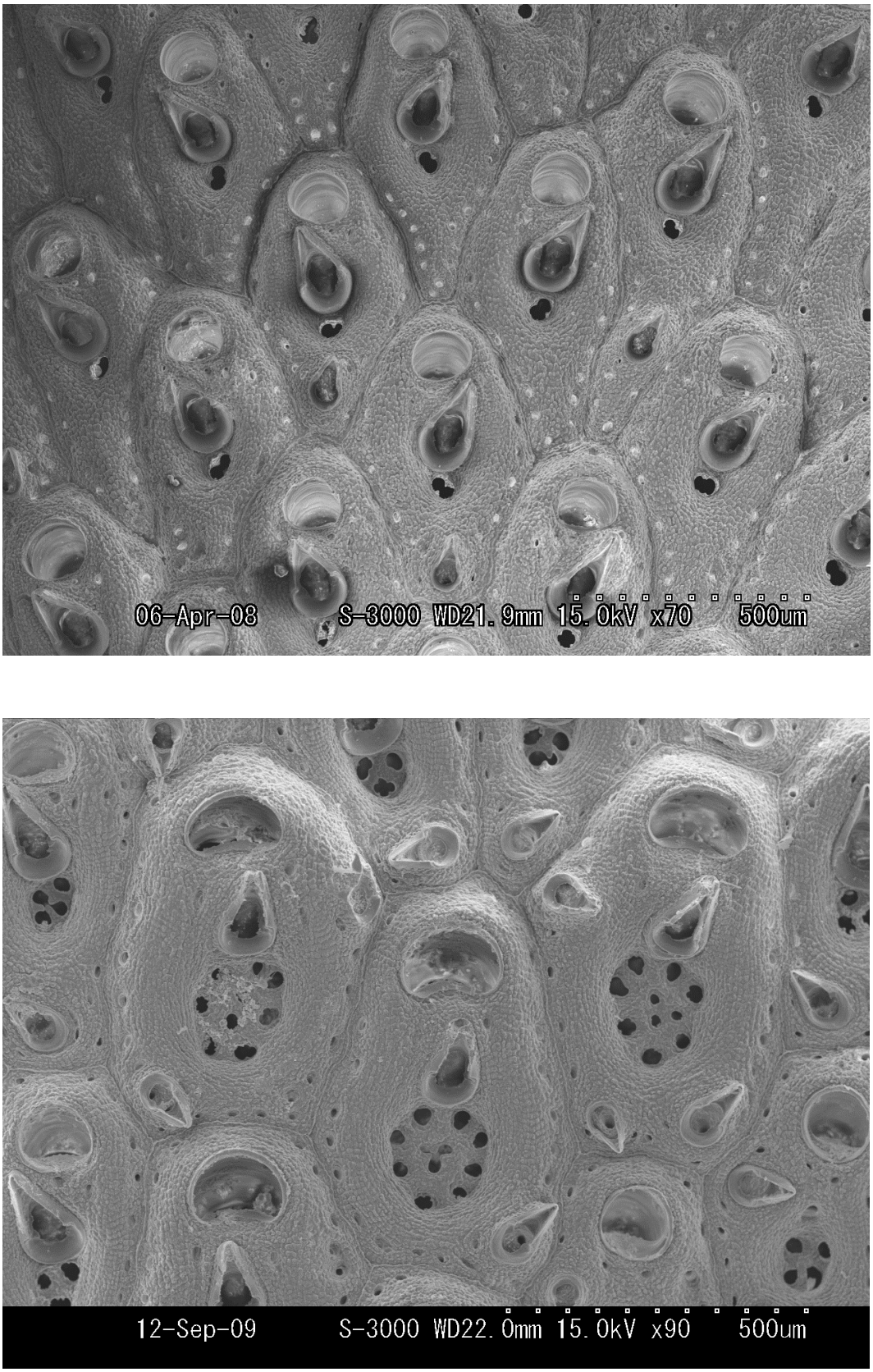

Appendix Figure 27. SEM, ***Adeonellopsis japonica*** Ortmann, 1890
Specimen ID: BLEED 49, Locality: off Otsuchi Bay, Iwate Pref., Japan, Photo credits: Masato Hirose

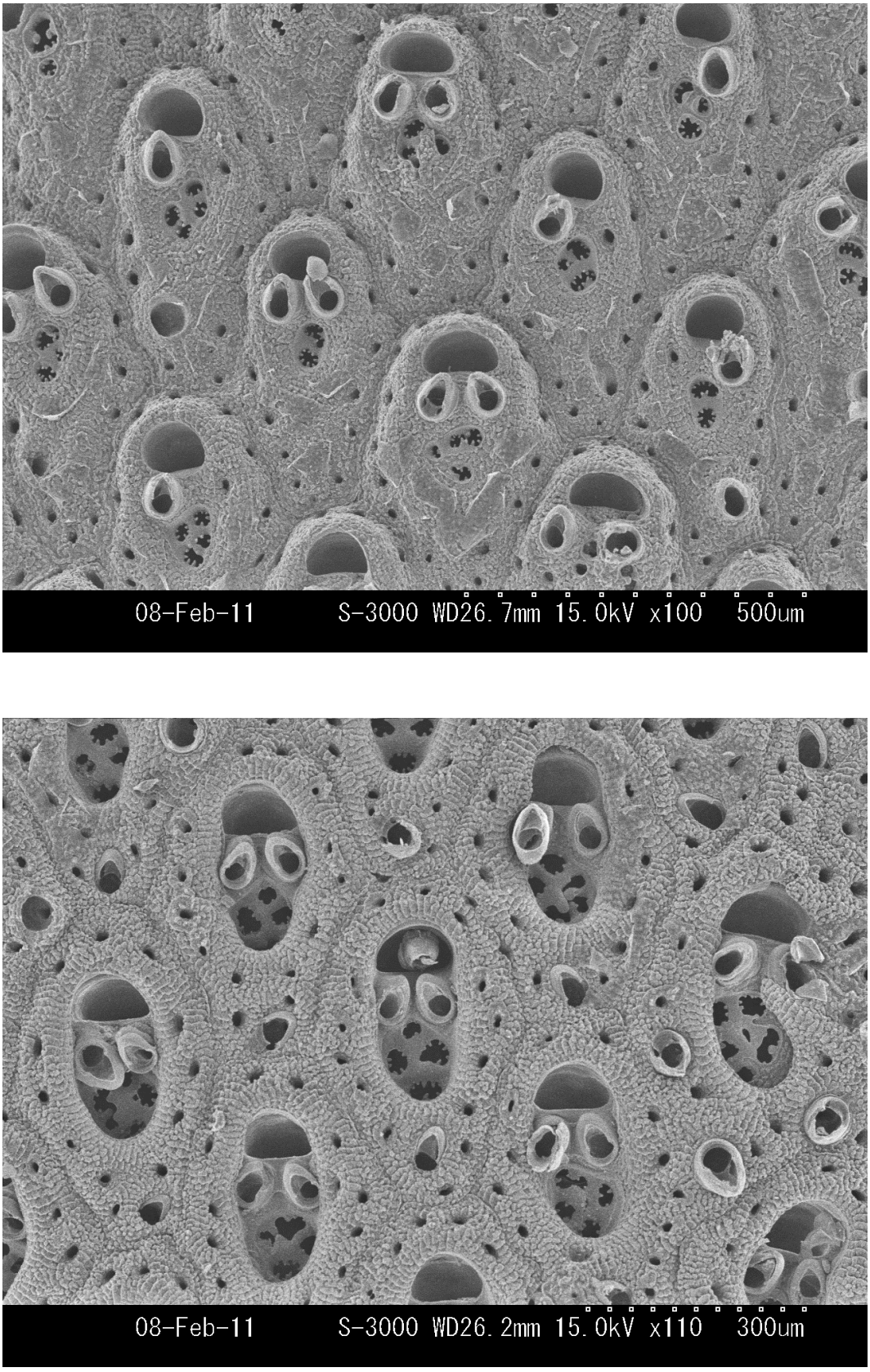

Appendix Figure 28. SEM, ***Adeonellopsis pentapora*** Canu & Bassler, 1929
Specimen ID: BLEED 50, Locality: off Otsuchi Bay, Iwate Pref., Japan, Photo credits: Masato Hirose

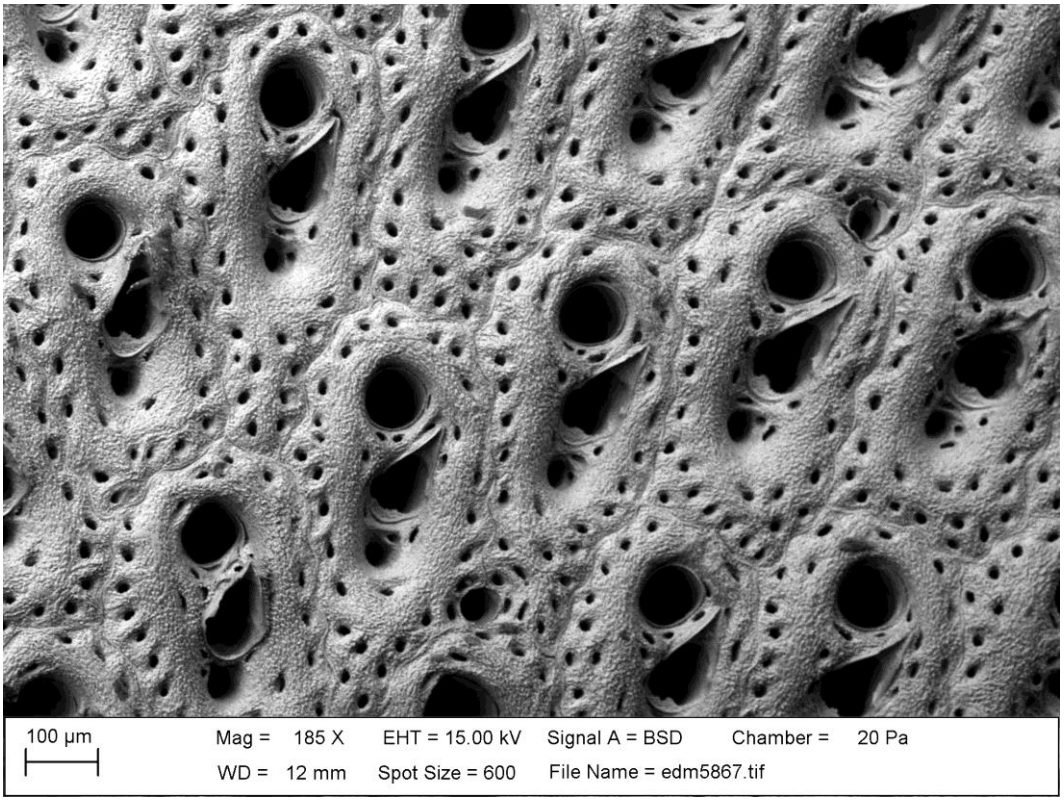

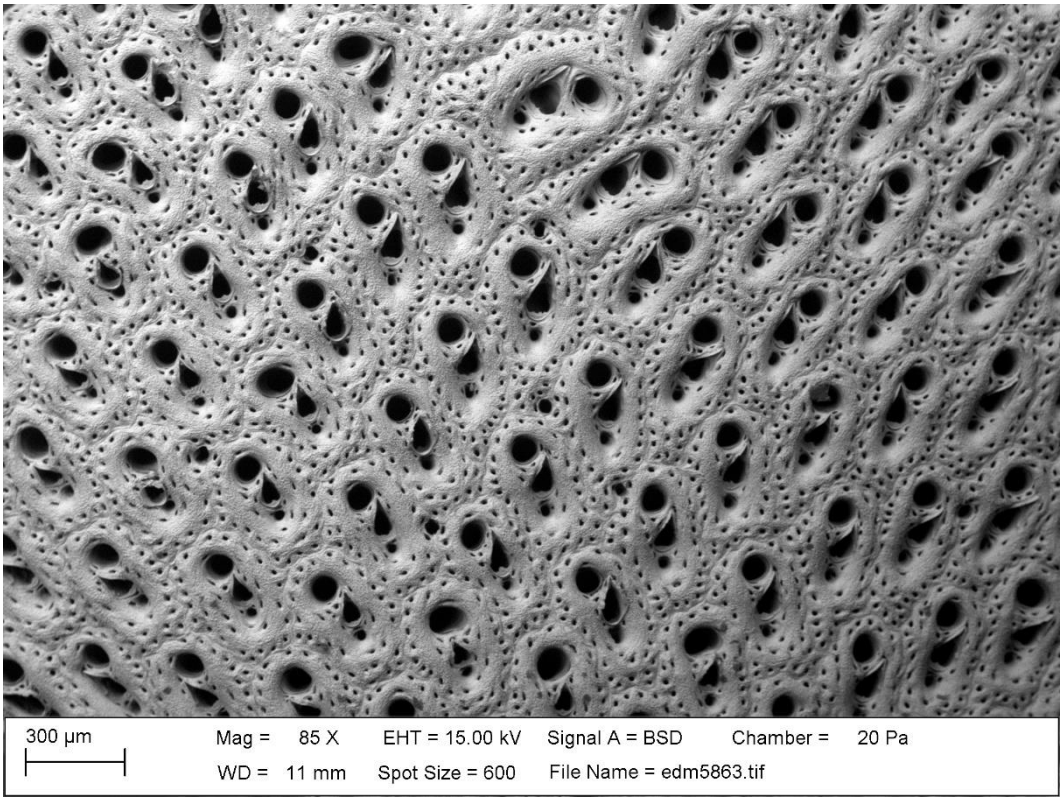

Appendix Figure 29. SEM, ***Adeona* sp.**
Specimen ID: BLEED 298, Locality: Abrolhos Shelf, Australia, Photo credits: Emanuela Di Martino

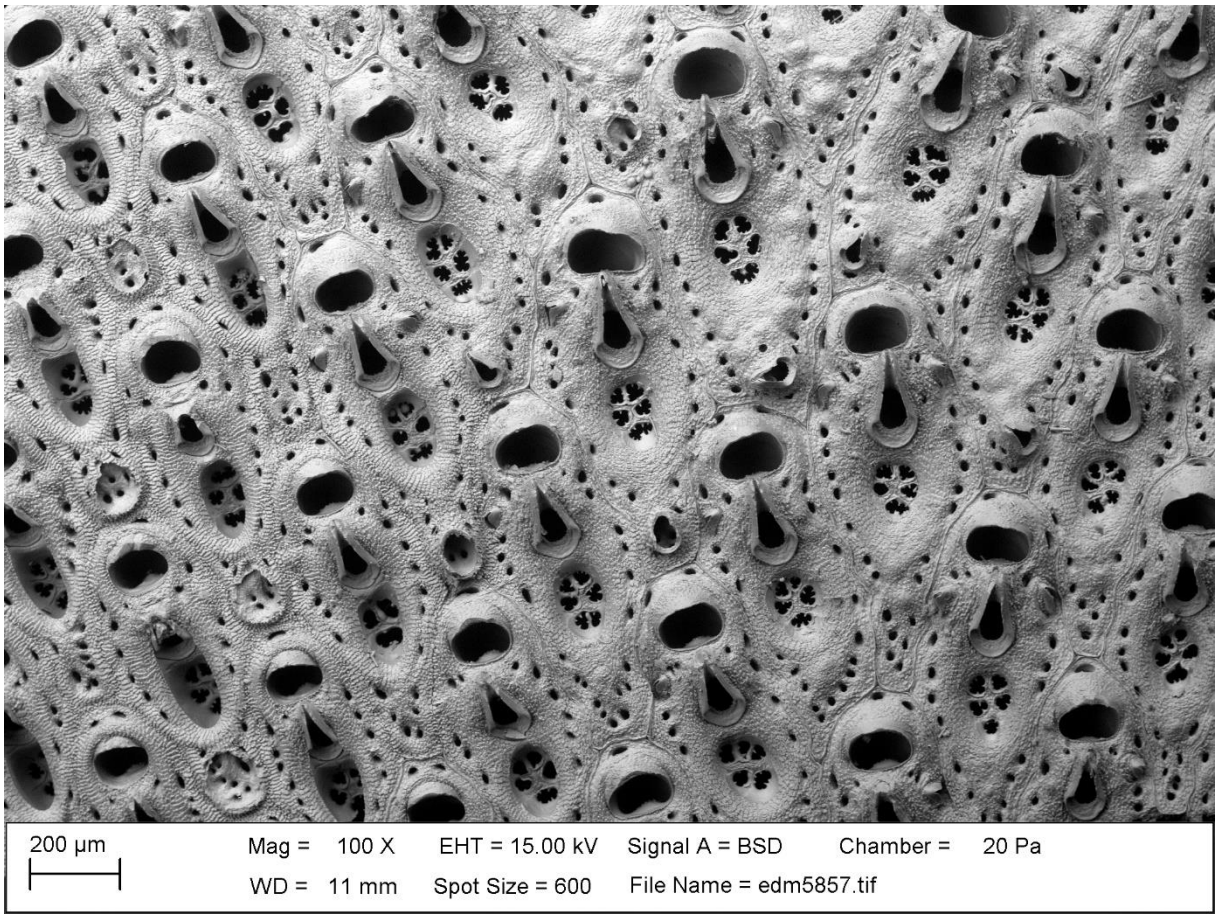

Appendix Figure 30. SEM, ***Adeonellopsis* sp.2**
Specimen ID: BLEED 301, Locality: off Bald Isld, Australia, Photo credits: Emanuela Di Martino

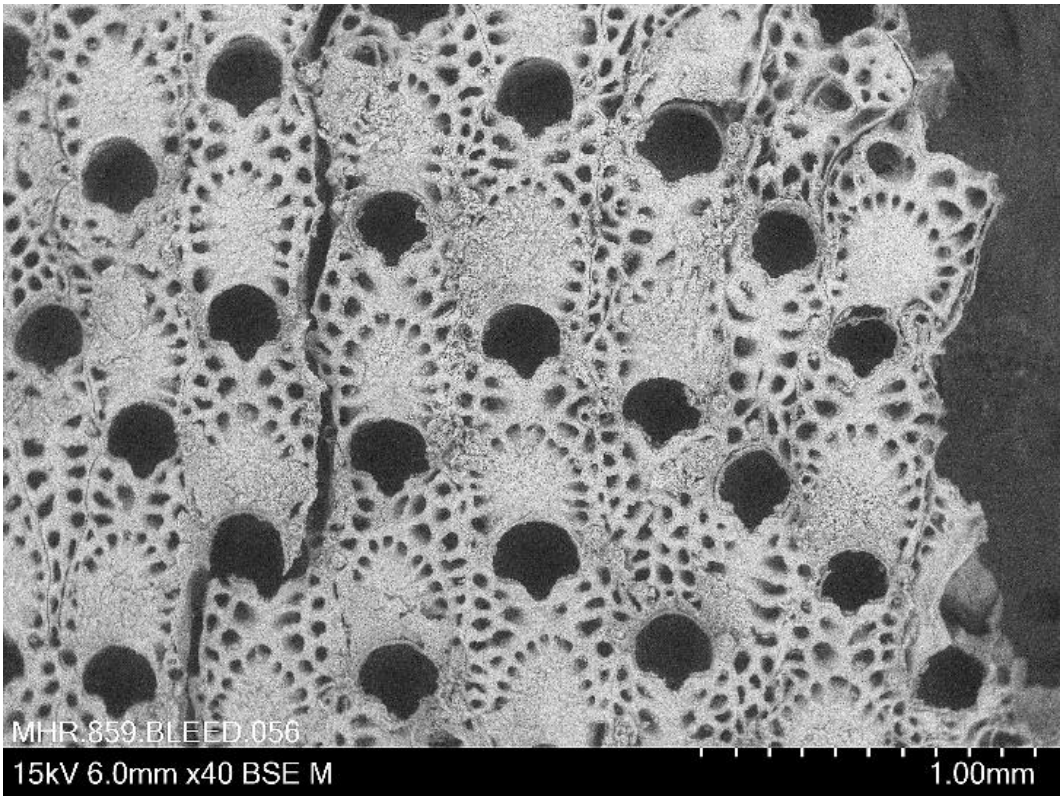

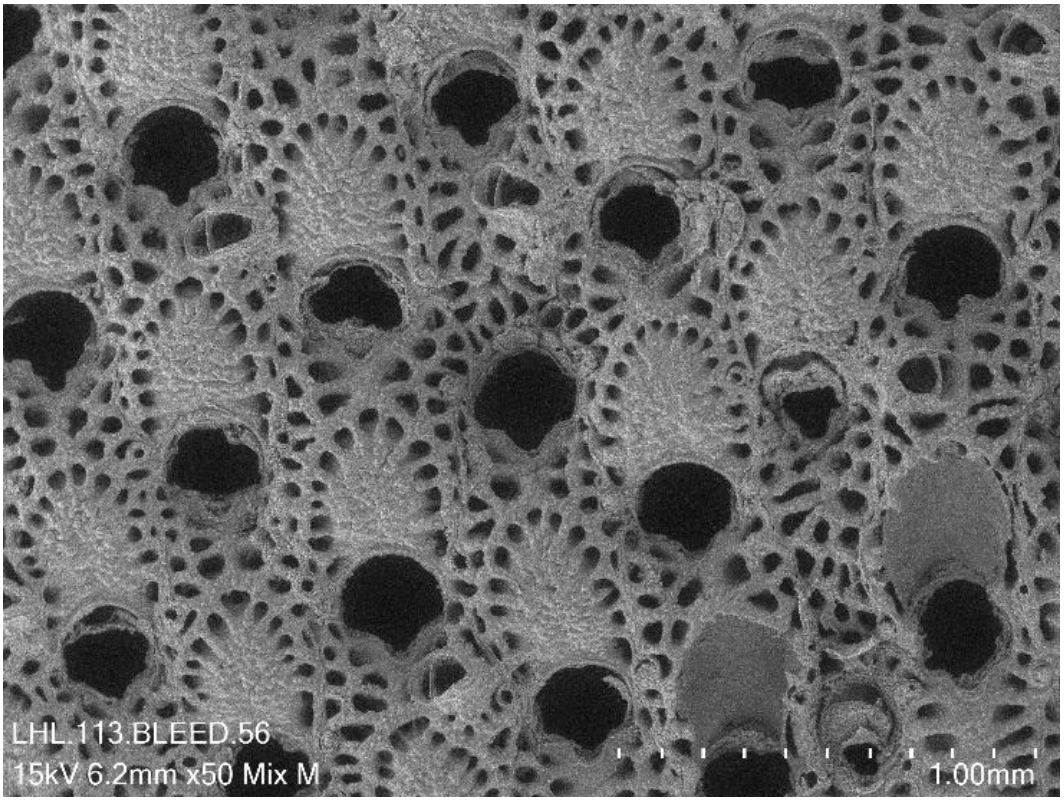

Appendix Figure 31. SEM, ***Chiastosella watersi*** Stach, 1937
Specimen ID: BLEED 56, Locality: Castlepoint, Wairarapa, New Zealand, Photo credits: Lee Hsiang Liow and Mali Hamre Ramsfjell

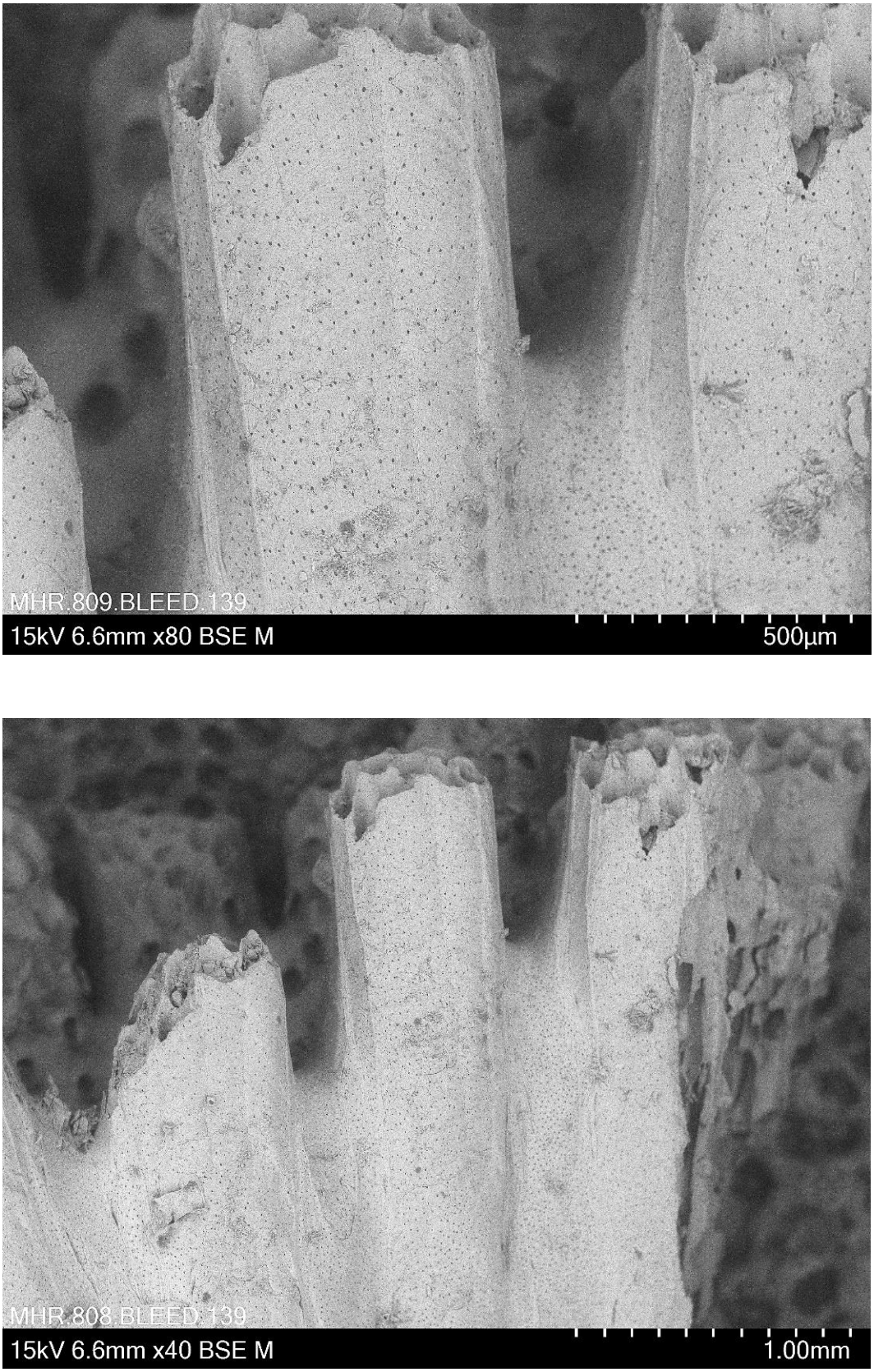

Appendix Figure 32. SEM, ***Telopora watersi*** Harmer, 1915
Specimen ID: BLEED 139, Locality: New Zealand, Photo credits: Mali Hamre Ramsfjell

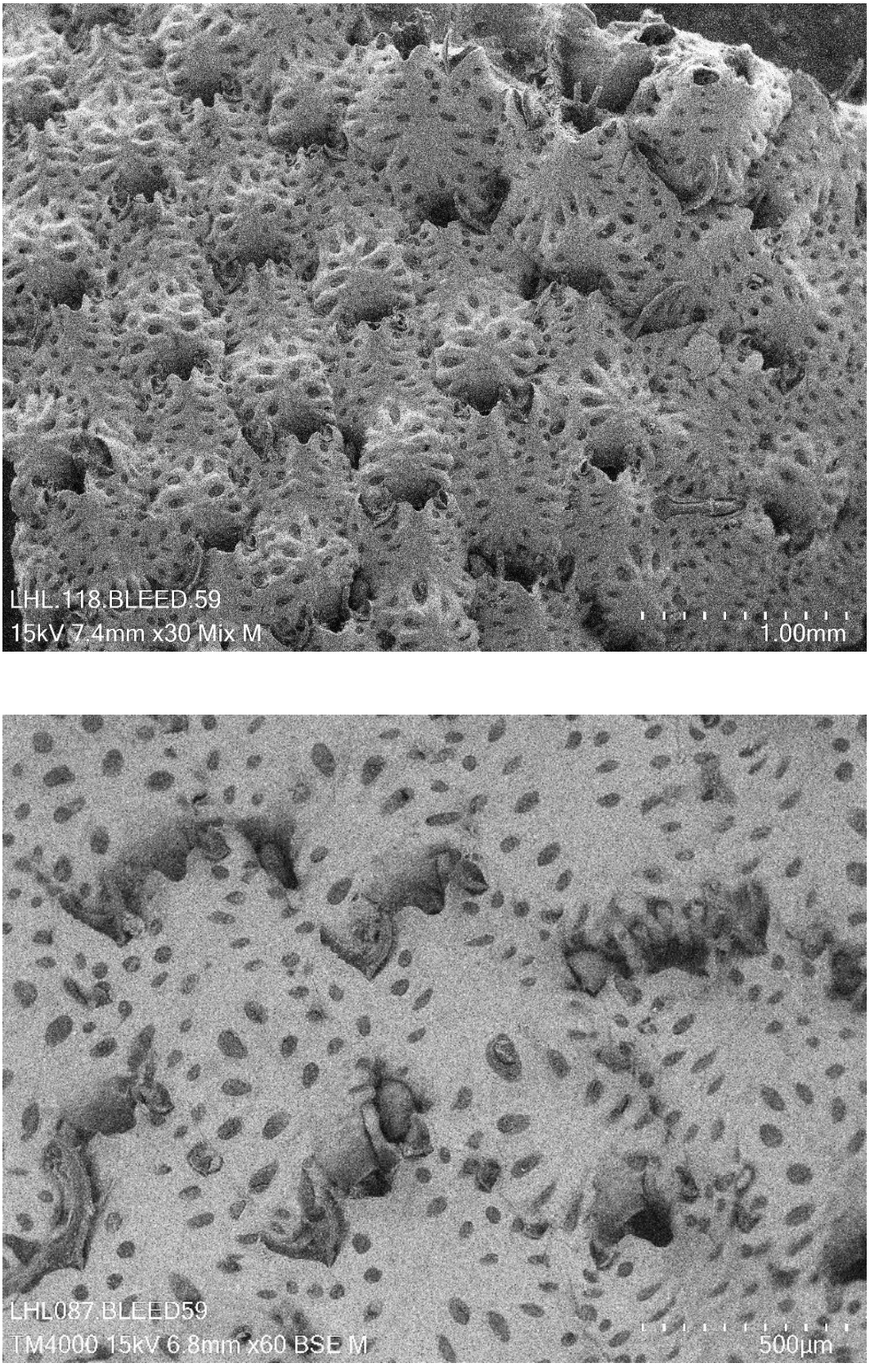

Appendix Figure 33. SEM, ***Escharoides angela*** Hutton, 1873
Specimen ID: BLEED 59, Locality: Middlesex Bank, New Zealand, Photo credits: Lee Hsiang Liow

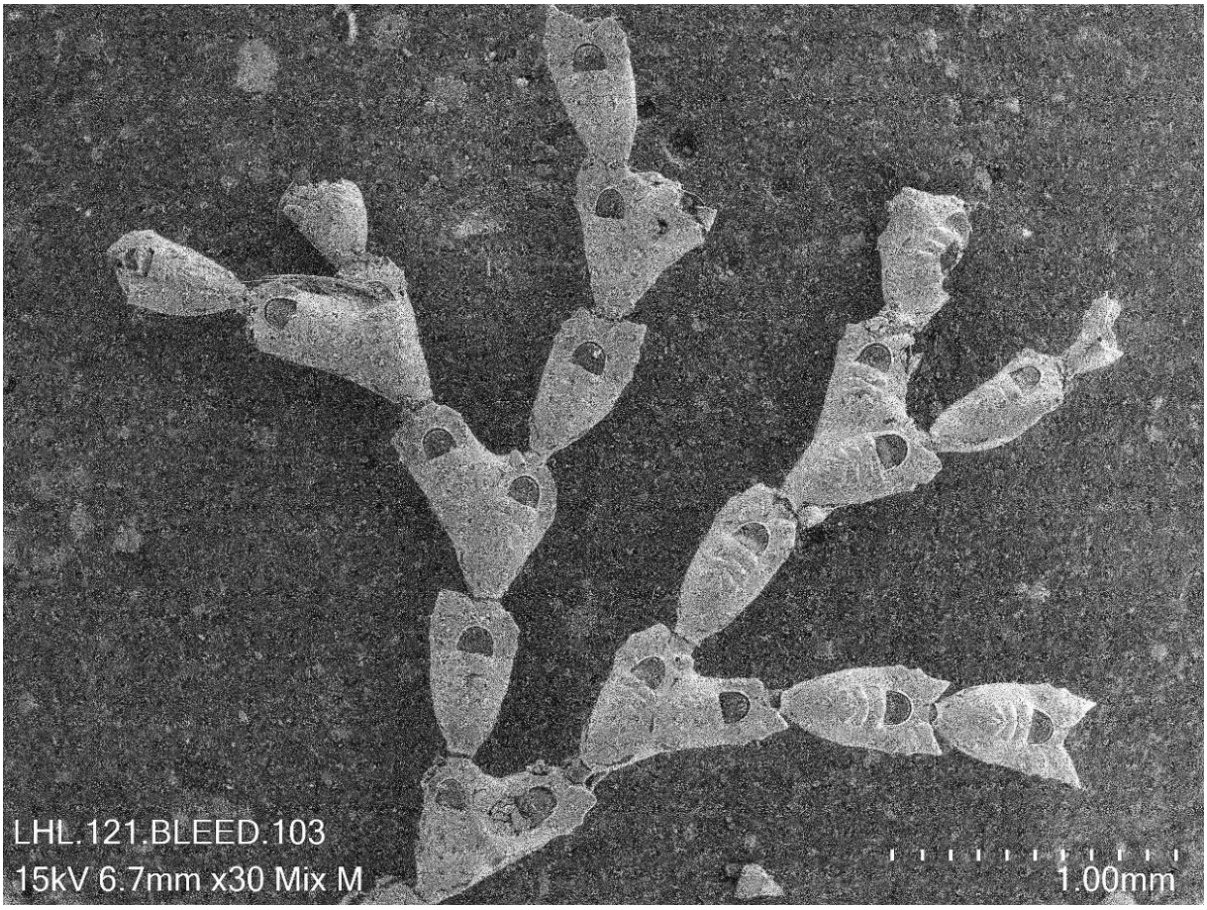

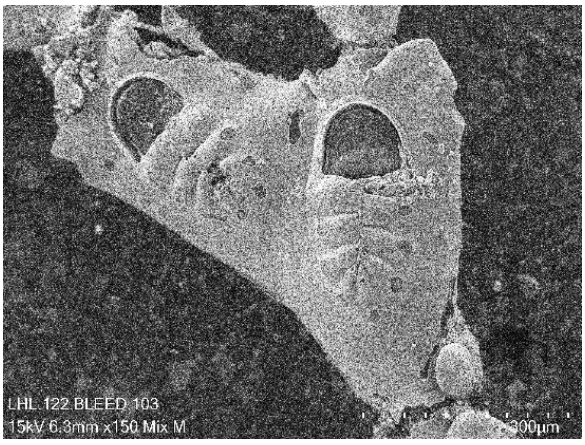

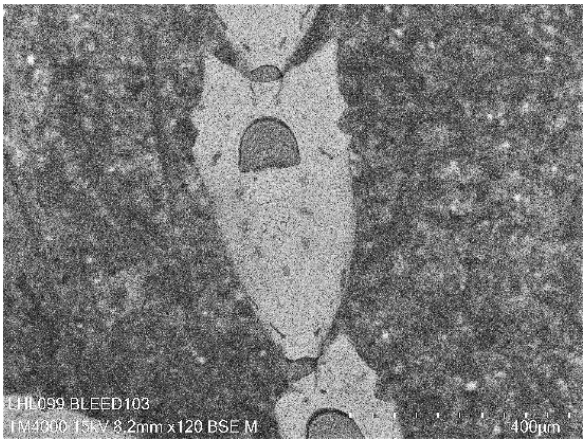

Appendix Figure 34. SEM, ***Costaticella bicuspis*** Gray, 1843
Specimen ID: BLEED 103, Locality: Middlesex Bank, New Zealand, Photo credits: Lee Hsiang Liow

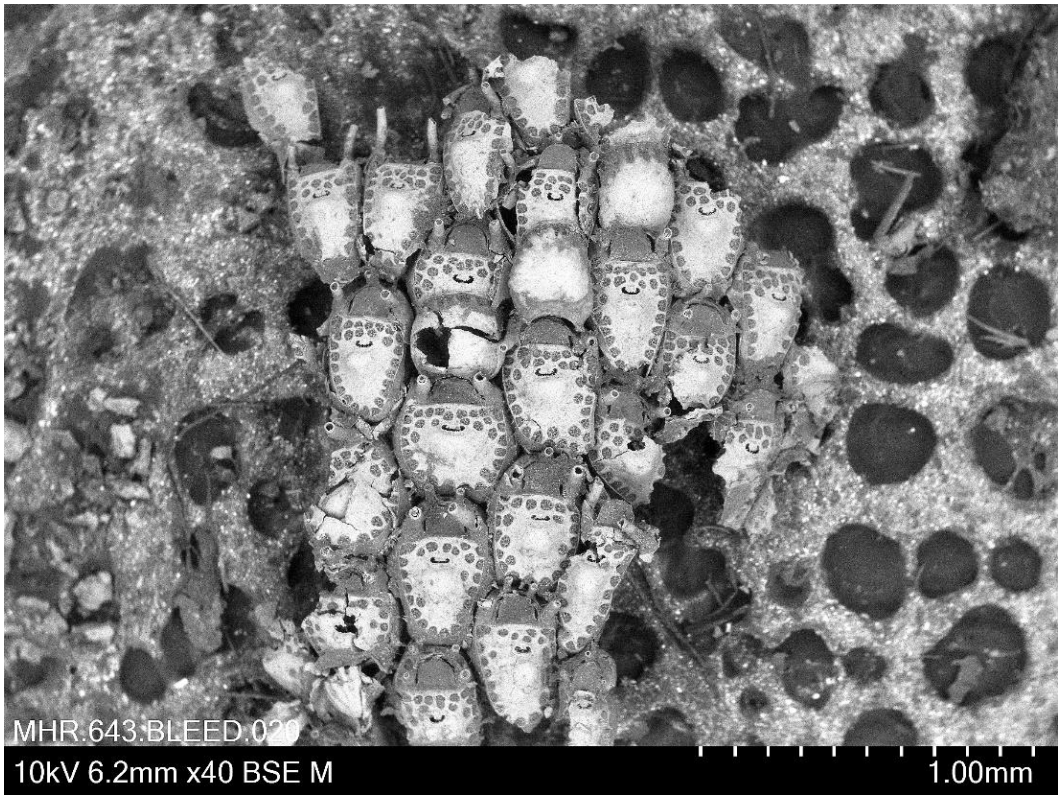

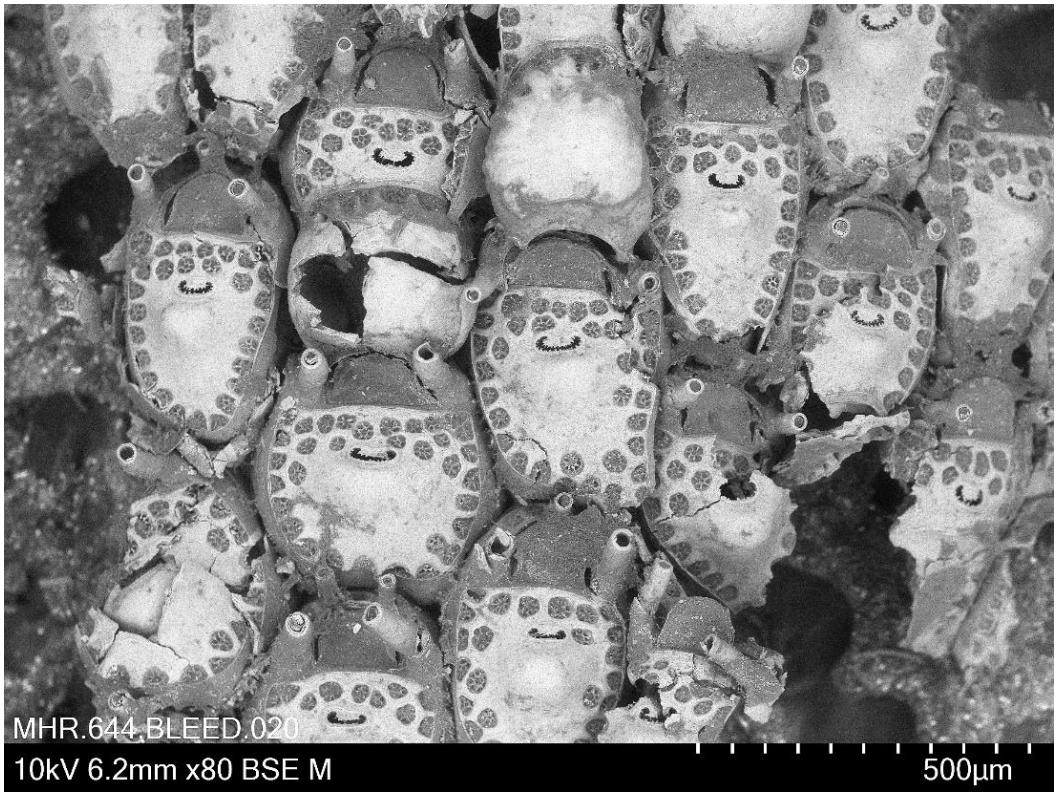

Appendix Figure 35. SEM, ***Fenestrulina*** **sp.**
Specimen ID: BLEED 20, Locality: Jik-do, Maldo-ri, Okdo-myeon, Gunsan-si, Jeollabuk-do, South Korea, Photo credits: Mali Hamre Ramsfjell

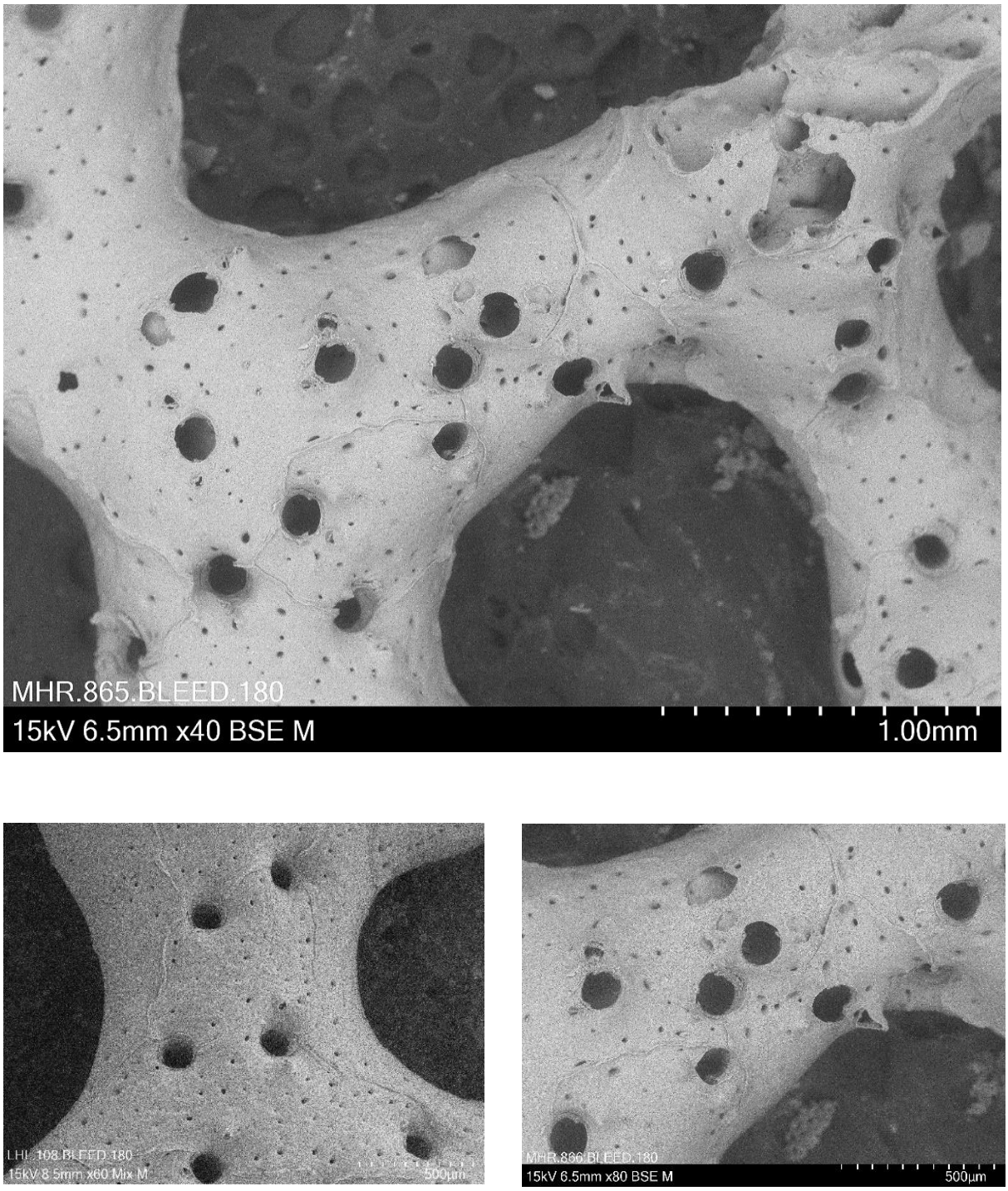

Appendix Figure 36. SEM, ***Bitectipora retepora*** Gordon, 1989
Specimen ID: BLEED 180, Locality: New Zealand, Photo credits: Lee Hsiang Liow and Mali Hamre Ramsfjell

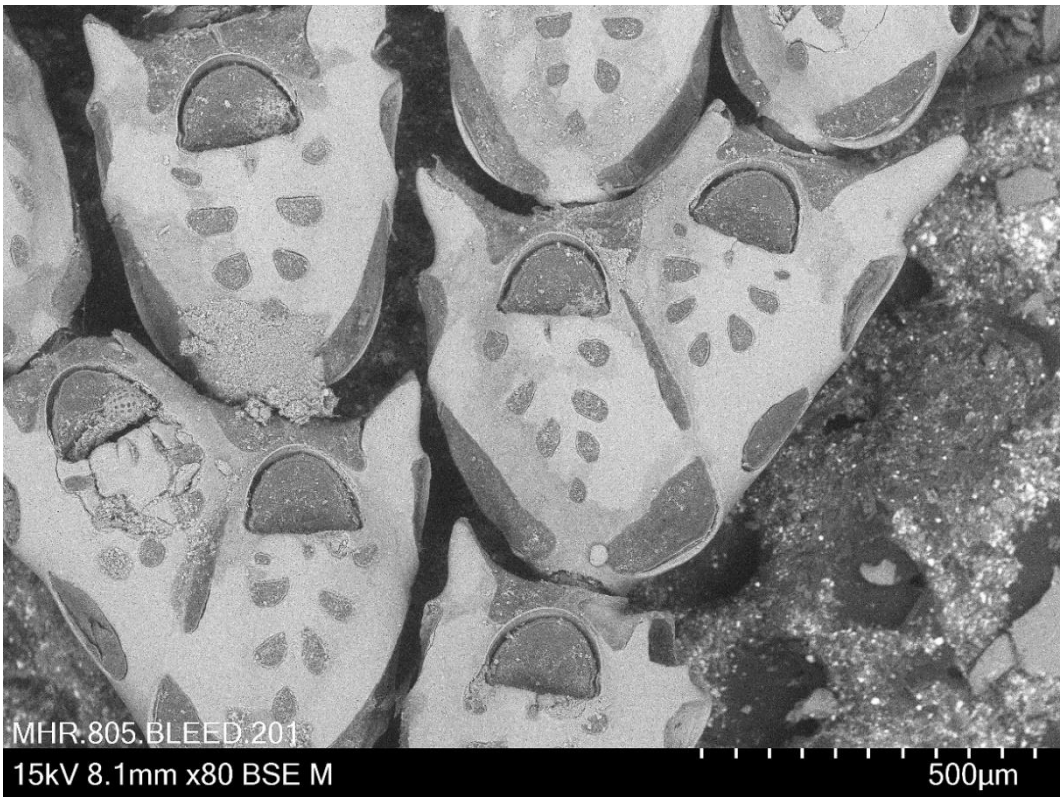

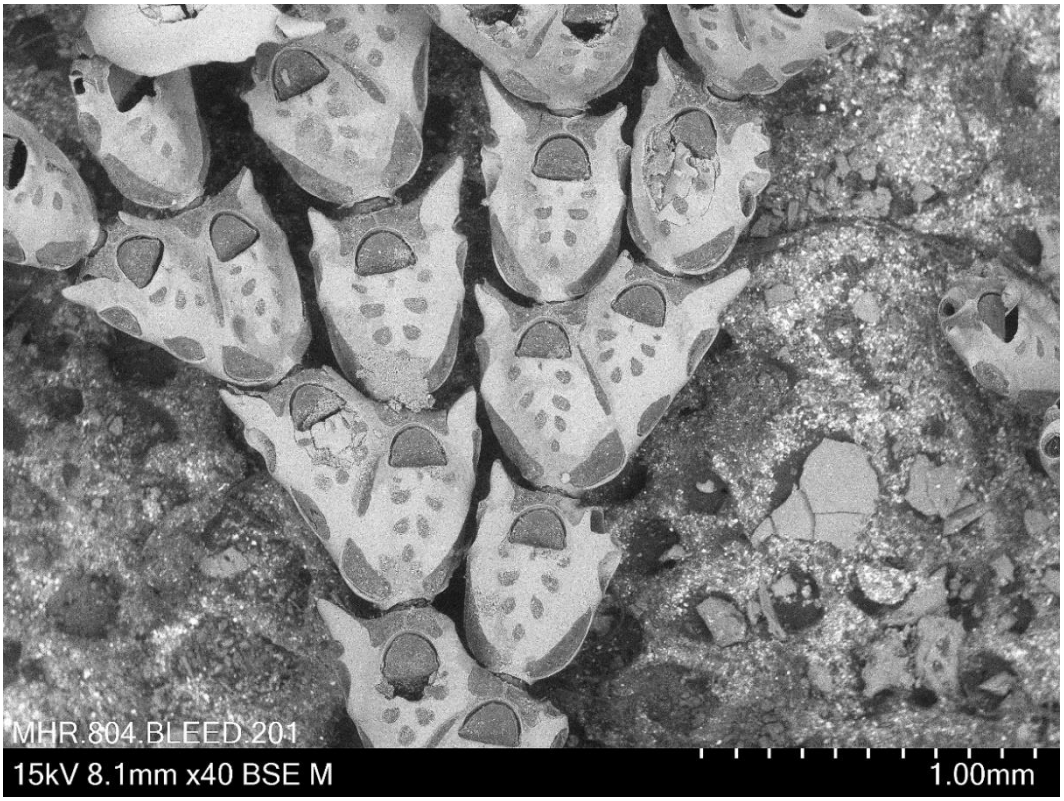

Appendix Figure 37. SEM, ***Orthoscuticella innominata*** Gordon, 1989
Specimen ID: BLEED 201, Locality: Orui,Wairarapa, New Zealand, Photo credits: Mali Hamre Ramsfjell

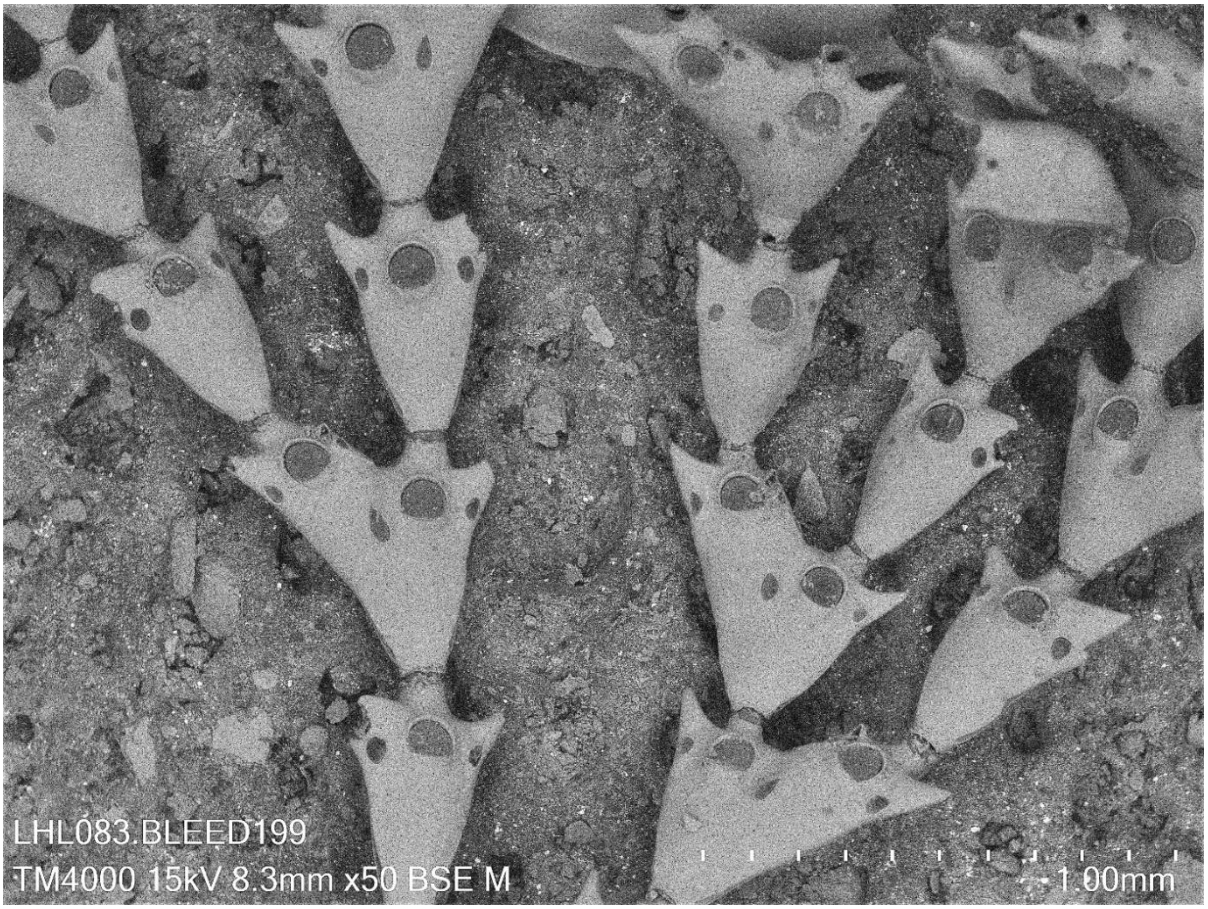

Appendix Figure 38. SEM, ***Cornuticella taurina*** Busk, 1852
Specimen ID: BLEED 199, Locality: Orui,Wairarapa, New Zealand, Photo credits: Lee Hsiang Liow

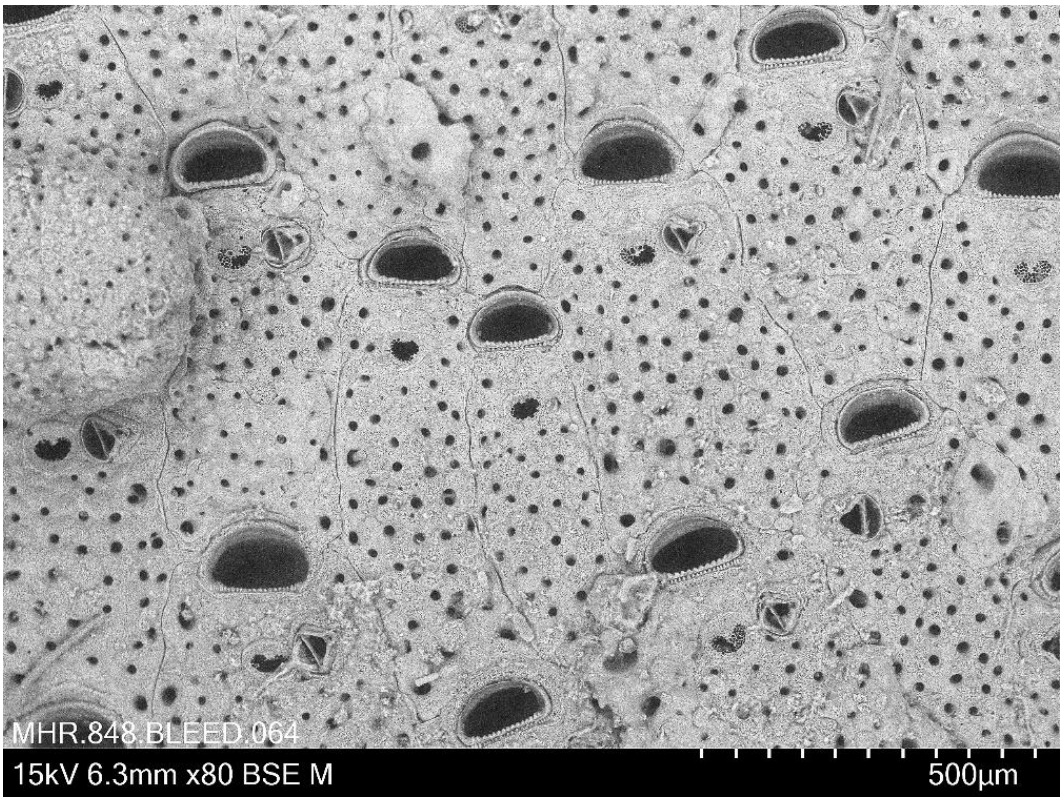

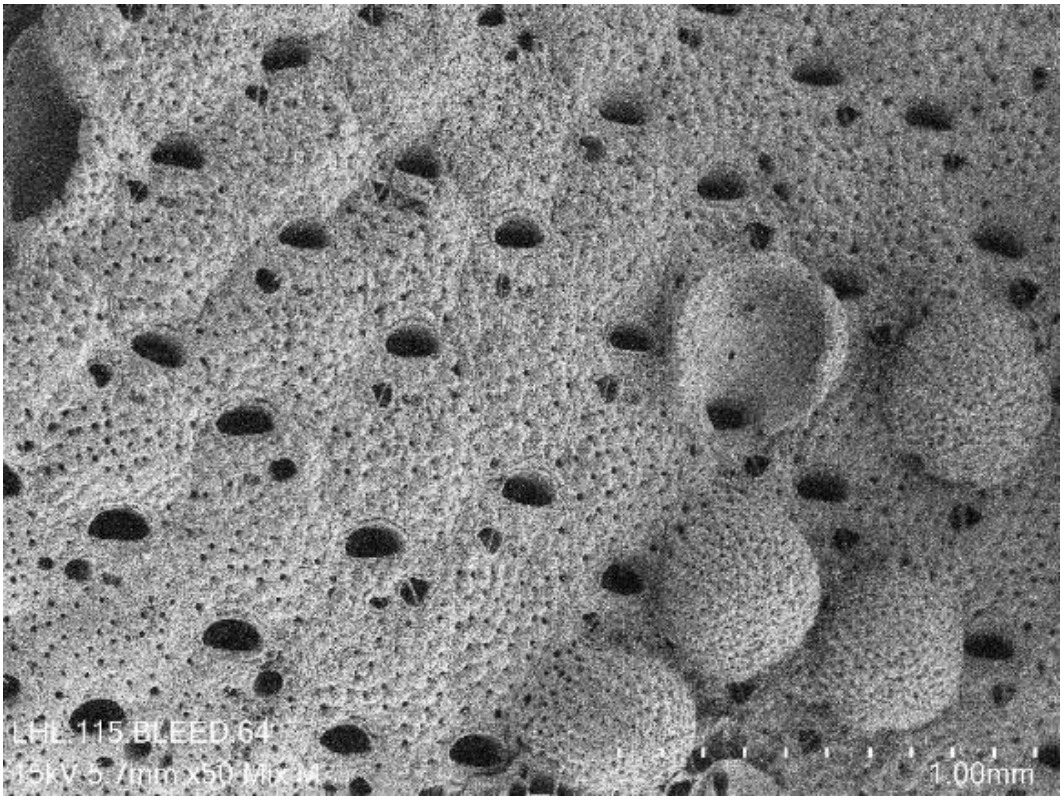

Appendix Figure 39. SEM, ***Microporella ordo*** Brown, 1952
Specimen ID: BLEED 64, Locality: New Zealand, Photo credits: Lee Hsiang Liow and Mali Hamre Ramsfjell

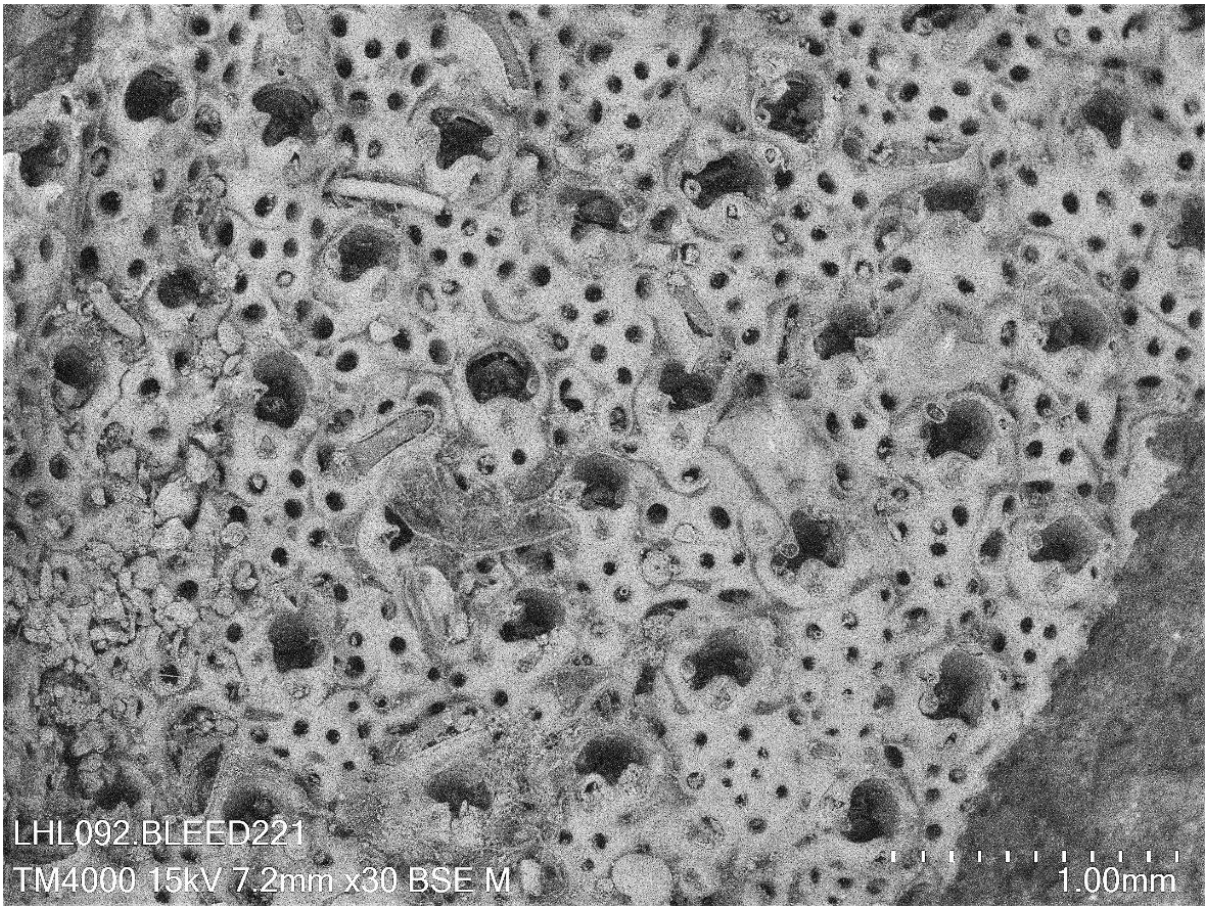

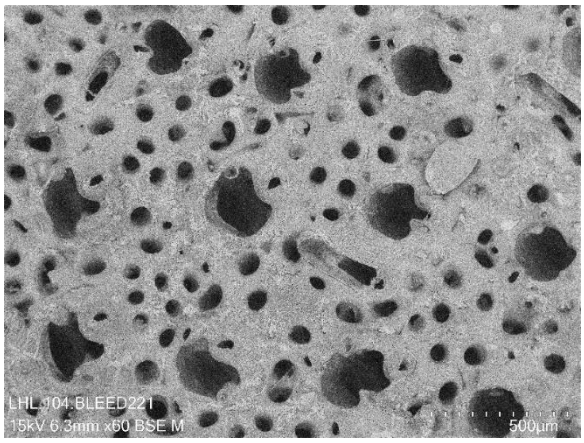

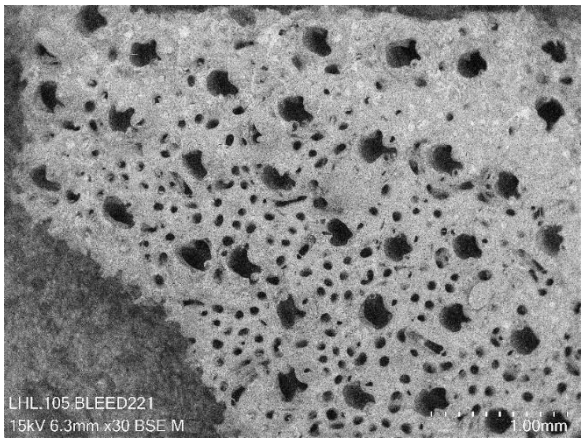

Appendix Figure 40. SEM, ***Arachnopusia unicornis*** Hutton, 1873
Specimen ID: BLEED 221, Locality: New Zealand, Photo credits: Lee Hsiang Liow

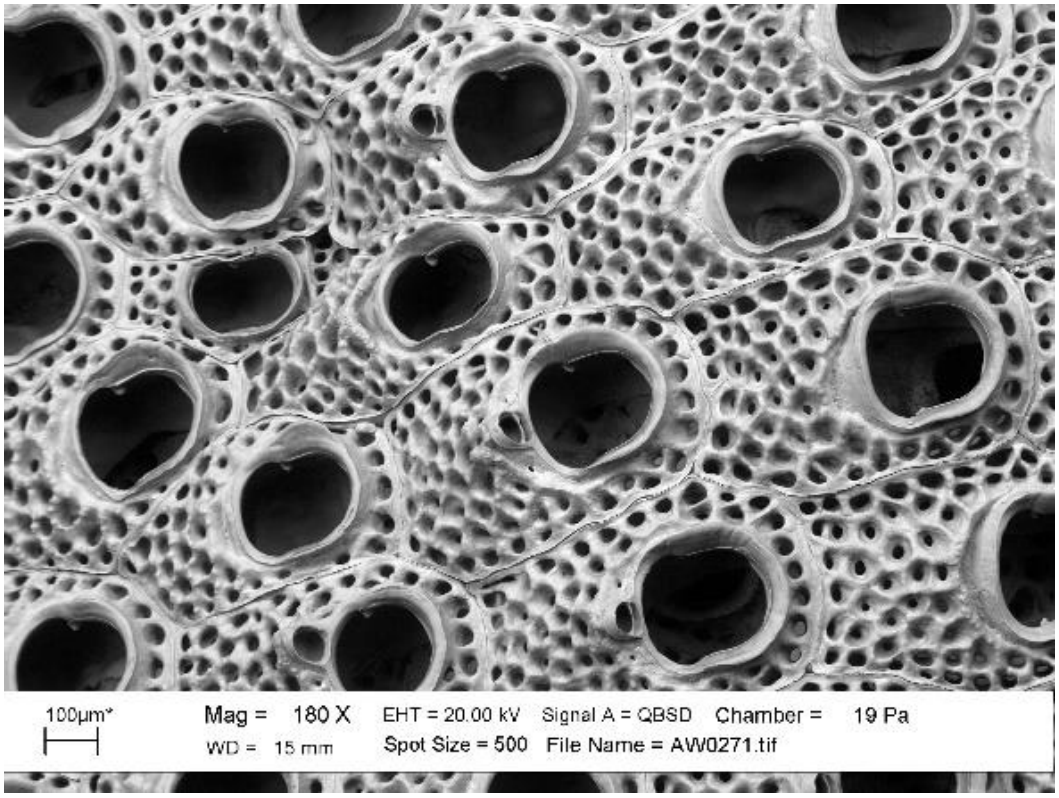

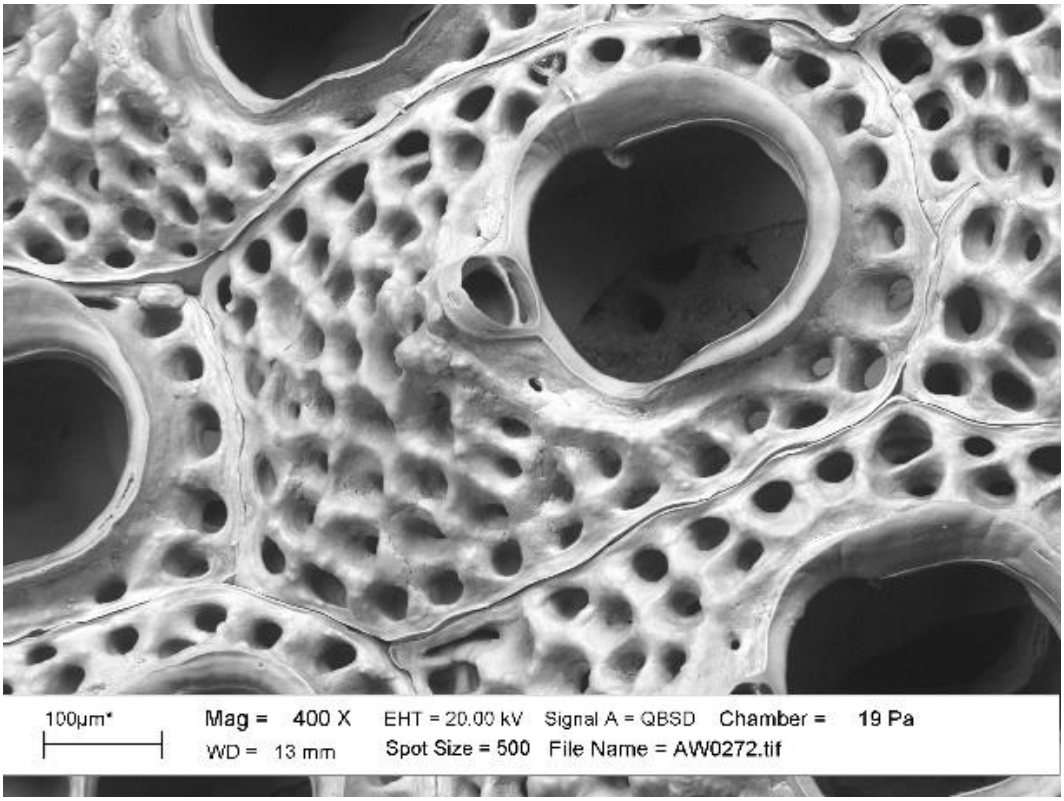

Appendix Figure 41. SEM, ***Cryptosula pallasiana*** Moll, 1803
Specimen ID: NZ011, Photo Credits: Andrea Waeschenbach

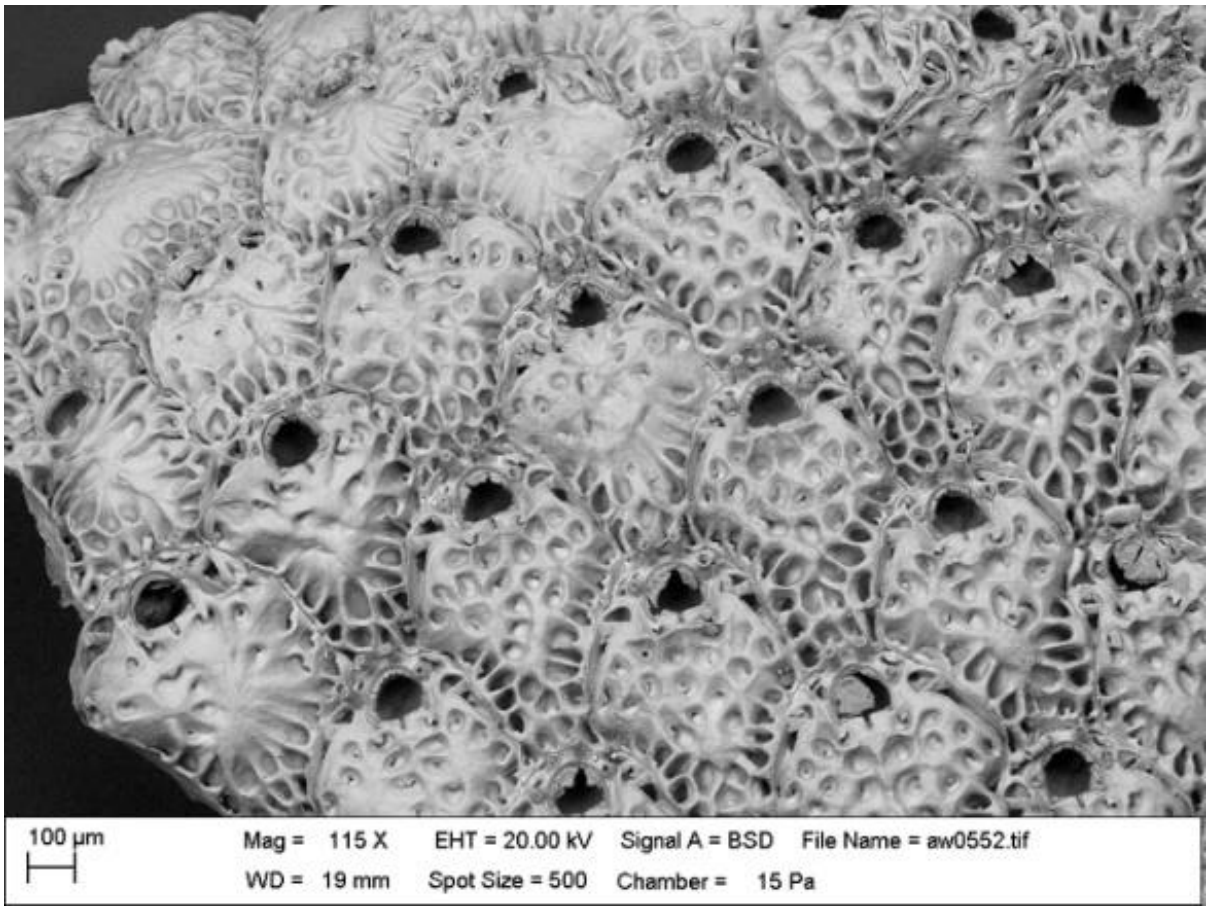

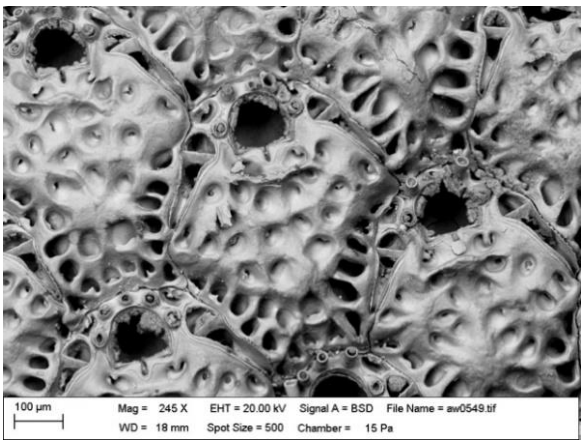

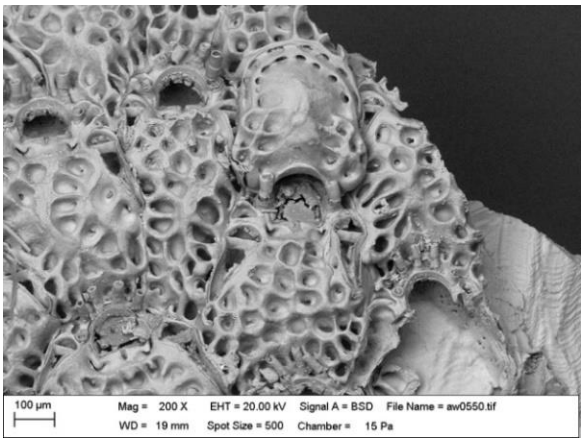

Appendix Figure 42. SEM, ***Chiastosella*** **sp.**
Specimen ID: AW459, Photo Credits: Andrea Waeschenbach

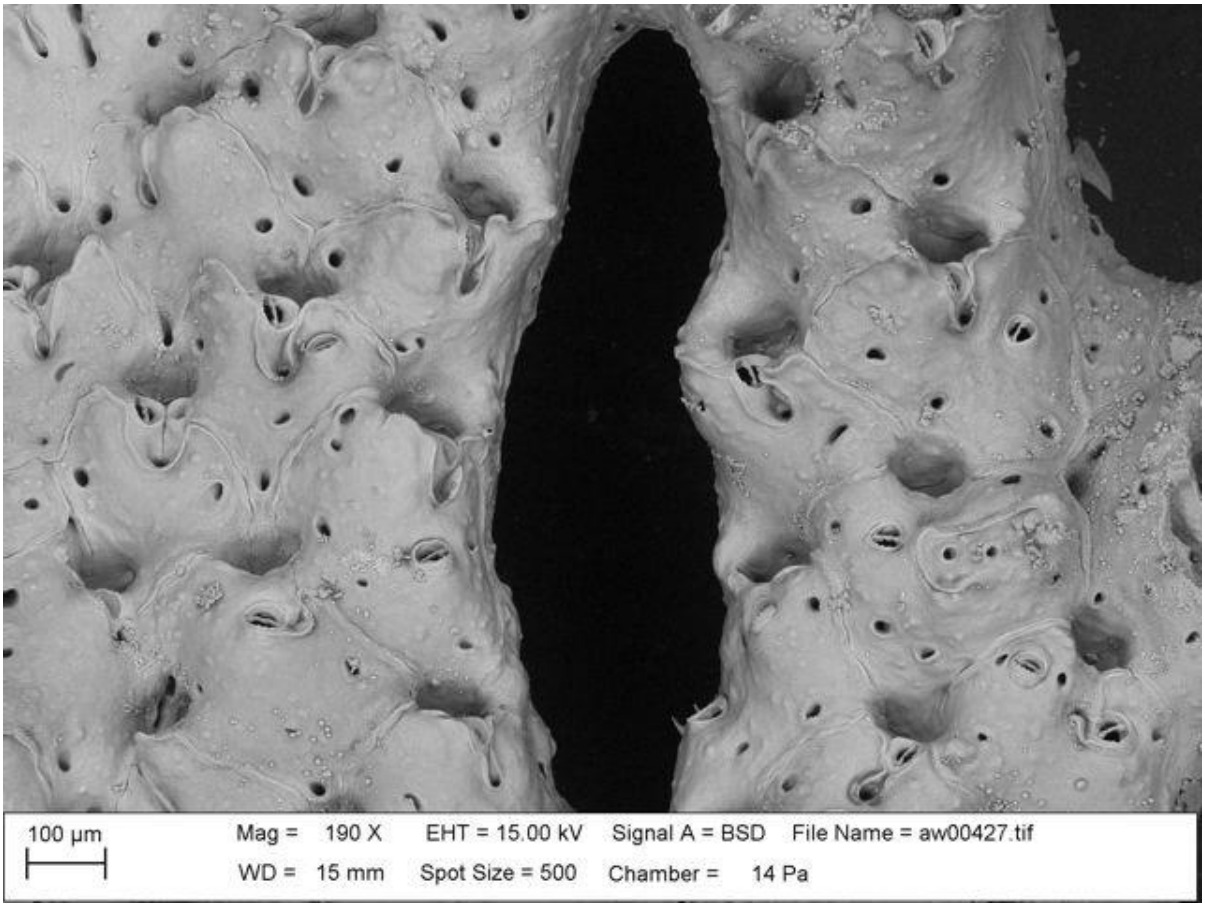

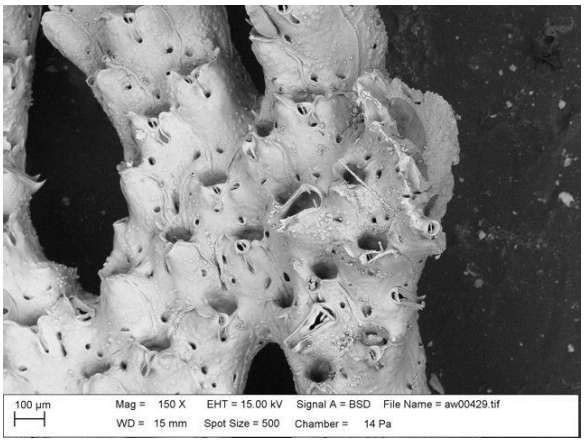

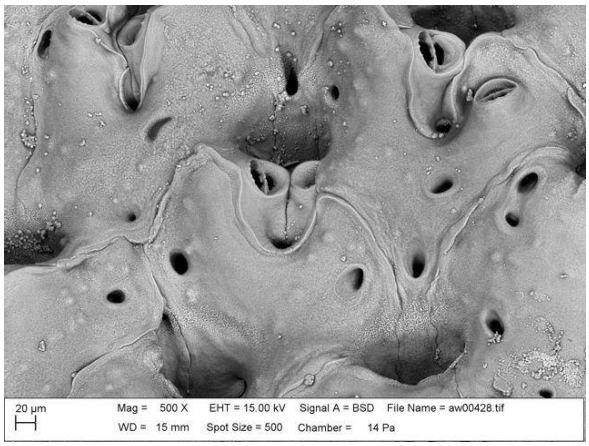

Appendix Figure 43. SEM, ***Reteporella ligulata*** Gordon, 1989
Specimen ID: AW286, Photo Credits: Andrea Waeschenbach

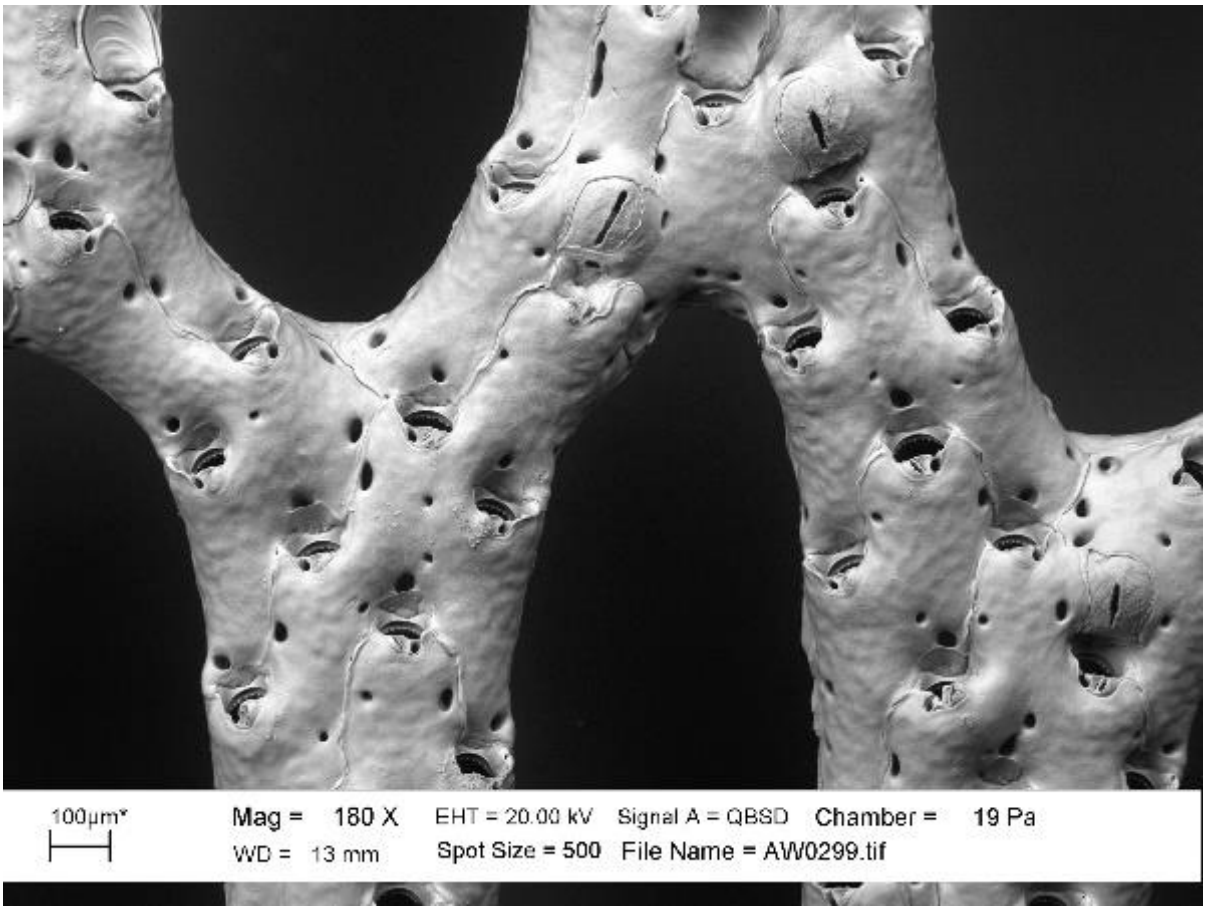

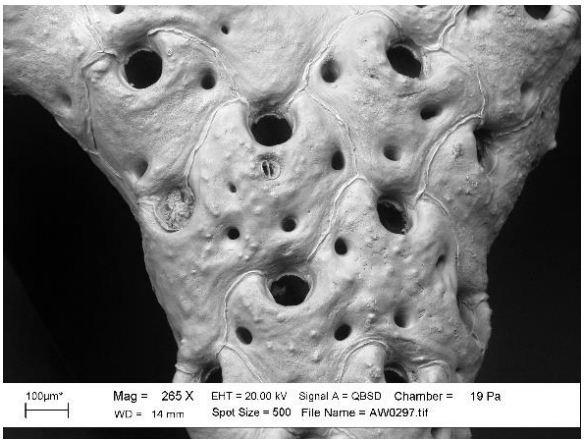

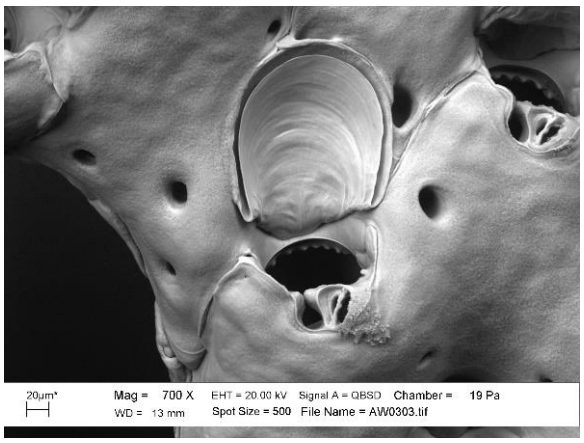

Appendix Figure 44. SEM, **Phidoloporidae indet.**
Specimen ID: AW006, Photo Credits: Andrea Waeschenbach

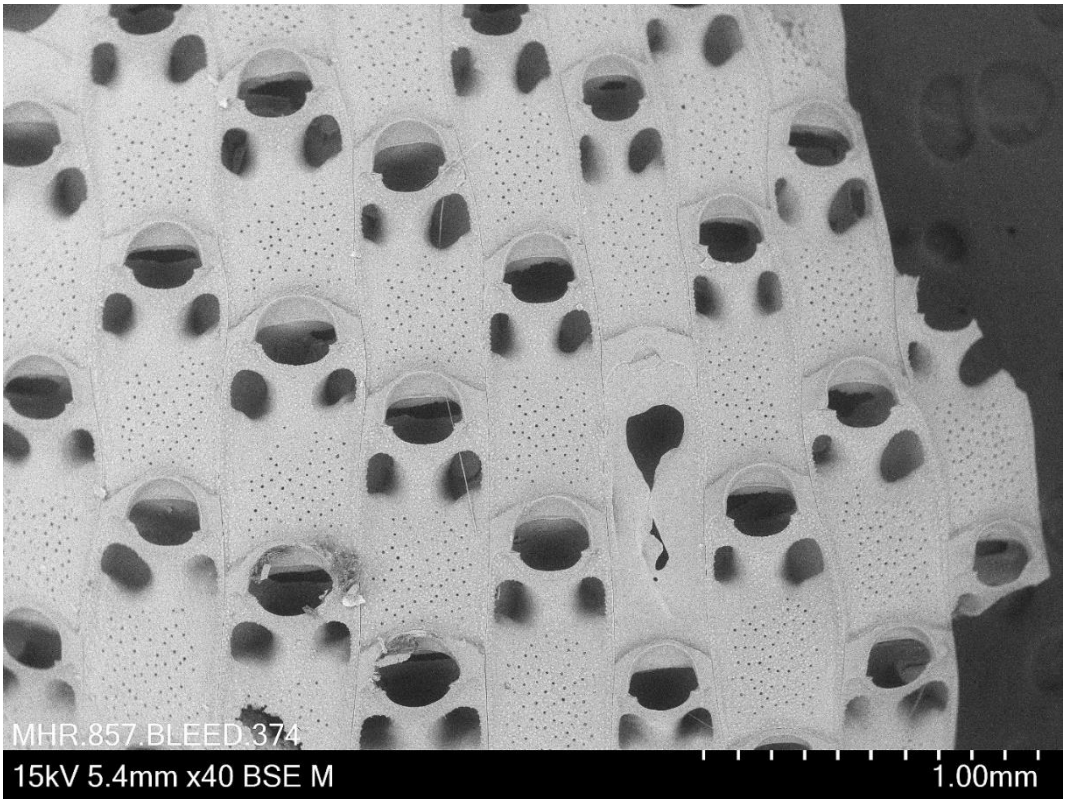

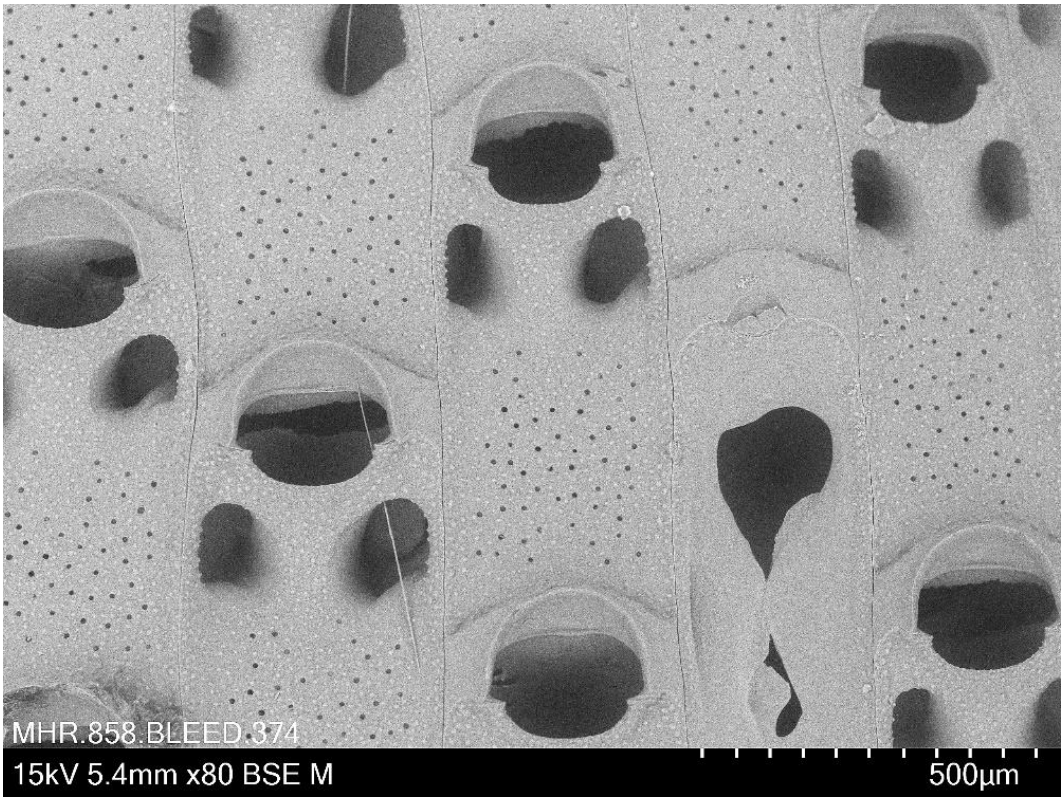

Appendix Figure 45. SEM, ***Thalamoporella*** **sp.**
Specimen ID: BLEED 374, Locality: St. Helena, Photo credits: Mali Hamre Ramsfjell

Appendix Figure 46. SEM, ***Euoplozoum*** **sp.**
Specimen ID: BLEED 322, Locality: New Zealand, Photo credits: Mali Hamre Ramsfjell

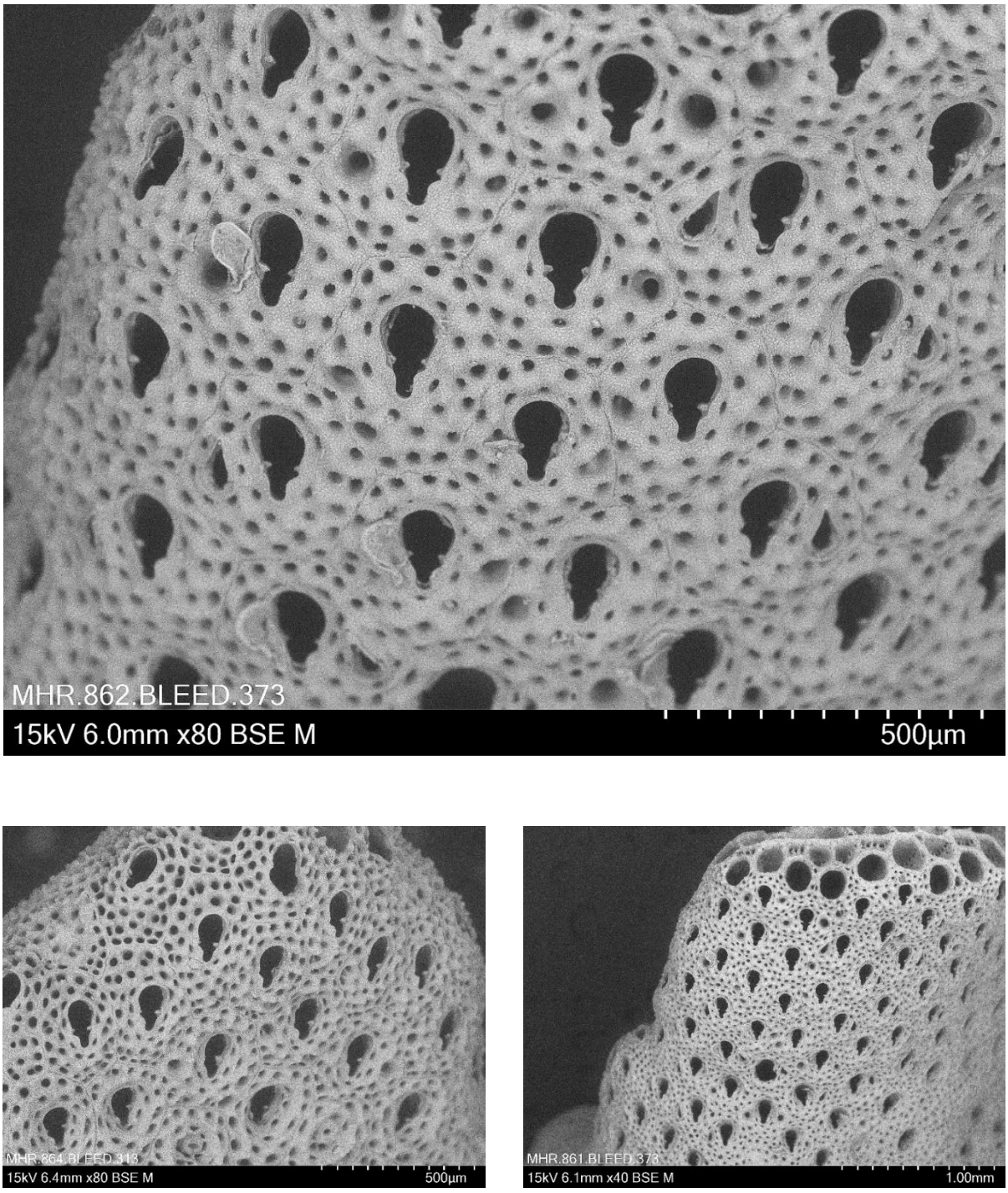

Appendix Figure 47. SEM, ***Laminopora contorta*** Michelin, 1842
Specimen ID: BLEED 373, Locality: Cape Verde, Photo credits: Mali Hamre Ramsfjell

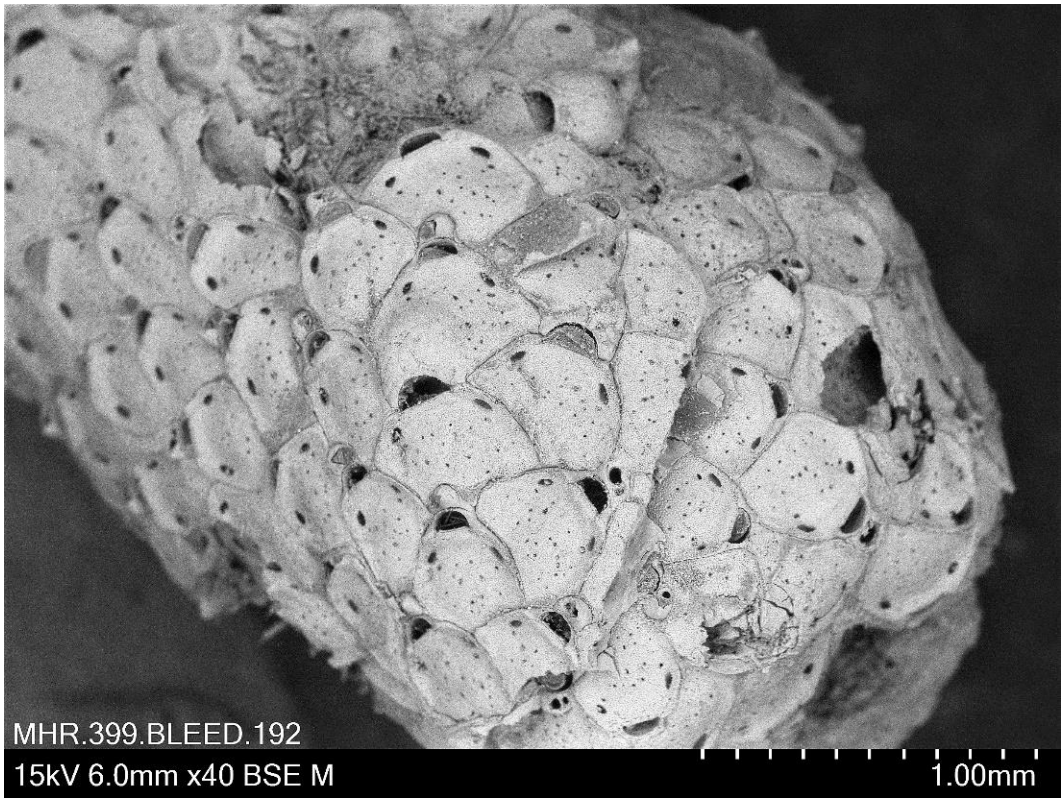

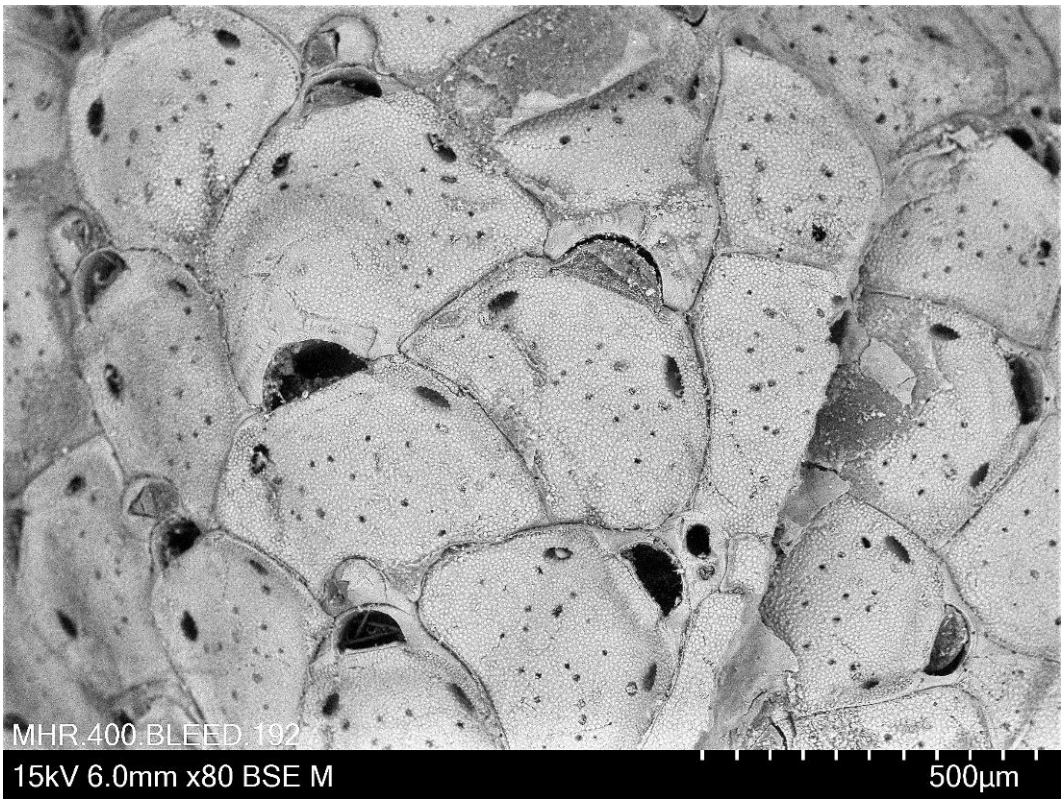

Appendix Figure 48. SEM, ***Micropora sp.***
Specimen ID: BLEED 192, Locality: New Zealand, Photo credits: Mali Hamre Ramsfjell

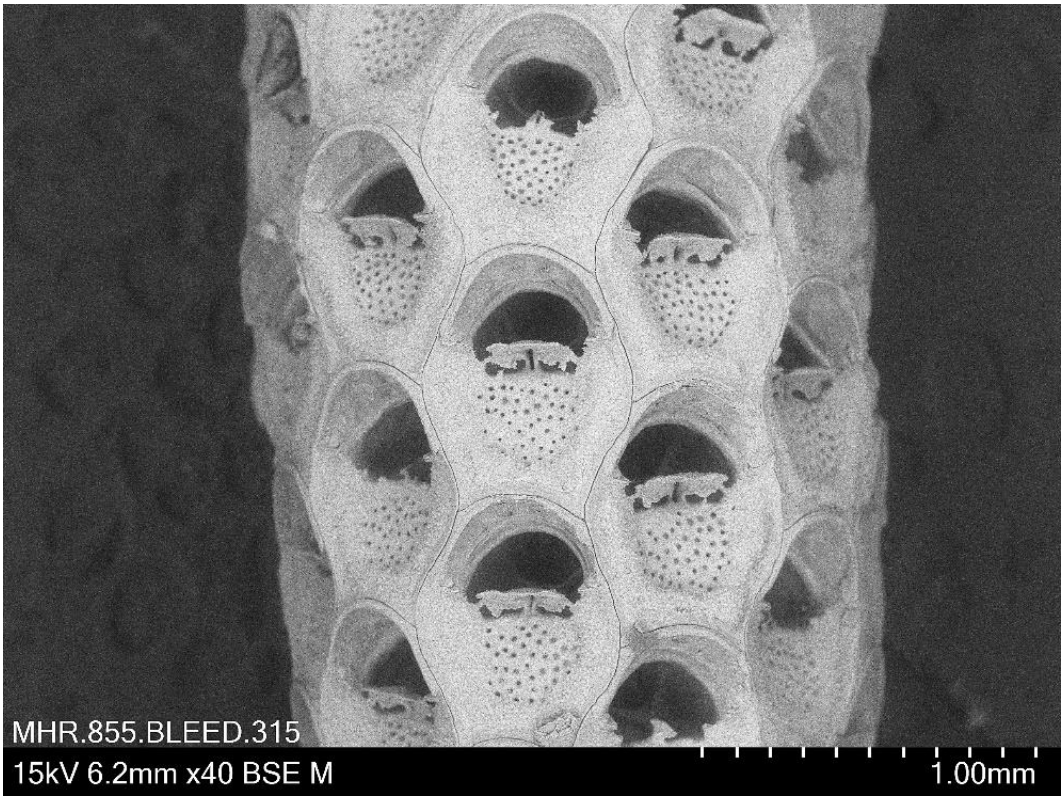

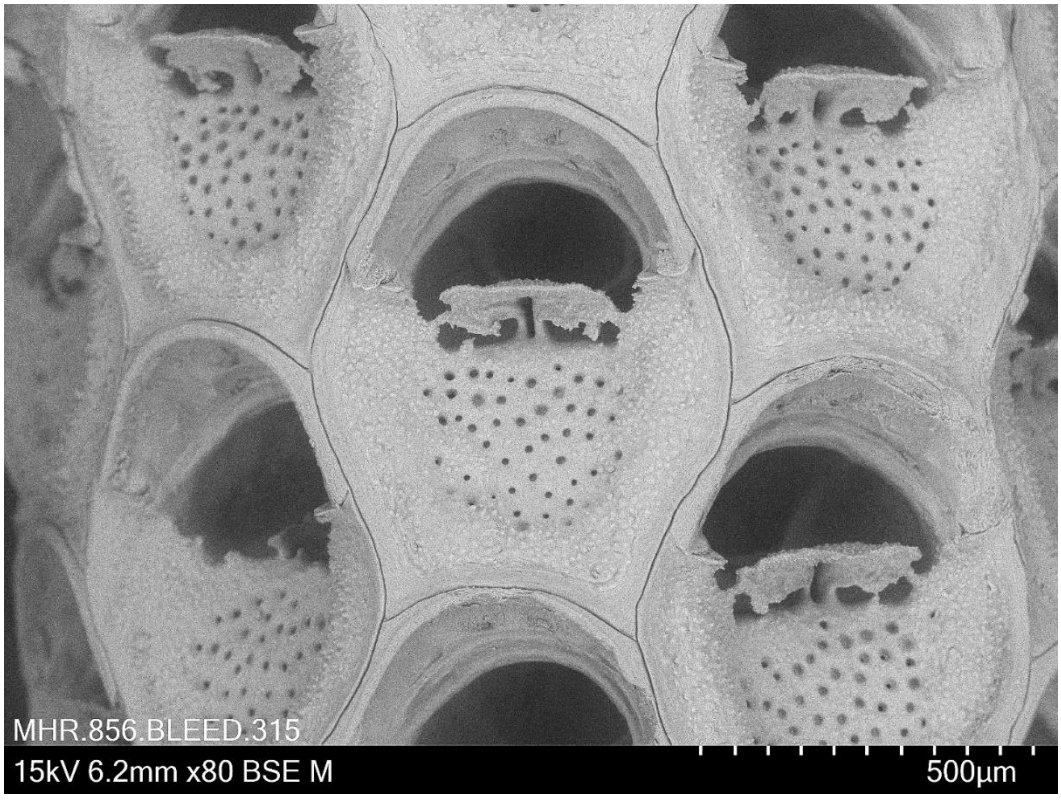

Appendix Figure 49. SEM, ***Steginoporella neozelanica*** Busk, 1861
Specimen ID: BLEED 315, Locality: New Zealand, Photo credits: Mali Hamre Ramsfjell

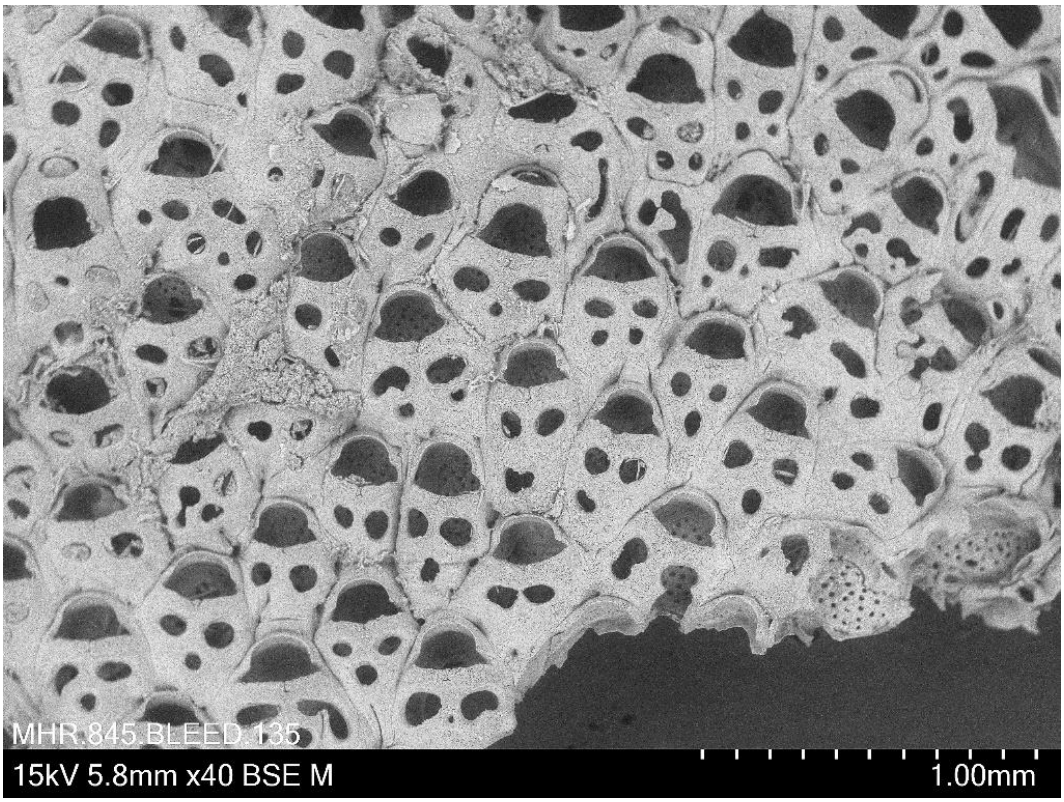

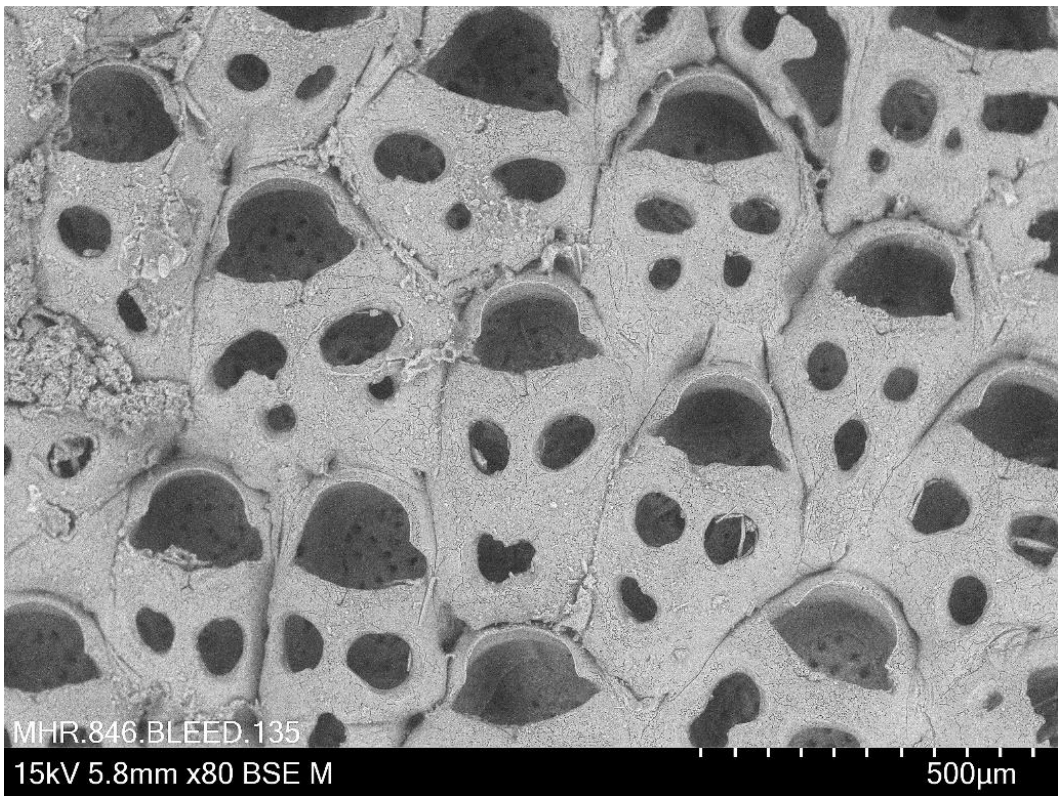

Appendix Figure 50. SEM, ***Eurystomella foraminigera*** Hincks, 1883
Specimen ID: BLEED 135, Locality: New Zealand, Photo credits: Mali Hamre Ramsfjell

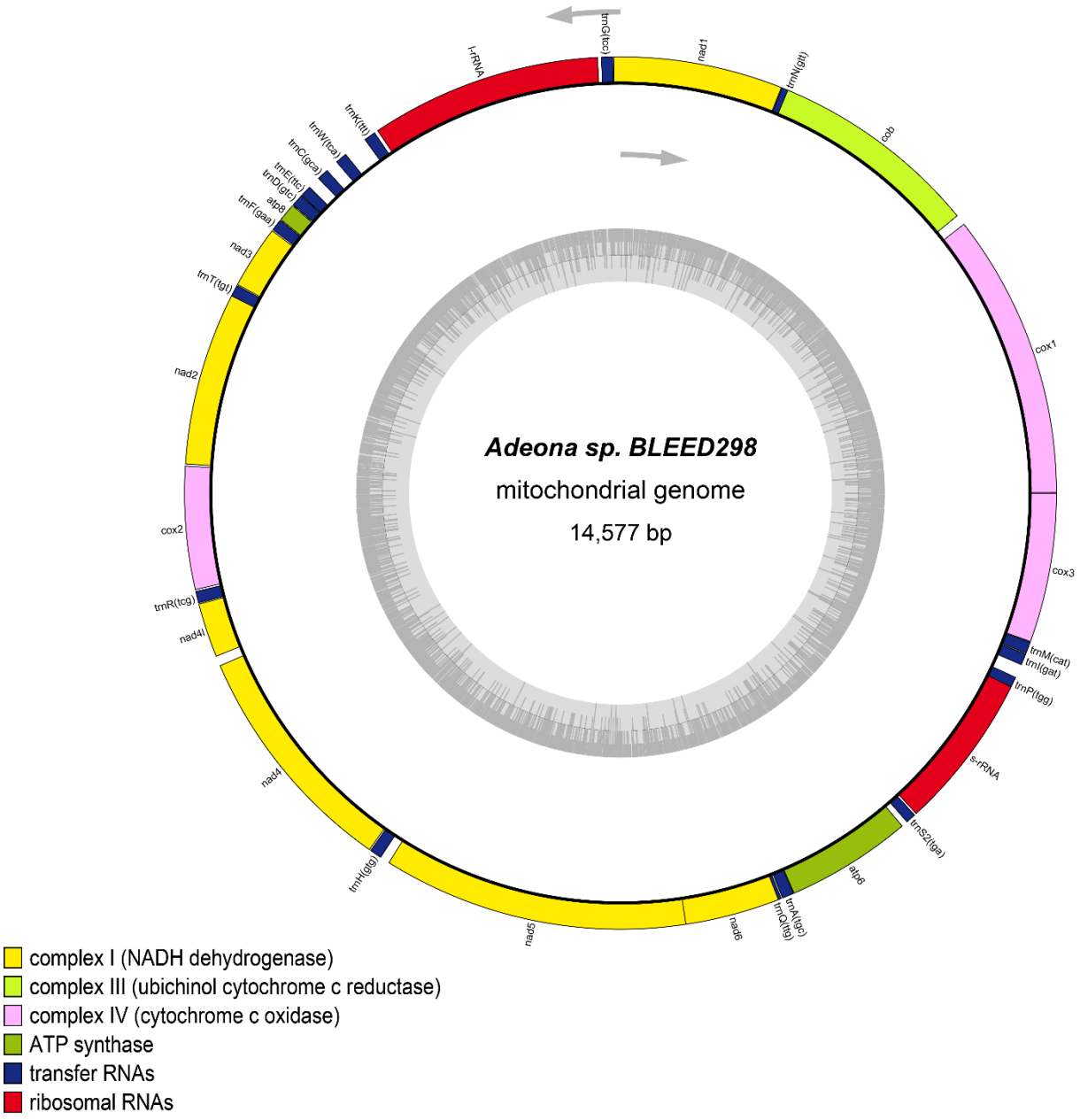

Appendix Figure 51. Complete mitochondrial genome of *Adeona* sp. Sequencing coverage: Average: 65x - Min: 7x.

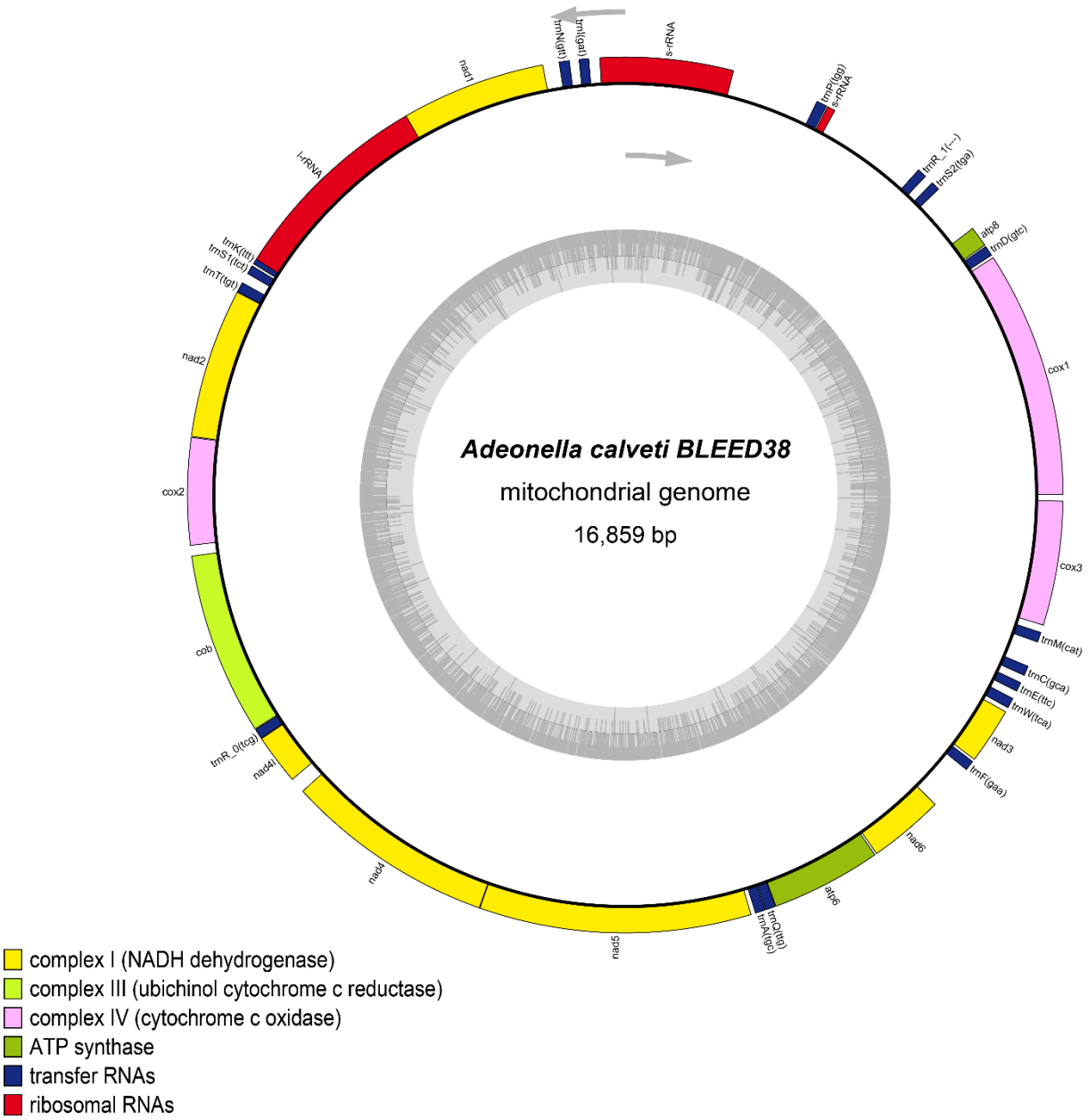

Appendix Figure 52. Complete mitochondrial genome of *Adeonella calveti*. Sequencing coverage: Average: 57x - Min: 6x.

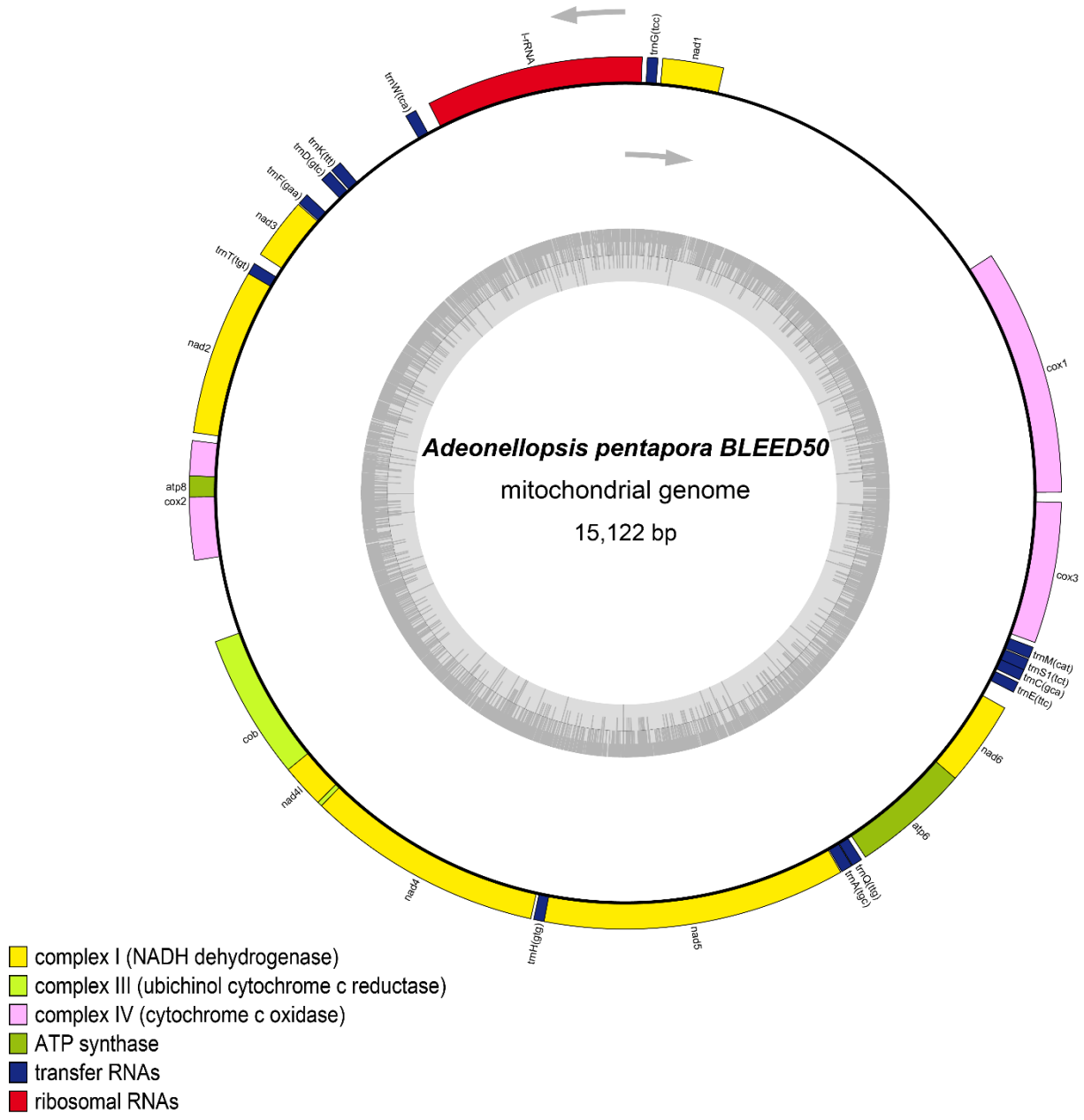

Appendix Figure 53. Complete mitochondrial genome of *Adeonellopsis pentapora.* Sequencing coverage: Average: 23x - Min: 5x.

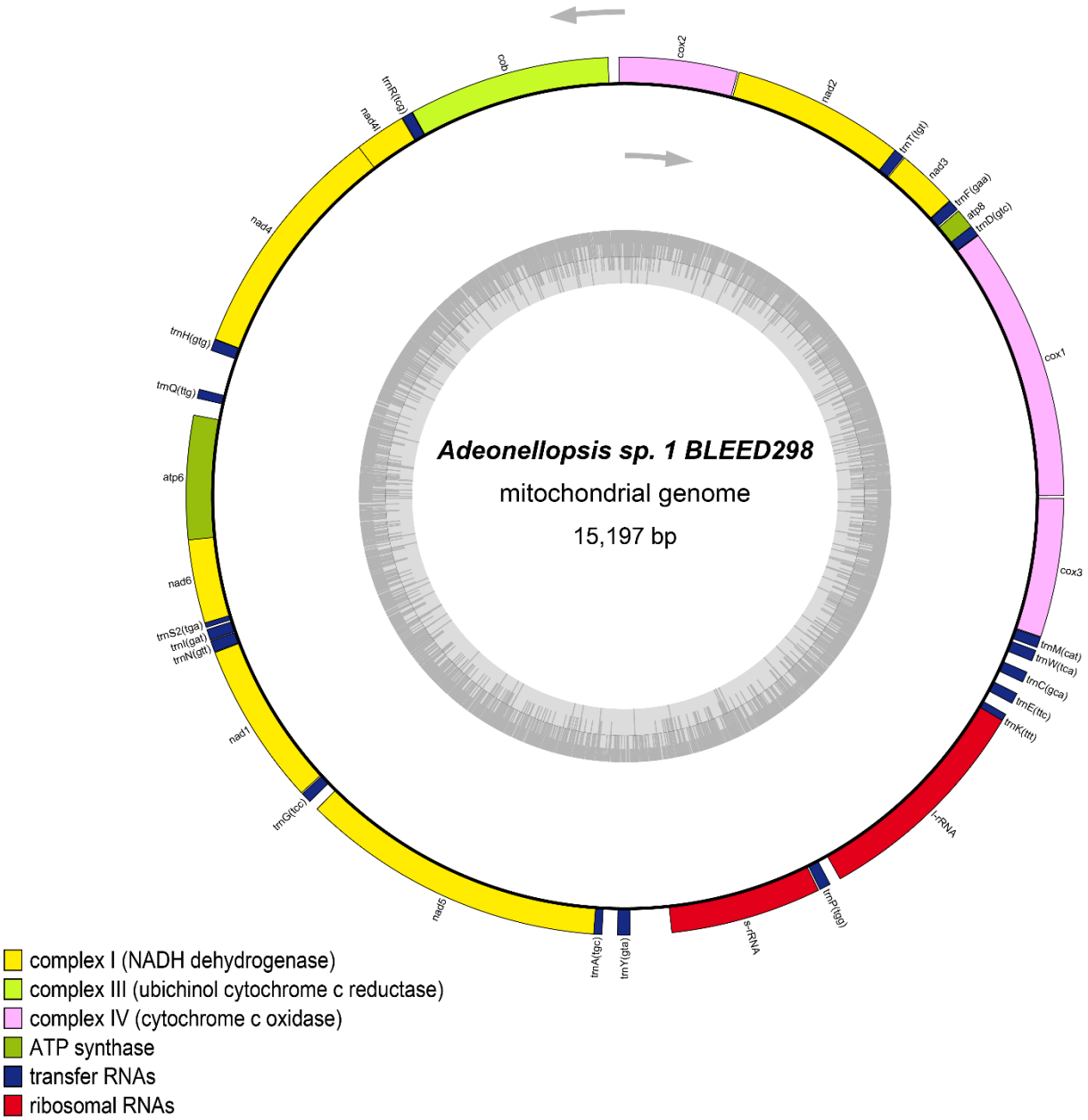

Appendix Figure 54. Complete mitochondrial genome of *Adeonellopsis* sp. 1. Sequencing coverage: Average: 83x - Min: 8x.

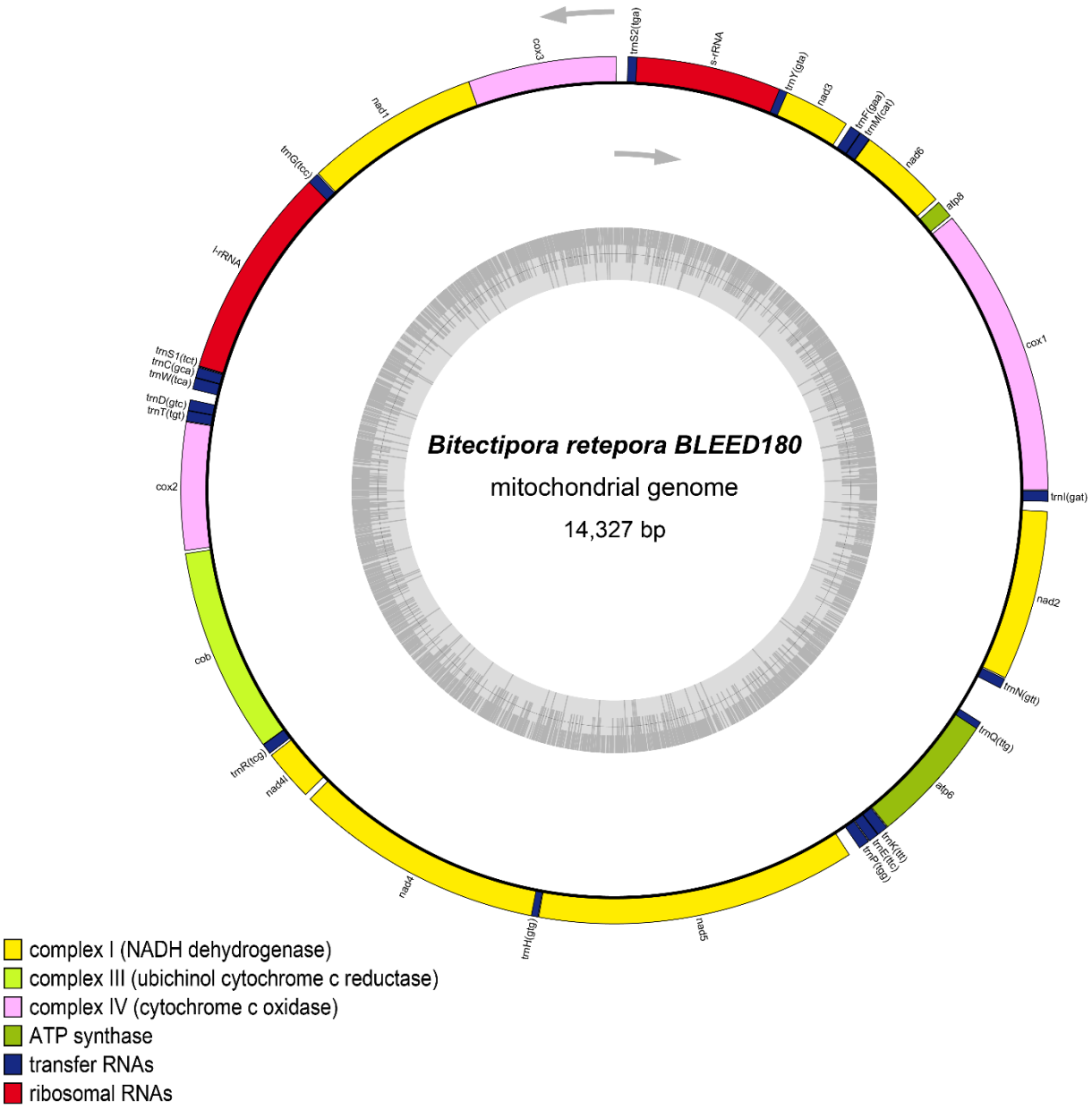

Appendix Figure 55. Complete mitochondrial genome of *Bitectipora retepora*. Sequencing coverage: Average: 50x - Min: 5x.

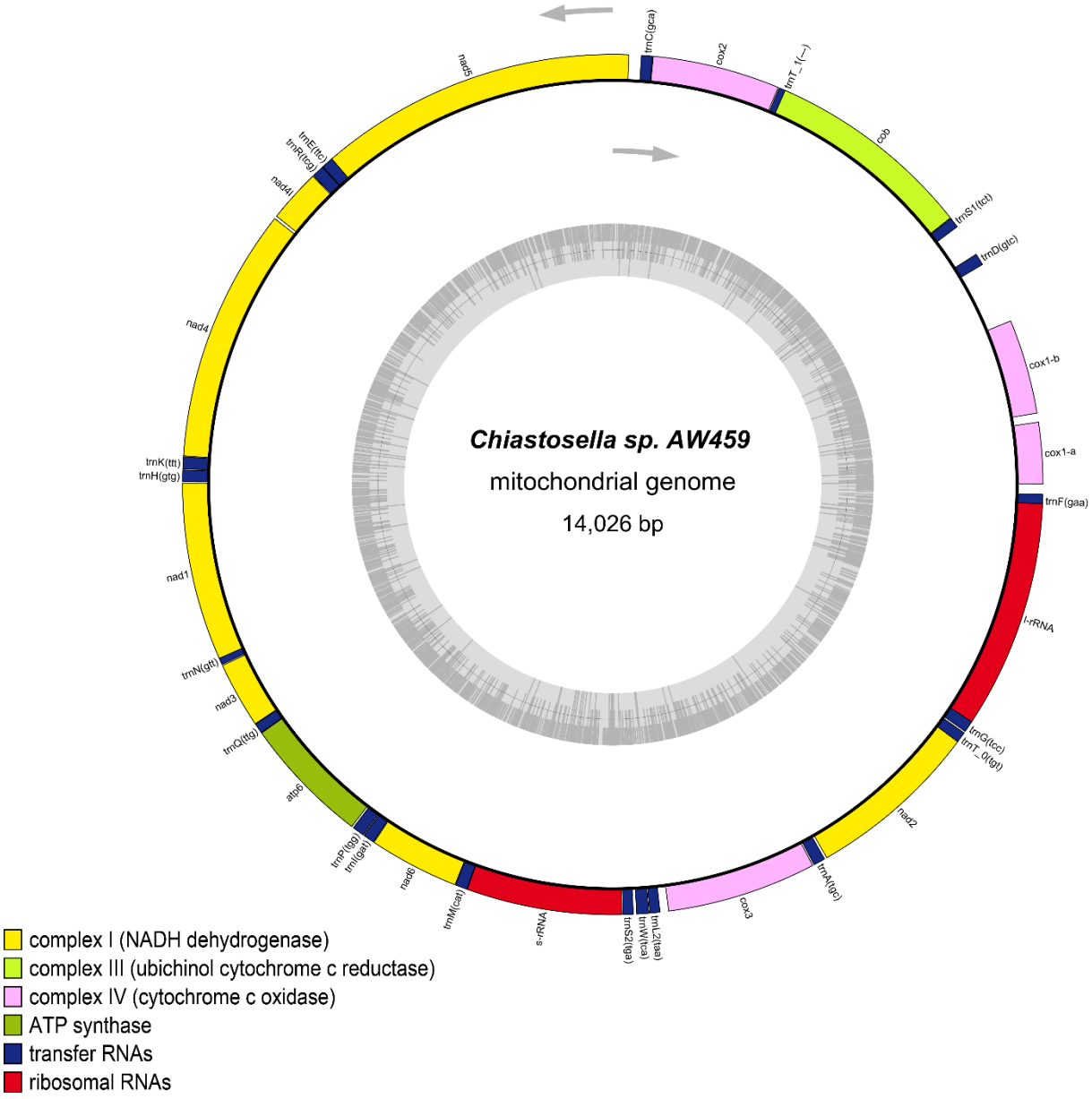

Appendix Figure 56. Complete mitochondrial genome of *Chiastosella* sp.

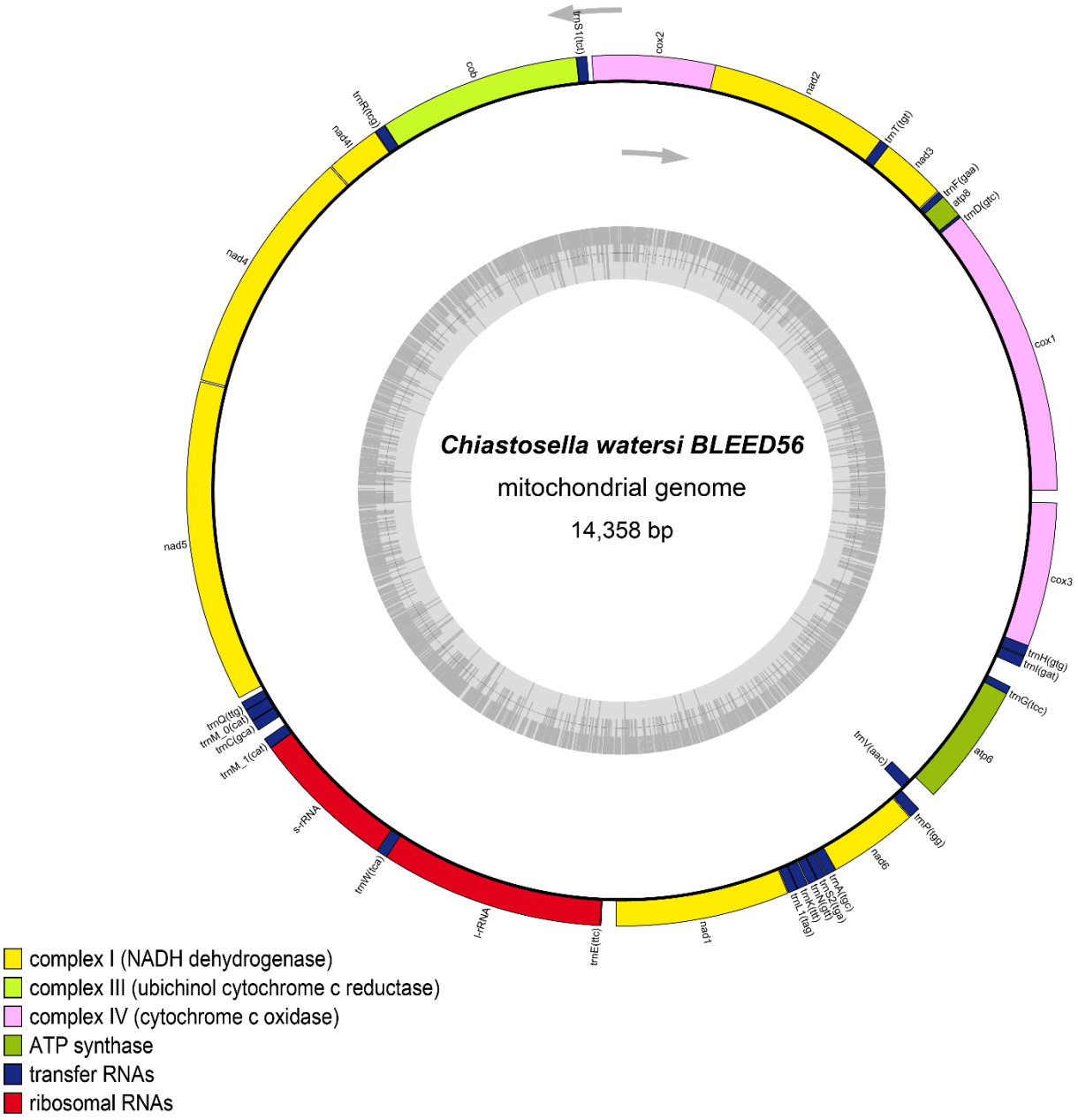

Appendix Figure 57. Complete mitochondrial genome of *Chiastosella watersi*. Sequencing coverage: Average: 57x - Min: 6x.

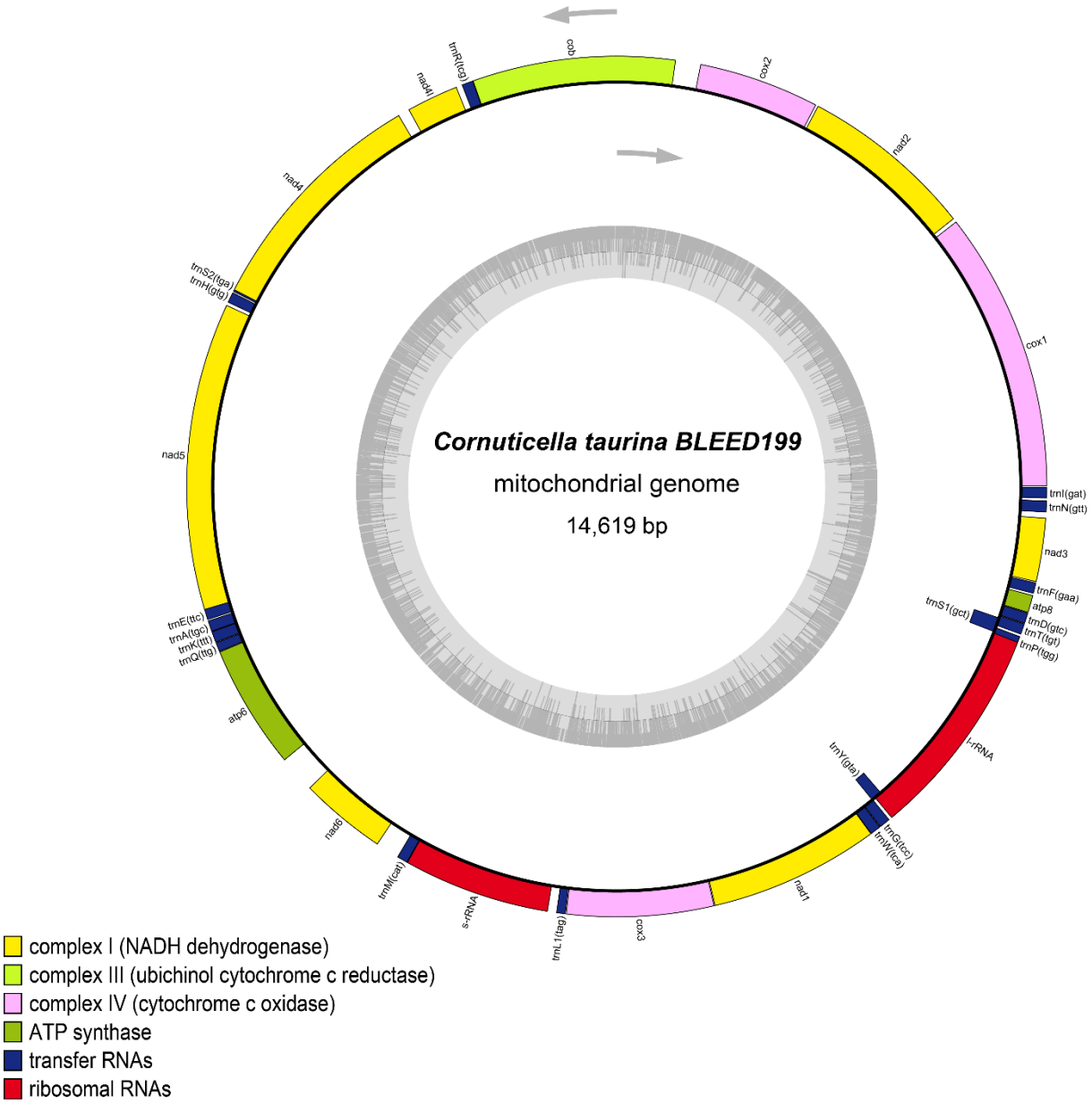

Appendix Figure 58. Complete mitochondrial genome of *Cornuticella taurina*. Sequencing coverage: Average: 36x - Min: 5x.

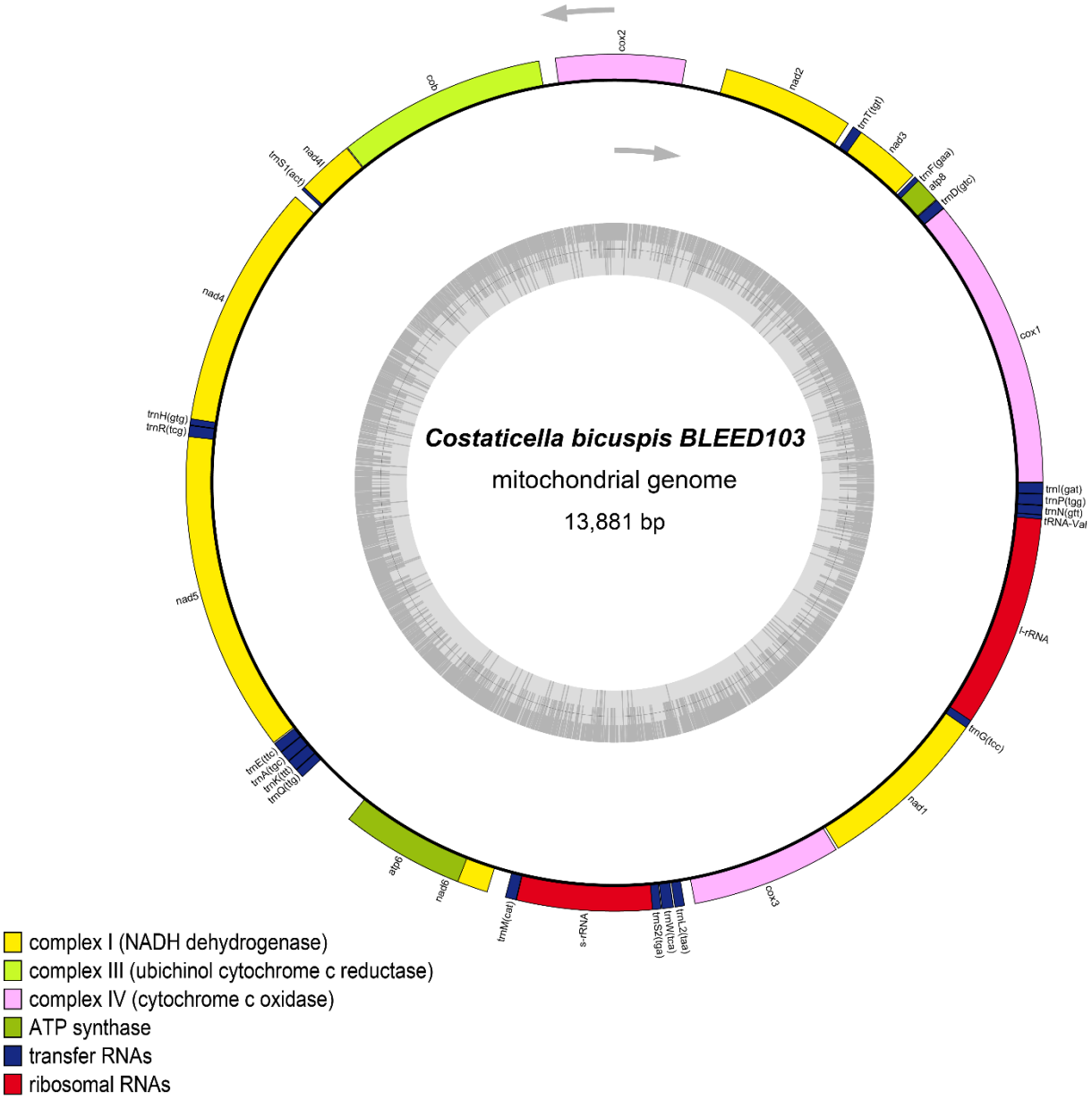

Appendix Figure 59. Complete mitochondrial genome of *Costaticella bicuspis*. Sequencing coverage: Average: 278x - Min: 28x.

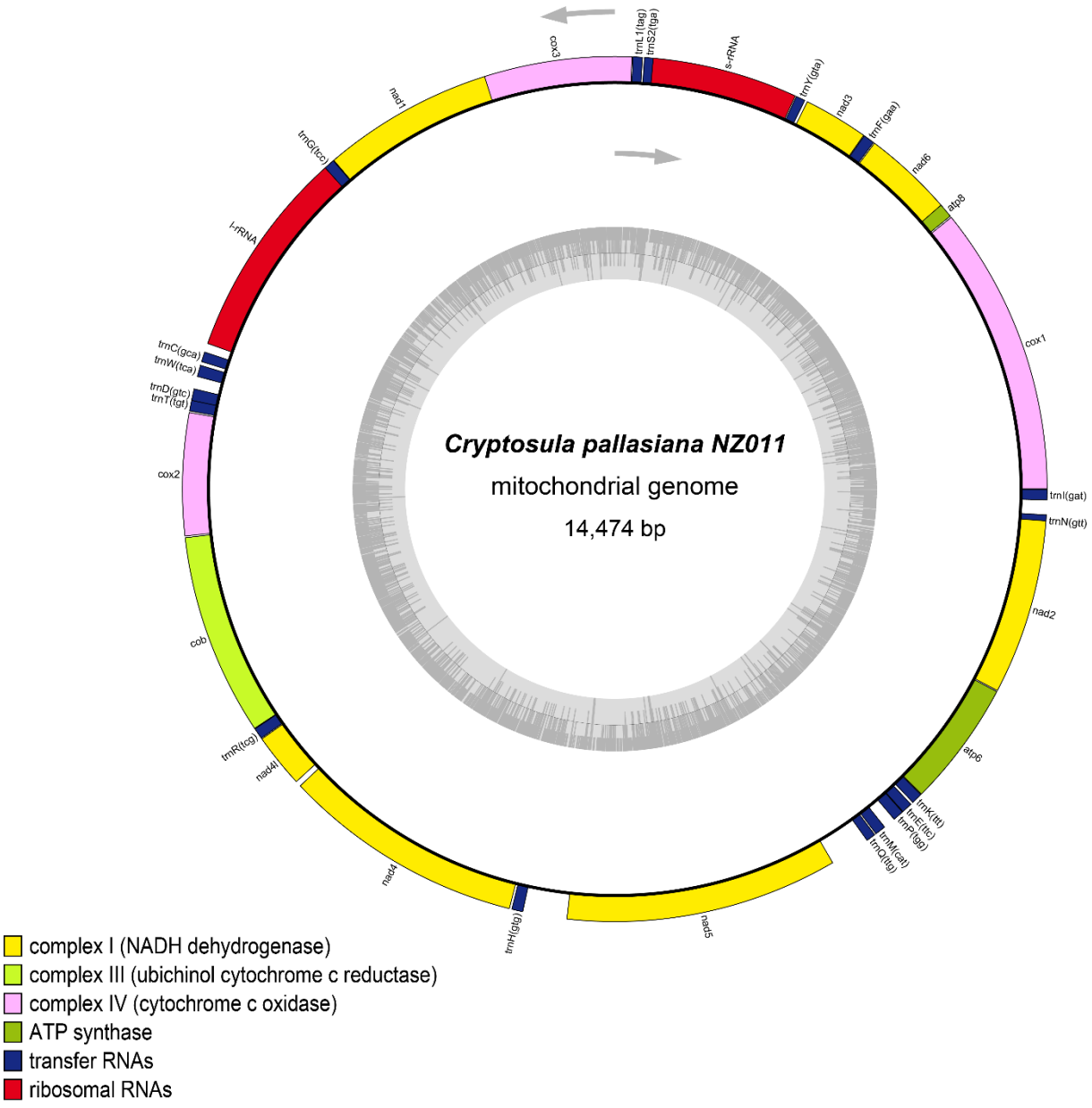

Appendix Figure 60. Complete mitochondrial genome of *Cryptosula pallasiana*.

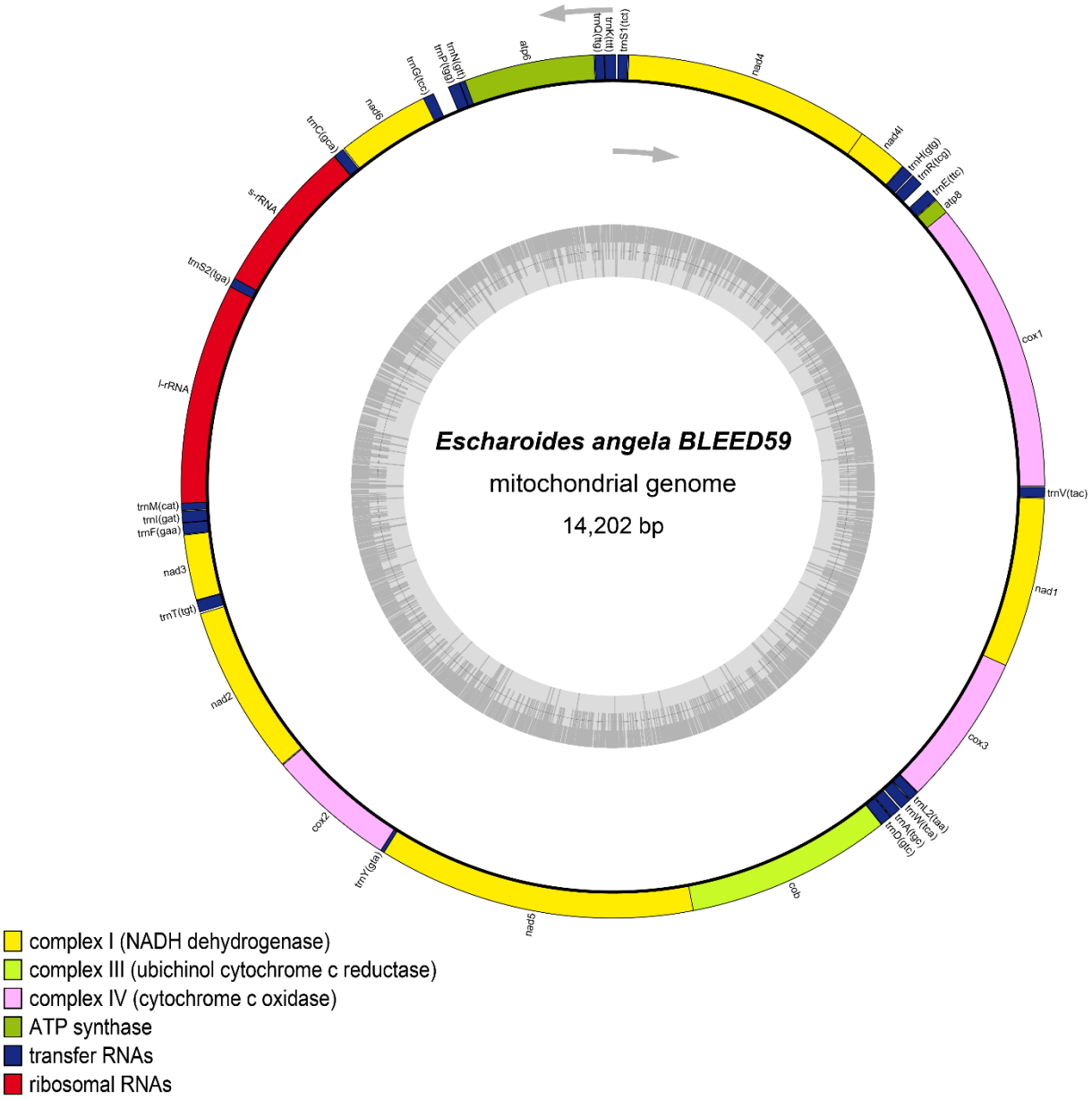

Appendix Figure 61. Complete mitochondrial genome of *Escharoides angela*. Sequencing coverage: Average: 68x - Min: 7x.

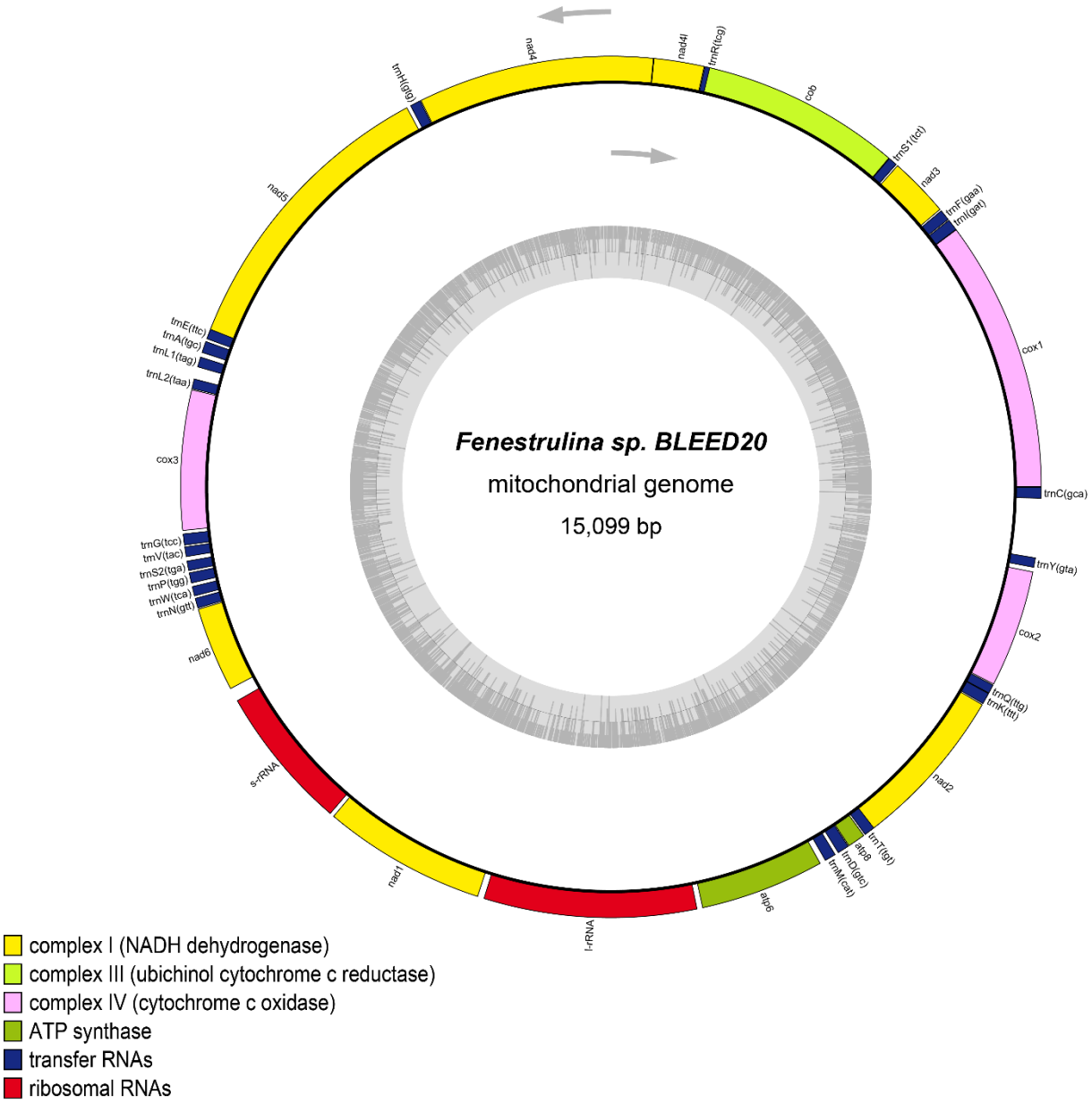

Appendix Figure 62. Complete mitochondrial genome of *Fenestrulina* sp. Sequencing coverage: Average: 164x - Min: 16x.

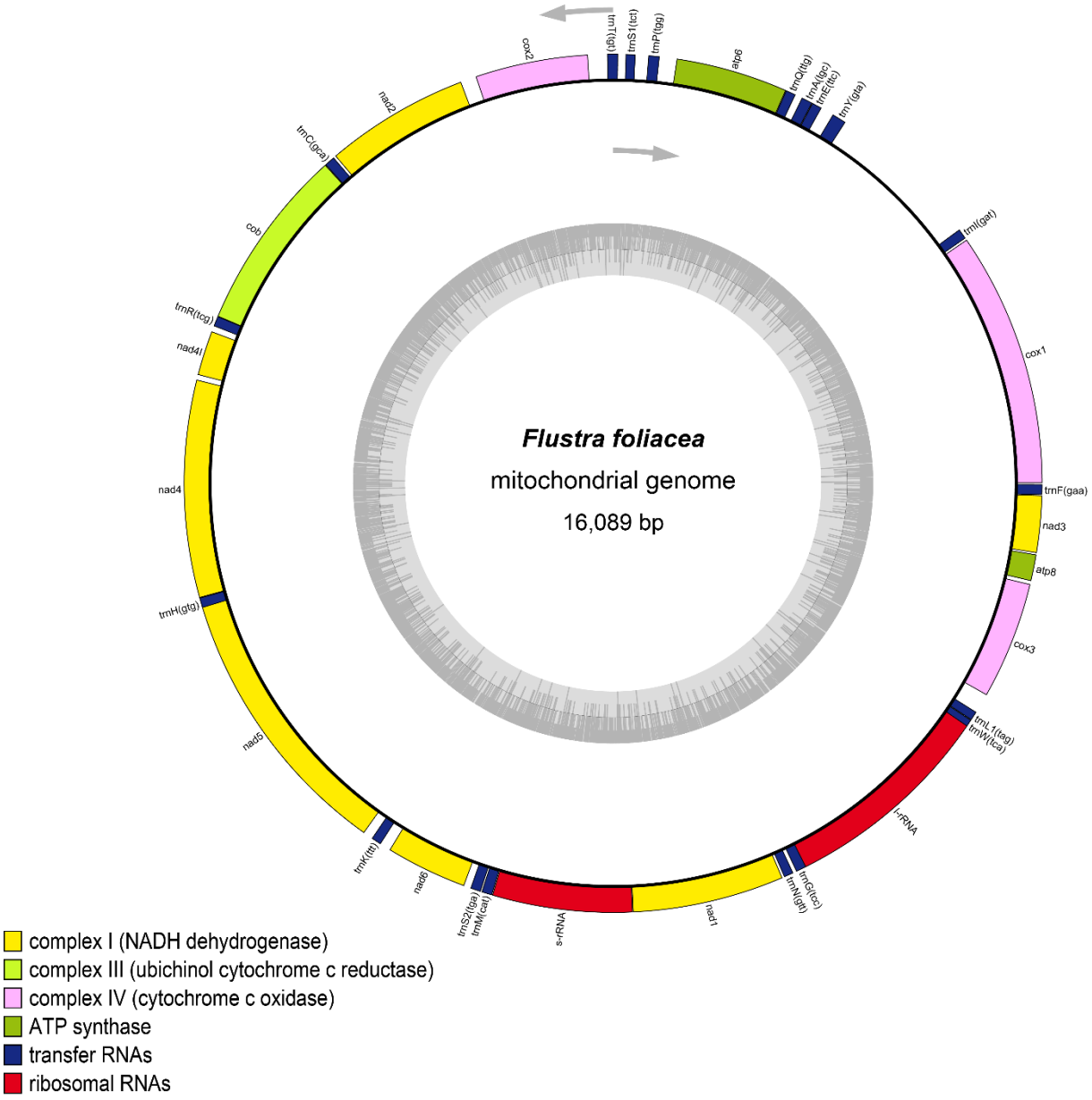

Appendix Figure 63. Complete mitochondrial genome of *Flustra foliacea.*

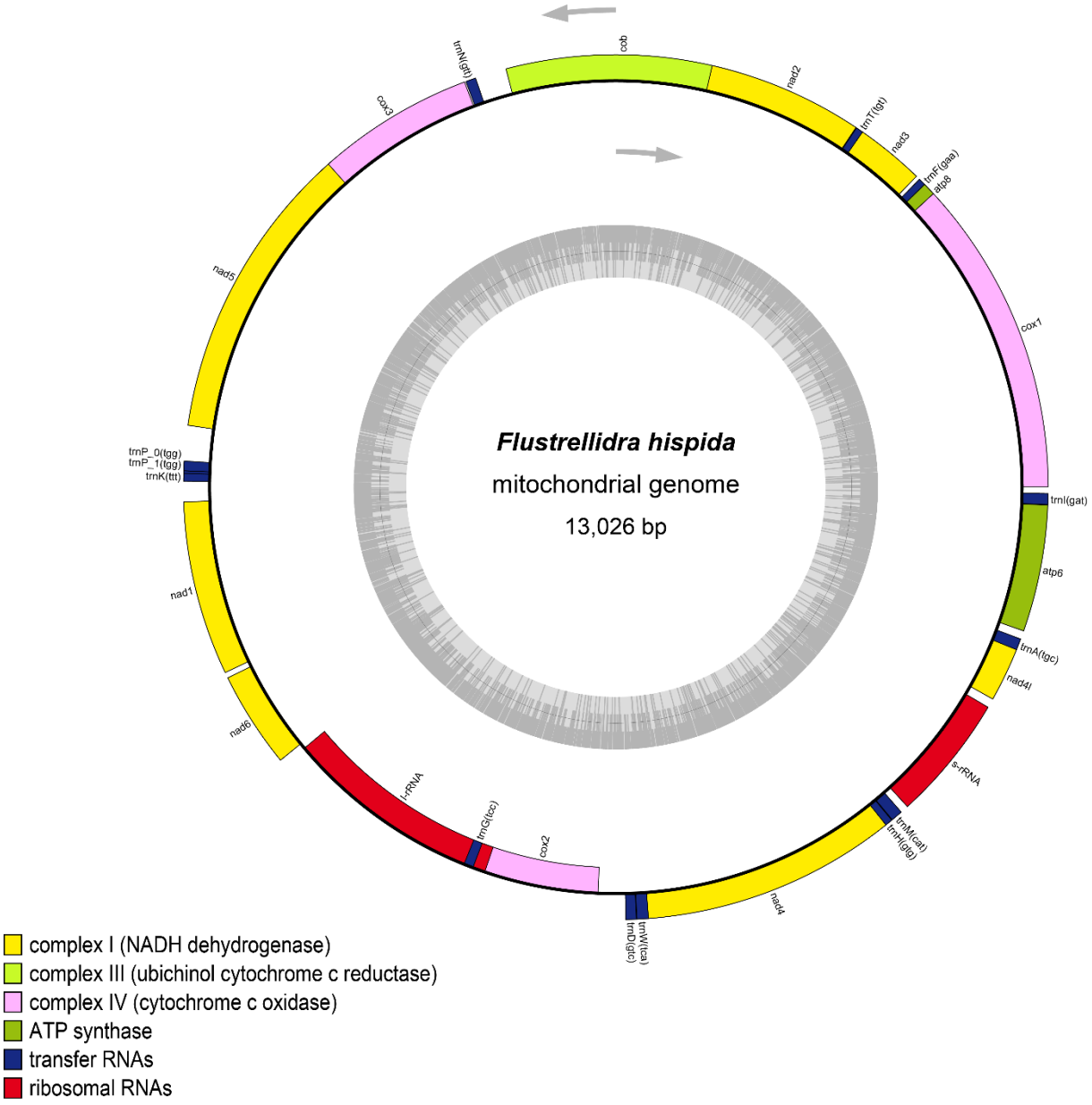

Appendix Figure 64. Complete mitochondrial genome of *Flustrellidra hispida.*

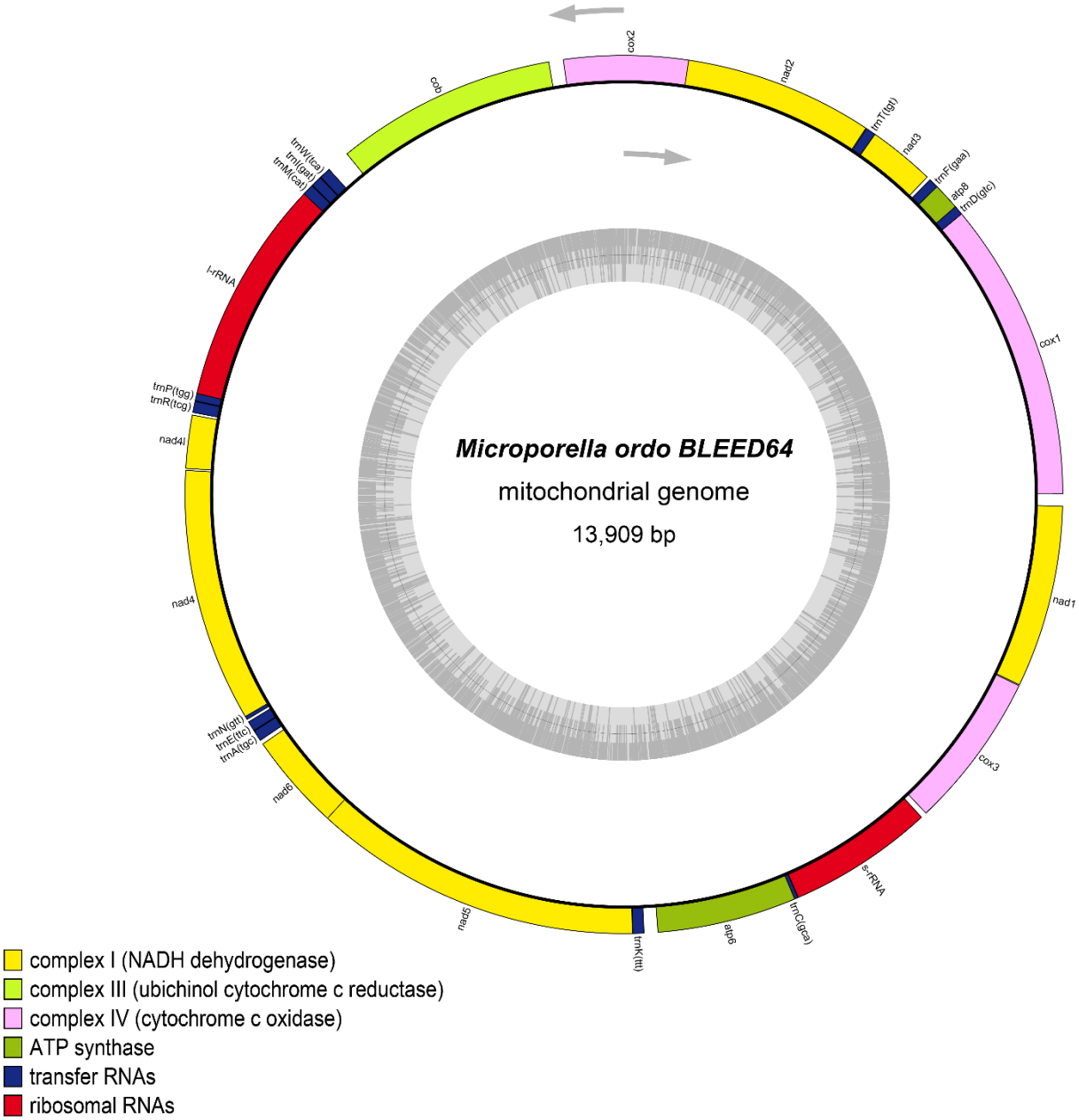

Appendix Figure 65. Complete mitochondrial genome of *Microporella ordo*. Sequencing coverage: Average: 28x - Min: 5x.

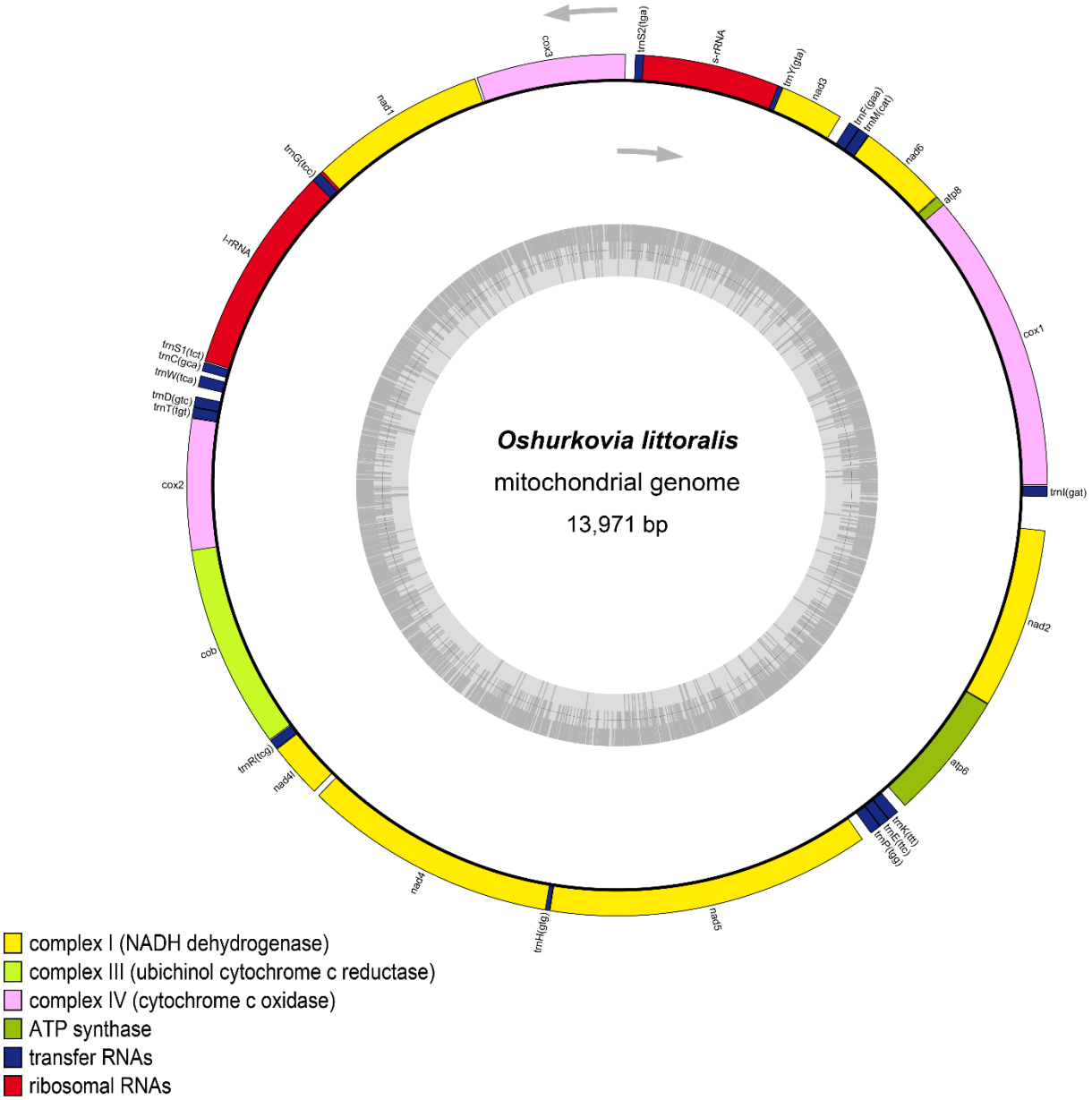

Appendix Figure 66. Complete mitochondrial genome of *Oshurkovia littoralis.* Please note: Previously named *Umbonula littoralis.*

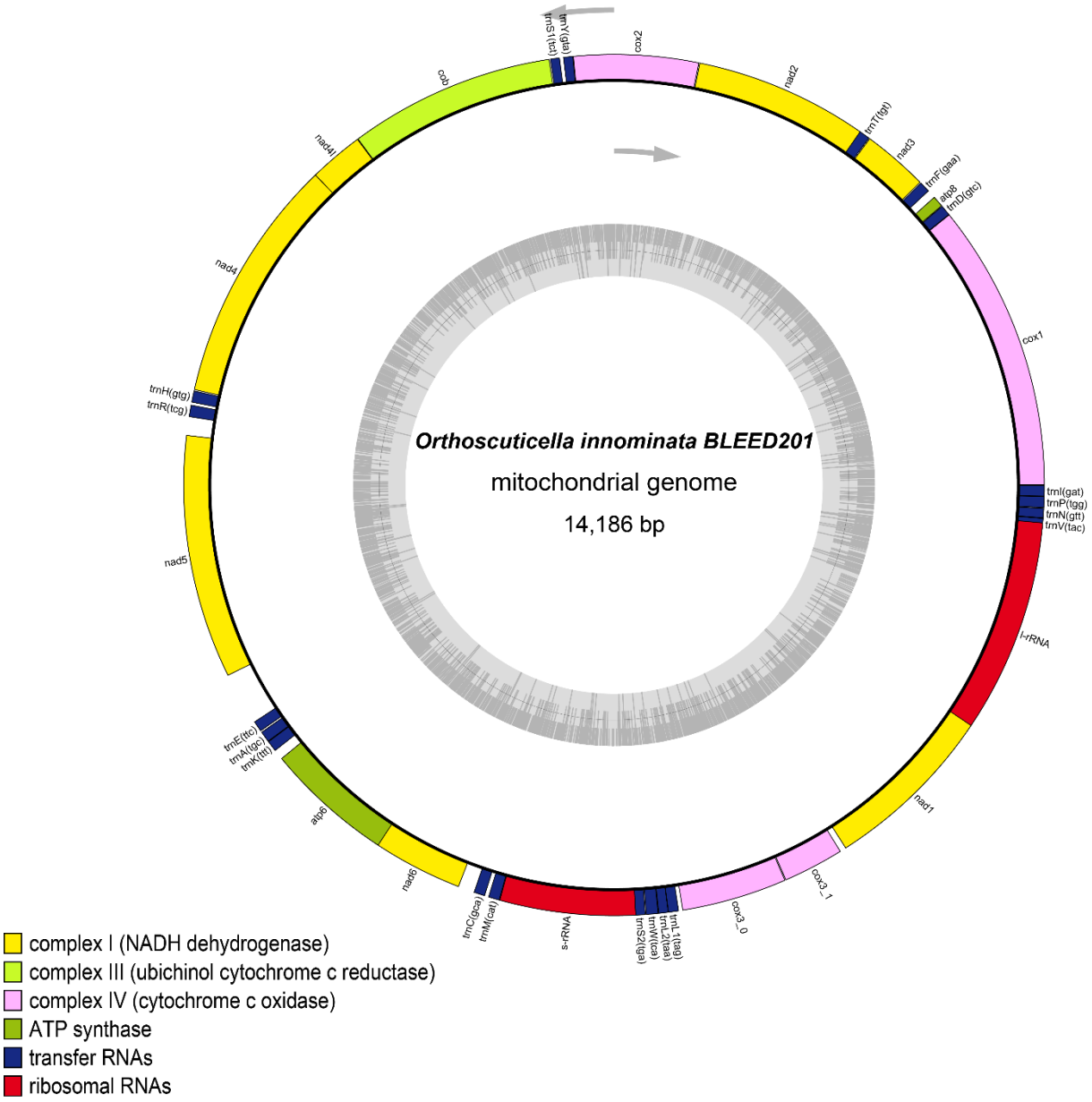

Appendix Figure 67. Complete mitochondrial genome of *Orthoscuticella innominata*. Sequencing coverage: Average: 75x - Min: 8x.

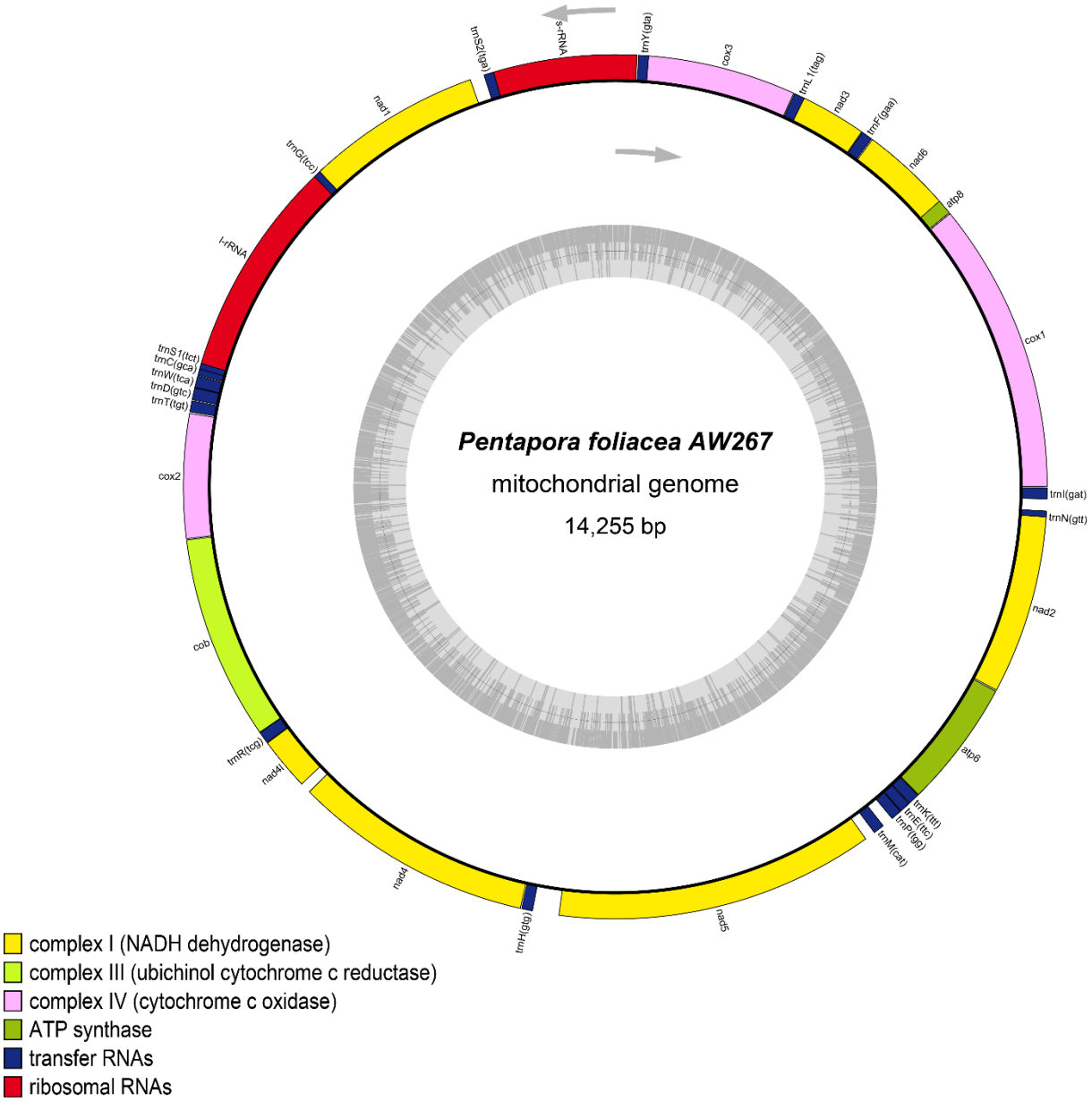

Appendix Figure 68. Complete mitochondrial genome of *Pentapora foliacea*.

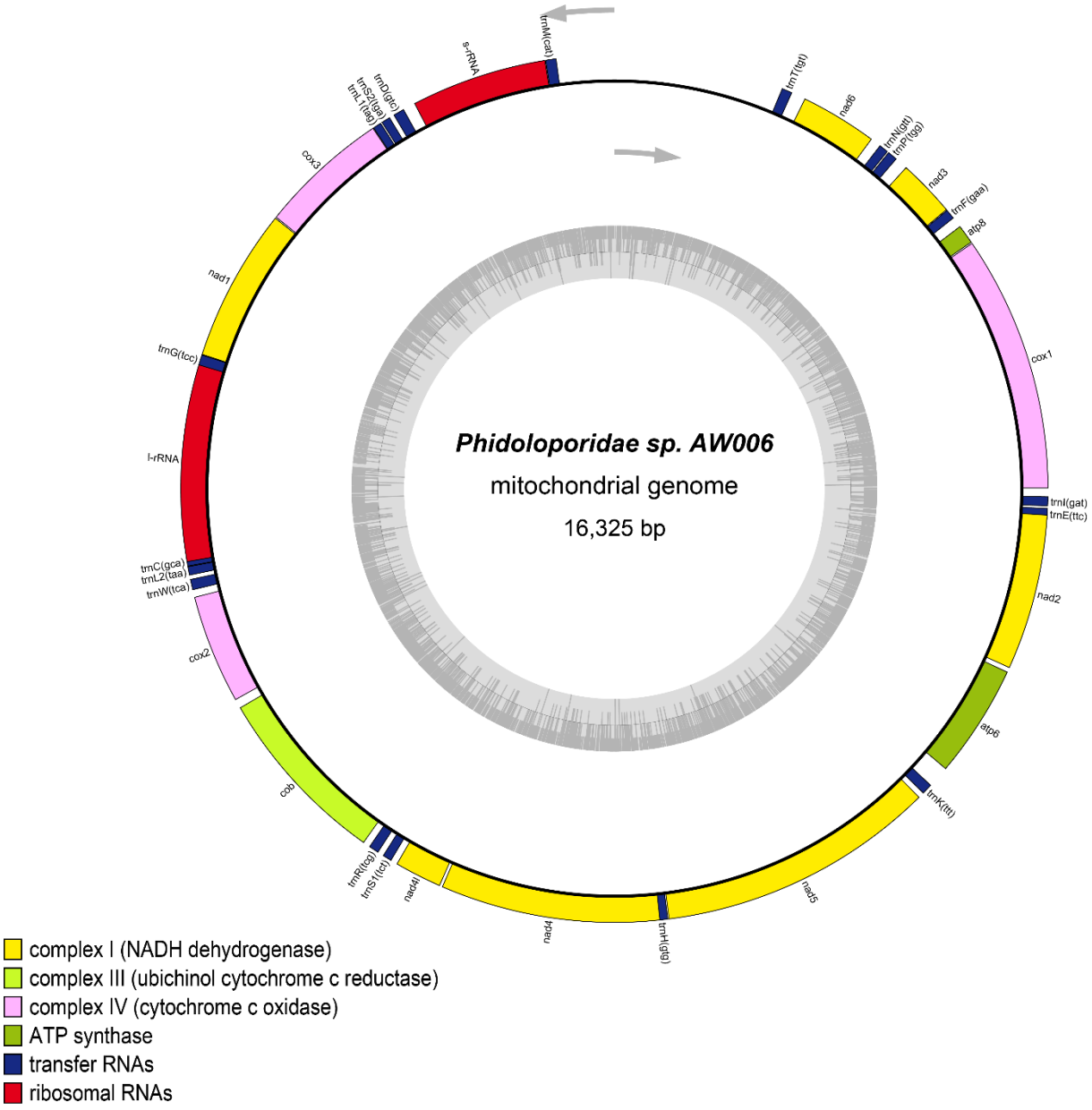

Appendix Figure 69. Complete mitochondrial genome of *Phidoloporidae* sp.

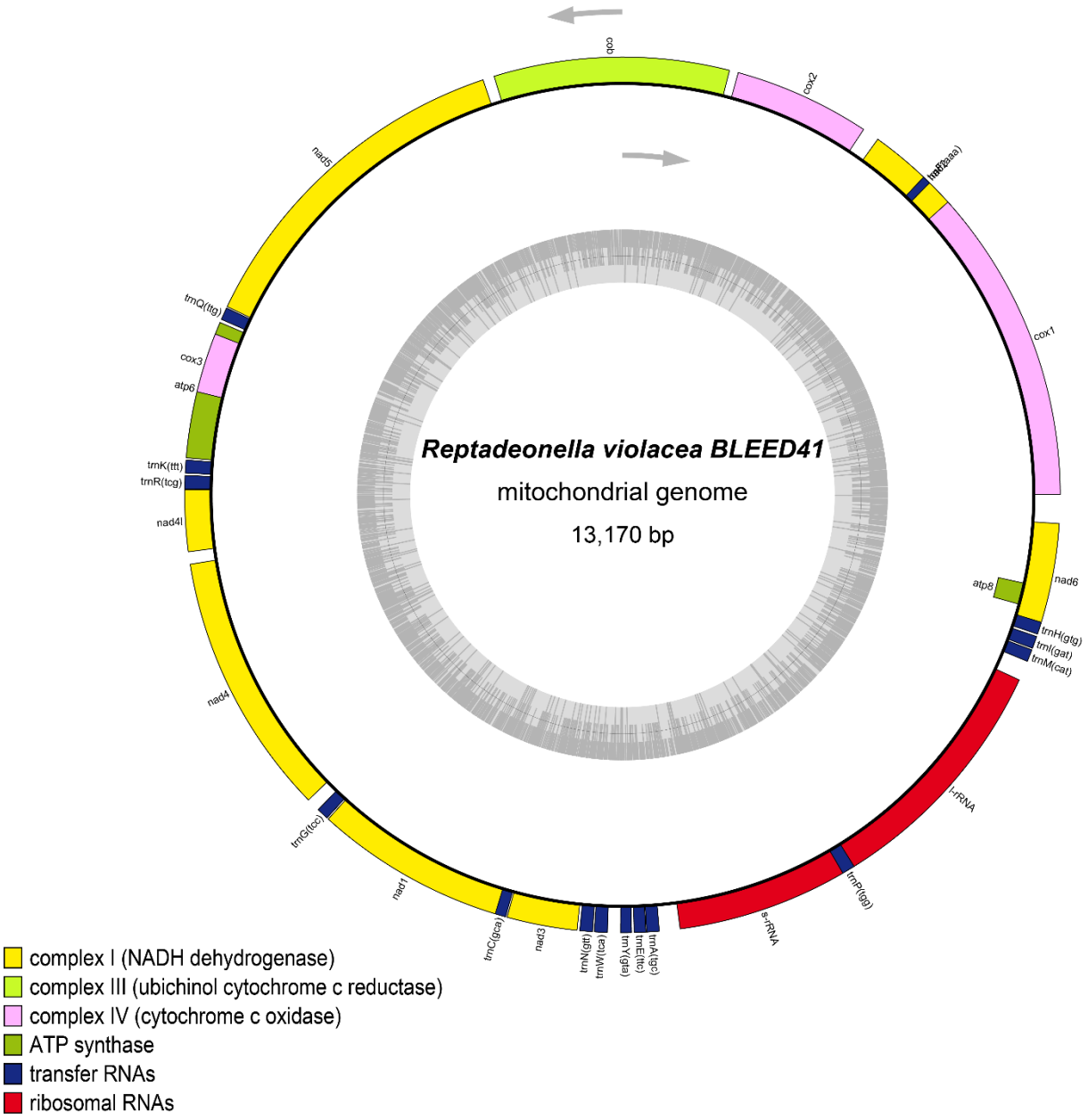

Appendix Figure 70. Complete mitochondrial genome of *Reptadeonella violacea*. Sequencing coverage: Average: 62x - Min: 6x.

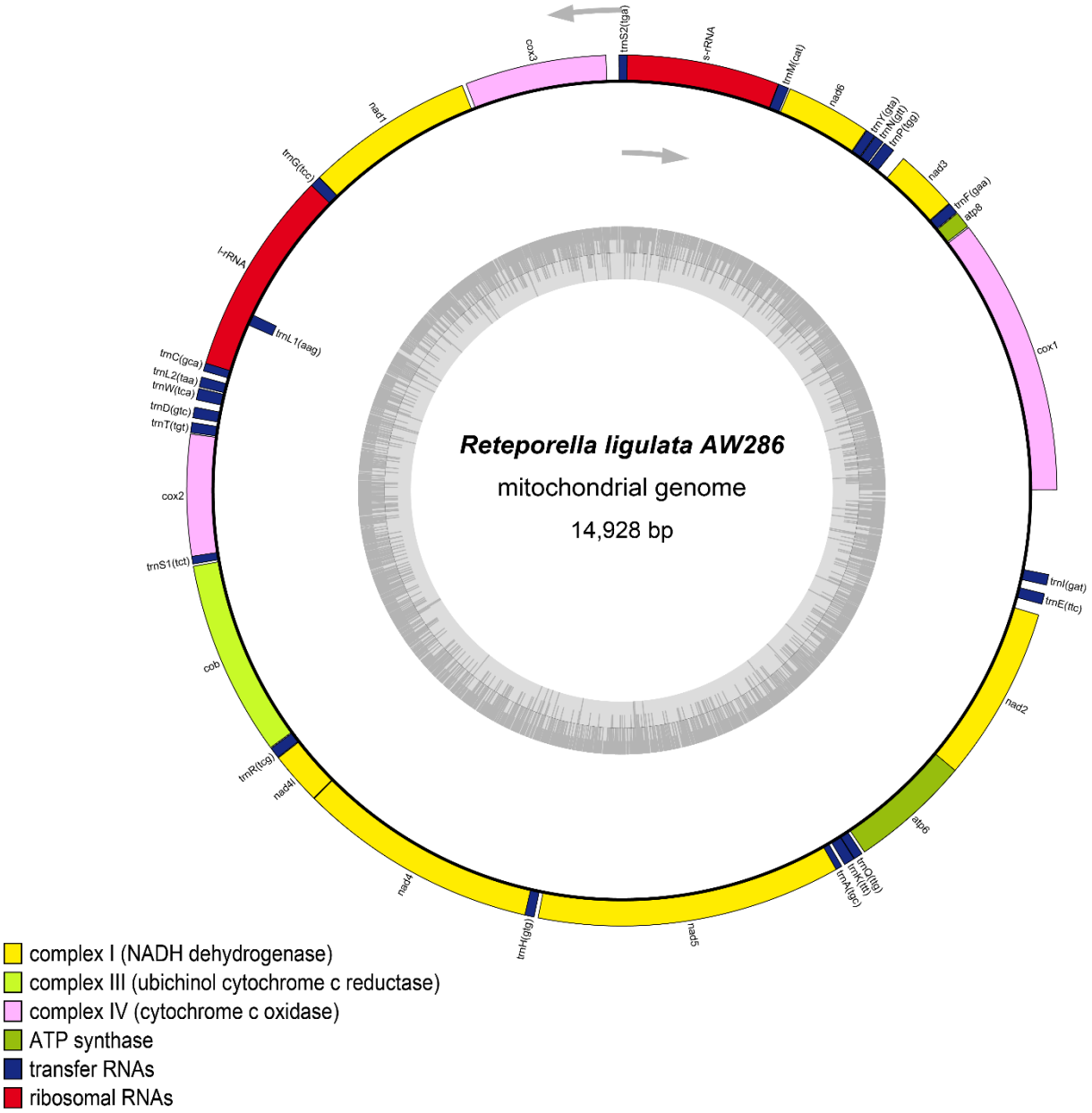

Appendix Figure 71. Complete mitochondrial genome of *Reteporella ligulata.*

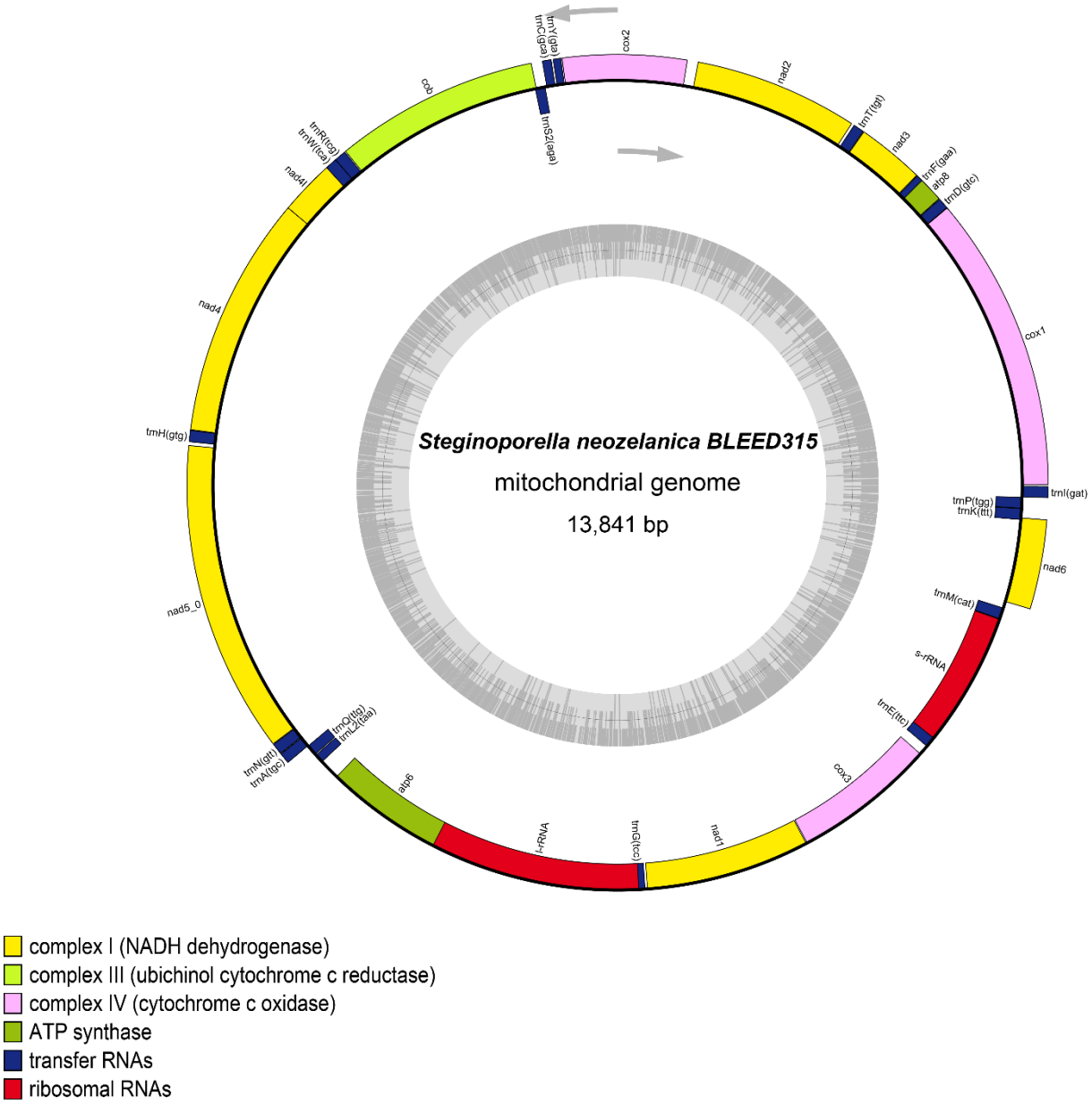

Appendix Figure 72. Complete mitochondrial genome of *Steginoporella neozelanica*. Sequencing coverage: Average: 234x - Min: 23x.

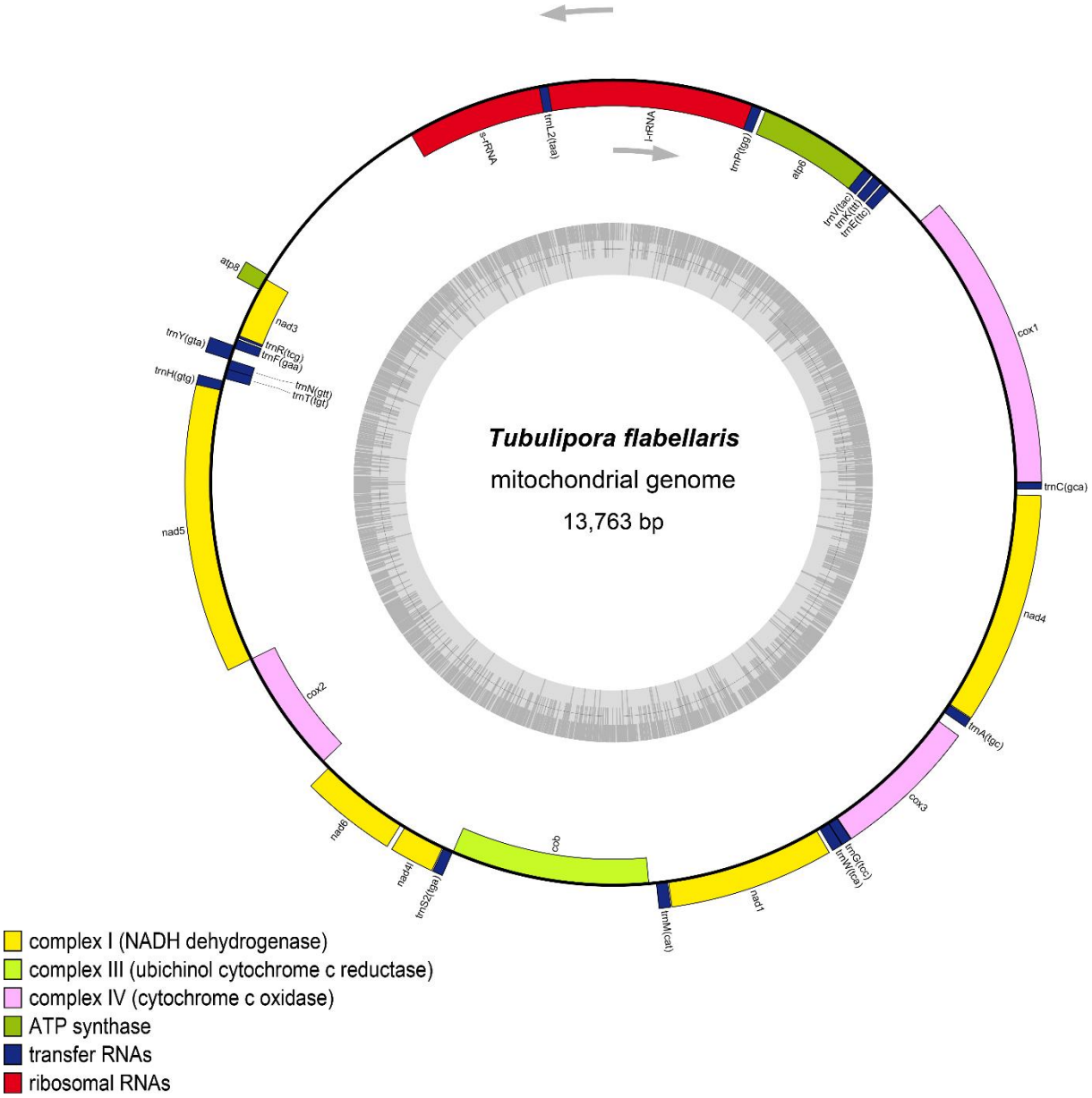

Appendix Figure 73. Complete mitochondrial genome of *Tubulipora flabellaris*.

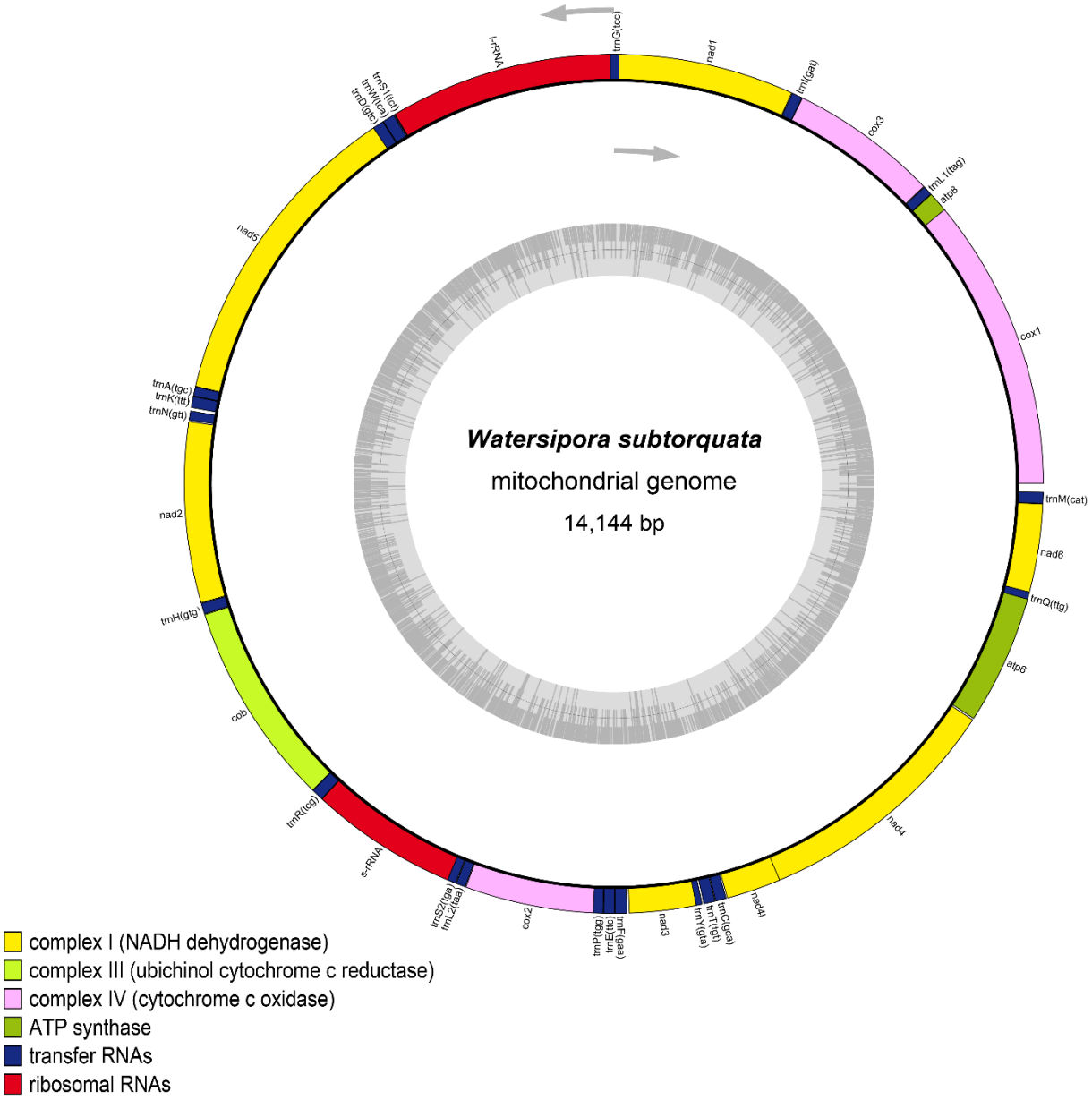

Appendix Figure 74. Complete mitochondrial genome of *Watersipora subtorquata.*

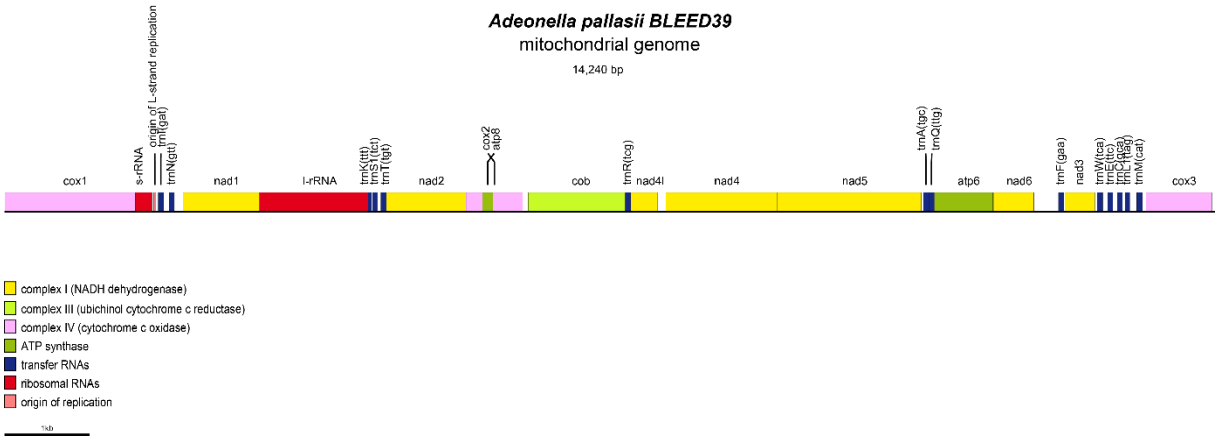

Appendix Figure 75. Incomplete mitochondrial genome of *Adeonella pallasii*. Sequencing coverage: Average: 86x - Min: 9x.

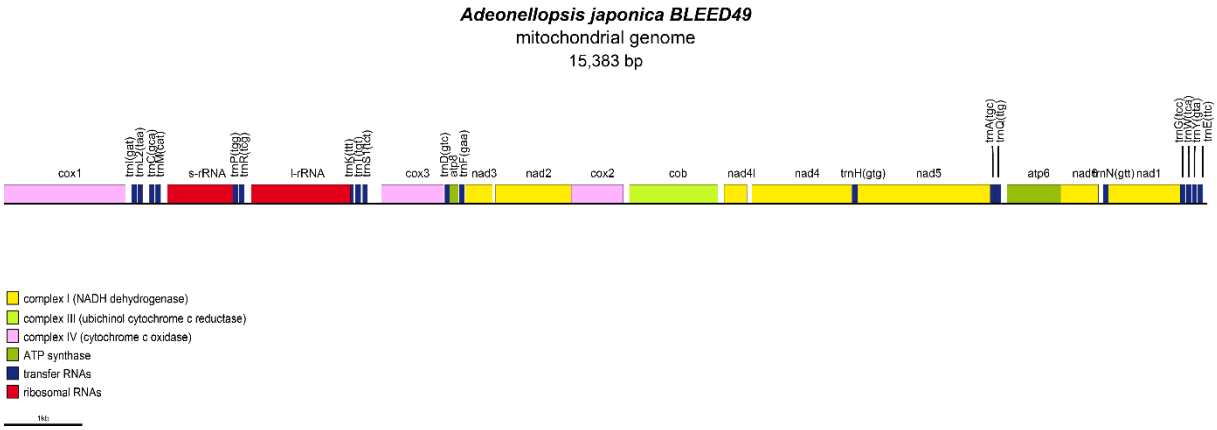

Appendix Figure 76. Incomplete mitochondrial genome of *Adeonellopsis japonica*. Sequencing coverage: Average: 55x - Min: 6x.

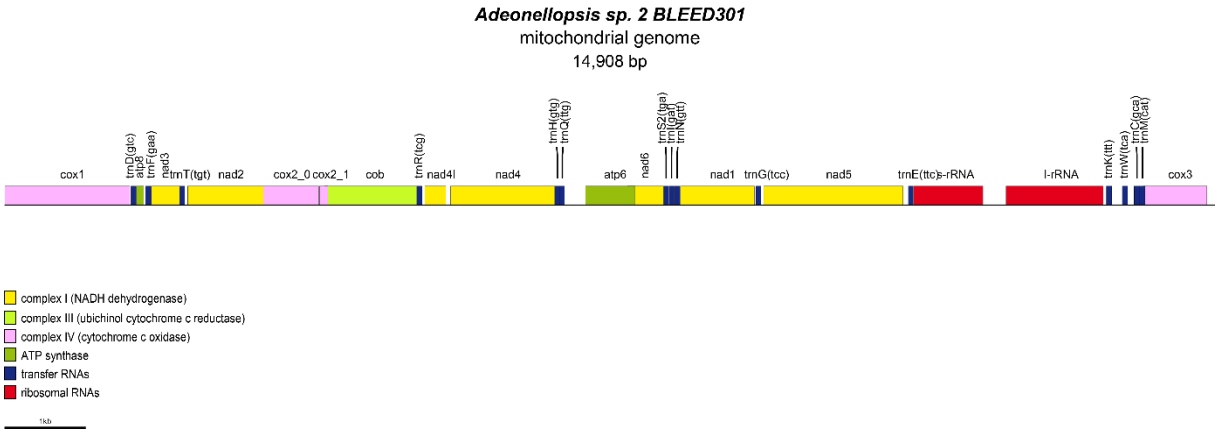

Appendix Figure 77. Incomplete mitochondrial genome of *Adeonellopsis* sp. 2. Sequencing coverage: Average: 13x - Min: 5x.

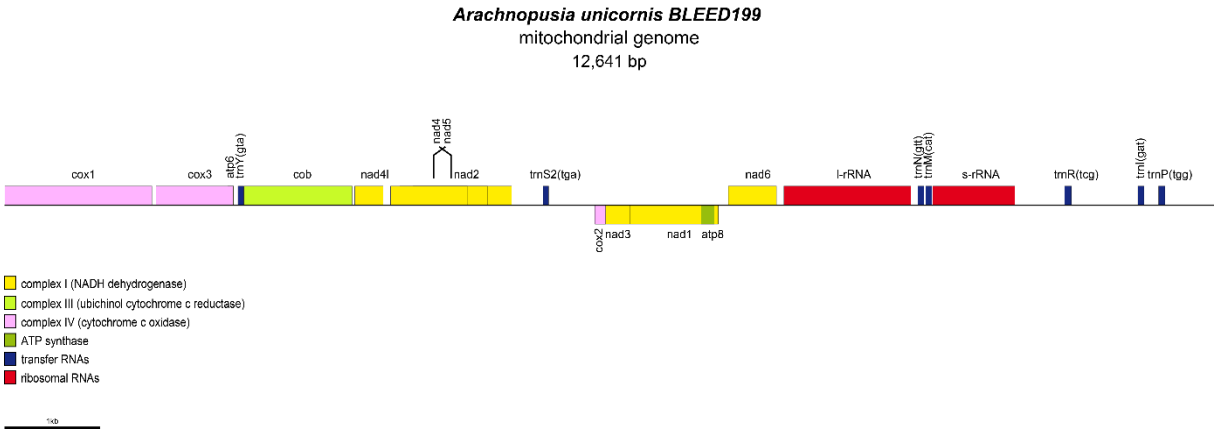

Appendix Figure 78. Incomplete mitochondrial genome of *Arachnopusia unicornis*. Sequencing coverage: Average: 60x - Min: 6x.

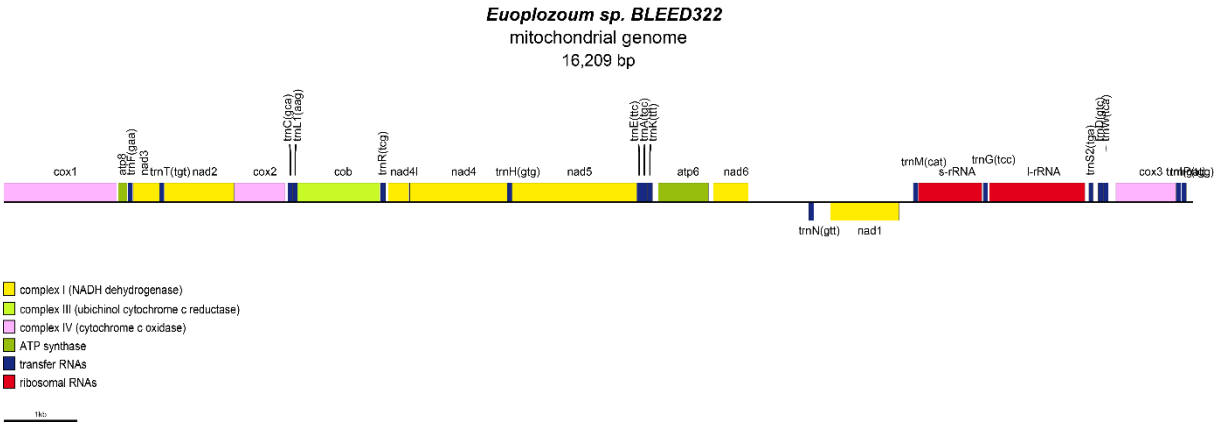

Appendix Figure 79. Incomplete mitochondrial genome of *Euoplozoum* sp. Sequencing coverage: Average: 165x - Min: 17x.

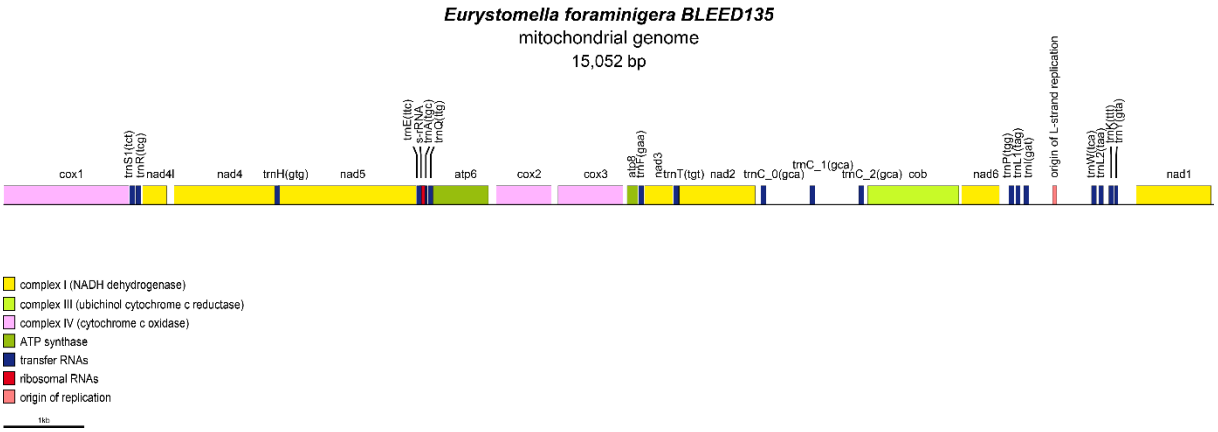

Appendix Figure 80. Incomplete mitochondrial genome of *Eurystomella foraminigera*. Sequencing coverage: Average: 137x - Min: 14x.

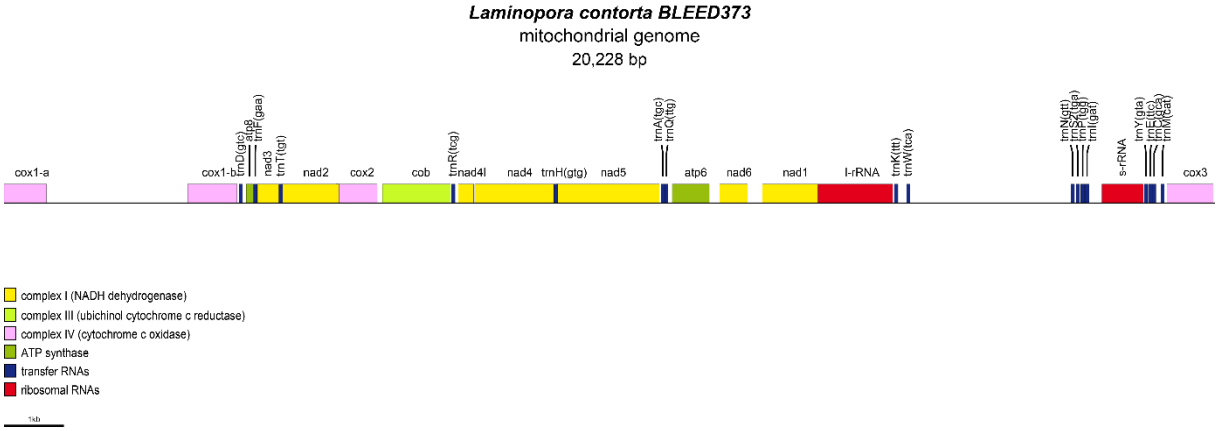

Appendix Figure 81. Incomplete mitochondrial genome of *Laminopora contorta*. Sequencing coverage: Average: 235x - Min: 24x.

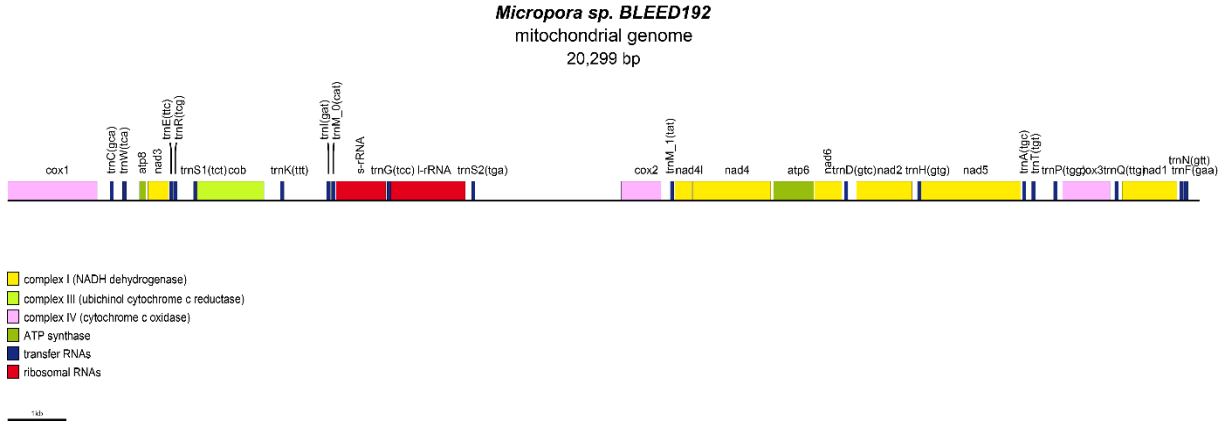

Appendix Figure 82. Incomplete mitochondrial genome of *Micropora* sp. Sequencing coverage: Average: 21x - Min: 5x.

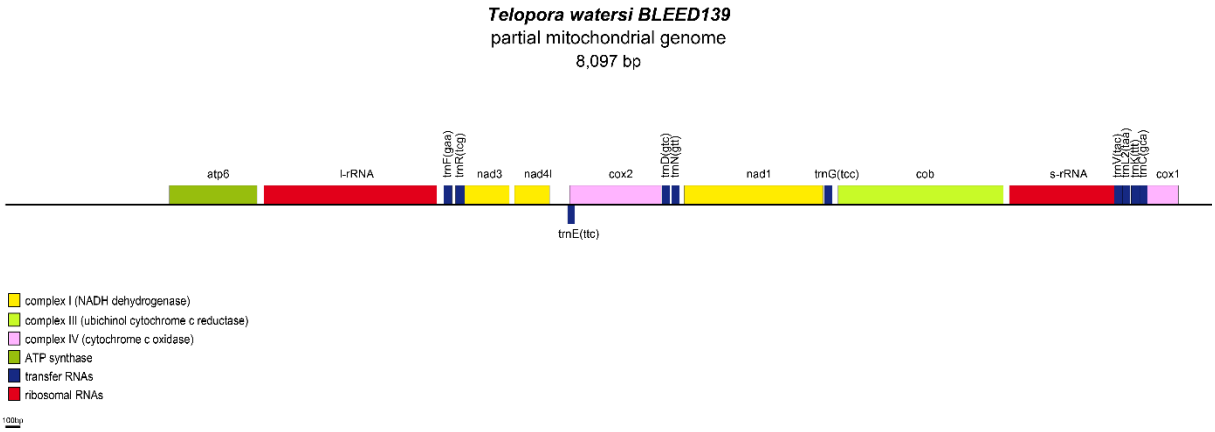

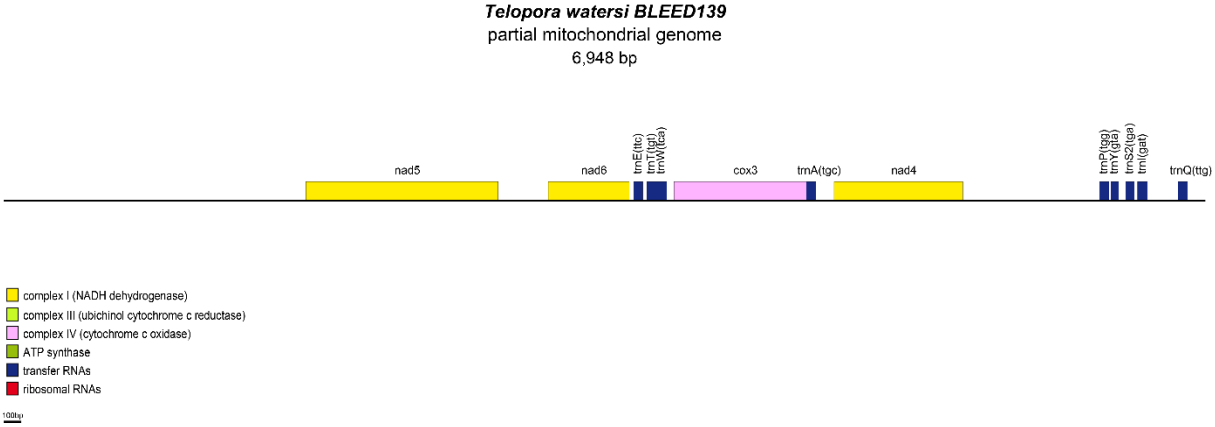

Appendix Figure 83. Incomplete, fragmented, mitochondrial genome of *Telopora watersi*. Sequencing coverage: Average: 78x - Min: 5x.

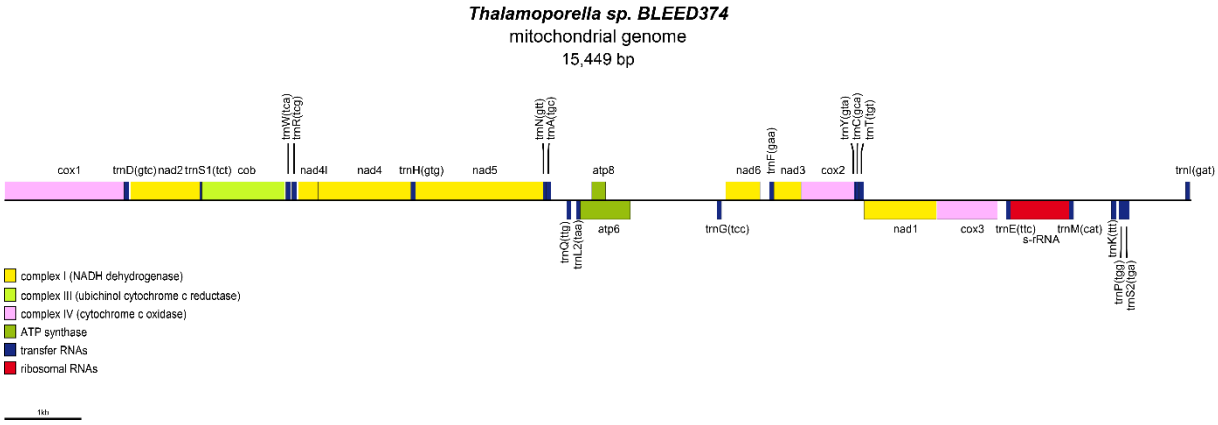

Appendix Figure 84. Incomplete mitochondrial genome of *Thalamoporella* sp. Sequencing coverage: Average: 132x - Min: 13x.